P-05-27

Oskarshamn site investigation

Formation factor logging in-situ and in the laboratory by electrical methods in KSH01A and KSH02

Measurements and evaluation of methodology

Martin Löfgren, Ivars Neretnieks
Department of Chemical Engineering and Technology
Royal Institute of Technology

April 2005

Svensk Kärnbränslehantering AB
Swedish Nuclear Fuel
and Waste Management Co
Box 5864
SE-102 40 Stockholm Sweden
Tel 08-459 84 00
+46 8 459 84 00
Fax 08-661 57 19
+46 8 661 57 19

ISSN 1651-4416
SKB P-05-27

Oskarshamn site investigation

Formation factor logging in-situ and in the laboratory by electrical methods in KSH01A and KSH02

Measurements and evaluation of methodology

Martin Löfgren, Ivars Neretnieks
Department of Chemical Engineering and Technology
Royal Institute of Technology

April 2005

Keywords: In-situ, Formation factor, Surface conduction, Rock, Resistivity, Electrical conductivity.

Abstract

This report presents measurements and interpretations of the formation factor of boreholes KSH01A and KSH02 in Simpevarp, Oskarshamn, Sweden. The formation factor was logged both in the laboratory and in-situ by electrical methods.

During the review process it was discovered that the nomenclature for fractures had been changed, and that the evaluation of the in-situ formation factor was based on "old" nomenclature (cores had also been remapped). This could imply minor uncertainties in the statistics of the reported "rock matrix formation factors", since data have been excluded. However, since the data still are judged useful (e.g. as indications of spatial variability) and a re-analysis will take some time, it was decided to publish this report and then evaluate the effects as a separate activity.

In order to meet future demands from models of radionuclide retention in fractured rock, the traditional formation factor was divided into two subgroups. The first subgroup is called the "rock matrix formation factor" and is the formation factor of the solid and non-fractured rock. The other subgroup is called the "fractured rock formation factor" and is the formation factor of fractured rock that do not contain hydraulically conductive fractures. The results presented in this report suggest that diffusion into open but non-conductive fractures may considerable increase the retention capacity of the rock.

The in-situ rock matrix formation factors obtained in KSH01A and KSH02 ranged from 1.0×10^{-5} to 4.4×10^{-4} and from 4.3×10^{-6} to 3.6×10^{-3} respectively. The in-situ fractured rock formation factors obtained ranged from 9.5×10^{-6} to 4.7×10^{-3} and from 4.3×10^{-6} to 1.3×10^{-1} in KSH01A and KSH02 respectively. The laboratory (rock matrix) formation factors obtained on bore core samples from KSH01A and KSH02 ranged from 1.3×10^{-6} to 9.0×10^{-4} and from 2.2×10^{-7} to 8.4×10^{-4} respectively. The formation factors appear to be distributed according to the log-normal distribution.

The rock type specific formation factor histograms presented in this report suggest that the formation factor within a rock type may range over at least two orders of magnitude.

For future work it is recommended to use an in-situ rock resistivity tool with a larger quantitative measuring range. The tool used at present may give rise to non-conservative formation factors in the lower formation factor region.

Sammanfattning

Denna rapport presenterar mätningar och tolkningar av formationsfaktorn i borrhålen KSH01A and KSH02 i Simpevarp, Oskarshamn, Sverige. Formationsfaktorn har loggats både in-situ och i laboratoriet med elektriska metoder.

Under granskningsfasen av denna rapport upptäcktes att nomenklaturen för sprickor hade ändrats och att utvärderingen av in-situ formationsfaktorn för bergmatrisen baserats på den gamla nomenklaturen (borrkärnorna hade även omkarterats). Detta kan medföra vissa osäkerheter i statistiken för de rapporterade ”rock matrix formation factors” eftersom vissa data utelämnats. Eftersom data trots detta bedömts vara användbara (t ex som indikation på rumslig variation) och att en ny analys tar tid, bestämdes att publicera denna rapport och genomföra en analys av effekterna som en separat aktivitet.

För att möta framtida krav från modeller som behandlar retention av radionuklider i sprickigt berg så delades den traditionella formationsfaktorn upp i två subgrupper. Den första subgruppen, kallad ”formationsfaktorn för bergmatrisen”, är formationsfaktorn för det solida ospruckna berget. Den andra subgruppen, kallad ”formationsfaktorn för sprickigt berg” är formationsfaktorn för berg som genomkorsas av öppna men hydrauliskt ickekonduktiva sprickor. Resultaten som presenteras i denna rapport tyder på att diffusion i öppna men ickekonduktiva sprickor påtagligt kan öka bergets retentionskapacitet.

Den erhållna in-situ formationsfaktorn för bergmatrisen för KSH01A och KSH02 varierade från $1{,}0\times10^{-5}$ till $4{,}4\times10^{-4}$ och från $4{,}3\times10^{-6}$ till $3{,}6\times10^{-3}$ för respektive borrhål. Den erhållna in-situ formationsfaktorn för sprickigt berg för KSH01A och KSH02 varierade från $9{,}5\times10^{-6}$ till $4{,}7\times10^{-3}$ och från $4{,}3\times10^{-6}$ till $1{,}3\times10^{-1}$ för respektive borrhål. Den erhållna laborativa formationsfaktorn (för bergmatrisen) för KSH01A och KSH02 varierade från $1{,}3\times10^{-6}$ till $9{,}0\times10^{-4}$ och från $2{,}2\times10^{-7}$ till $8{,}4\times10^{-4}$ för respektive borrhål.

De bergartsspecifika formationsfaktorhistogrammen som presenteras i denna rapport tyder på att formationsfaktorn inom samma bergart kan variera över åtminstone två tiopotenser.

För framtida arbete rekommenderas det att använda ett in-situ verktyg för att mäta bergets resistivitet som har ett större kvantitativt mätområde. Det verktyg som används för närvarnade kan ge upphov till ickekonservativa formationsfaktorer i det lägre formations-faktorområdet.

Contents

1 Introduction

This document reports the data gained from measurements of the formation factor of boreholes KSH01A and KSH02 within the site investigation at Oskarshamn. The formation factor was logged both in the laboratory and in-situ by electrical methods.

The laboratory work was performed by Chemical Engineering and Technology at the Royal Institute of Technology in Stockholm, Sweden, during the time period from the 12th of January to the 24th of May 2004. The work in the field and the results from this work that were used when obtaining in-situ formation factor logs are outside the framework of this activity and was performed by other contractors. The interpretation of in-situ data and compilation of in-situ formation factor logs were performed by Chemical Engineering and Technology at the Royal Institute of Technology in Stockholm, Sweden.

This work was conducted according to the activity plan AP PS 400-03-041 (SKB internal controlling document). The reference to SICADA for the data of this activity are field note no 634 differential flow logging, 699 specific-EC differential logging and 756 resistivity logging.

Figure 1-1 shows the sub area of Simpevarp. KSH01A is the forth borehole from the right and KSH02 is the second borehole from the left.

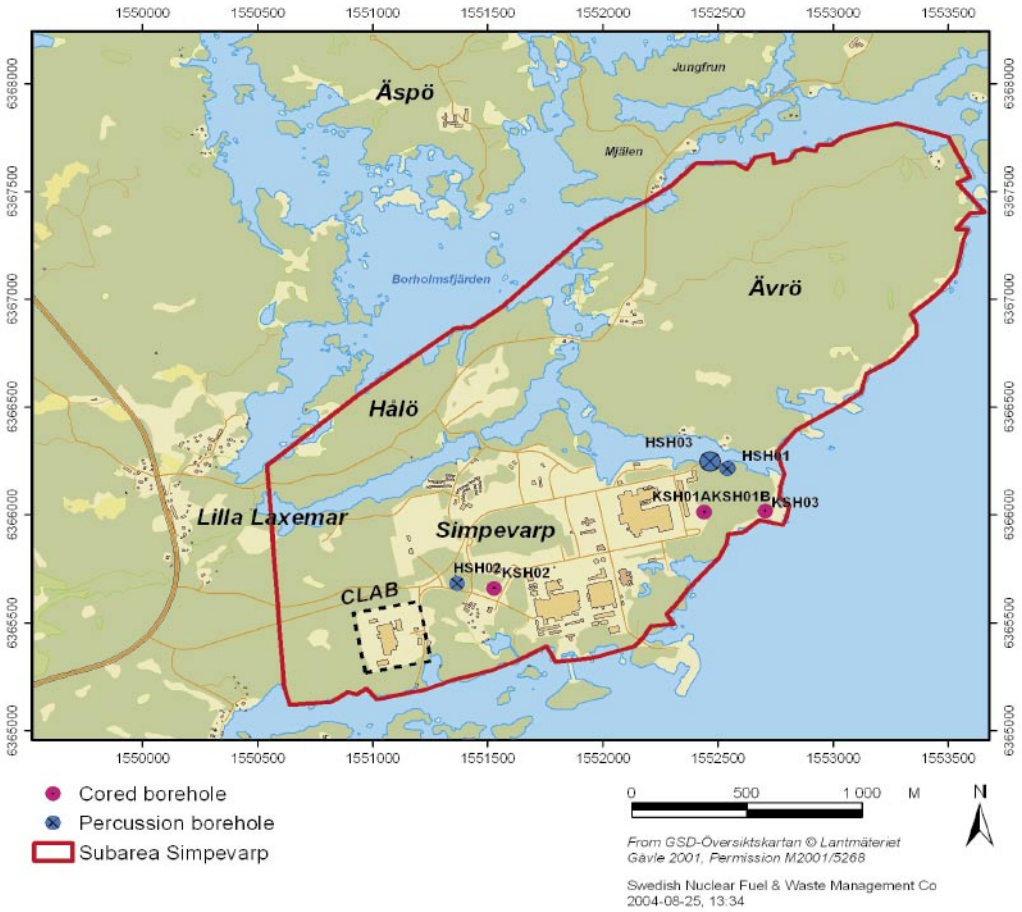

Figure 1-1. *General overview over the Simpevarp subarea.*

2 Objective and scope

The main objective of this work was to obtain the formation factor of the rock mass around the boreholes KSH01A and KSH02. This was achieved by performing formation factor loggings by electrical methods both in-situ and in the laboratory. To obtain the in-situ formation factor, results from previous loggings were used. The laboratory formation factor was obtained by performing measurements on rock samples from the bore cores of KSH01A and KSH02. The formation factor is an important parameter that may be used directly in the safety assessment. Prior to this work, formation factors have generally been obtained in the laboratory on a limited number of disturbed rock samples. The in-situ method gives a great number of formation factors obtained under more natural conditions.

A secondary objective of this work was to evaluate and, if necessary, improve the methodology used. At the end of this report suggestions on improvements are given. A number of different ways of representing the results is also presented.

3 Equipment

3.1 Rock resistivity measurments

The rock resistivity of KSH01A and KSH02 was logged in two separate campaigns using the focused rock resistivity tools Century 9072 and Century 9030. In this report data from the Century 9030 is not used. These tools emit an alternating current perpendicular to the borehole axis from a main current electrode. The shape of the current field is controlled by electric fields emitted by guard electrodes. By using focused tools the disturbance from the borehole is minimized.

The rock resistivity of KSH01A was logged between the borehole lengths 0.3 and 1,002.9 m on the 12th of February 2003. The campaign is described in /1/. The rock resistivity of KSH02 was logged between 78.1 and 1,001.7 m on the 1st of July 2003, and the campaign is described in /2/. The quantitative measuring range of the Century 9072 tool is 0–50,000 ohm.m according to the manufacturer. In Section 4.2.1 in this report a discussion concerning the measuring range is given. For further details concerning the campaigns, methods and tools used please consult the publications mentioned above.

3.2 Groundwater electrical conductivity measurments

The EC (electrical conductivity) of the borehole fluid in KSH01A was logged between the borehole lengths 22.9 and 998.2 m using the POSIVA difference flow meter. The tool is shown in Figure 3-1.

When logging the EC of the borehole fluid, the lower rubber disks of the tool are not used. Measurements in KSH01A were carried out before pumping in the borehole between the 19th and the 20th of February 2003, and after pumping in the borehole on the 1st of March 2003. The measurements are described in /3/.

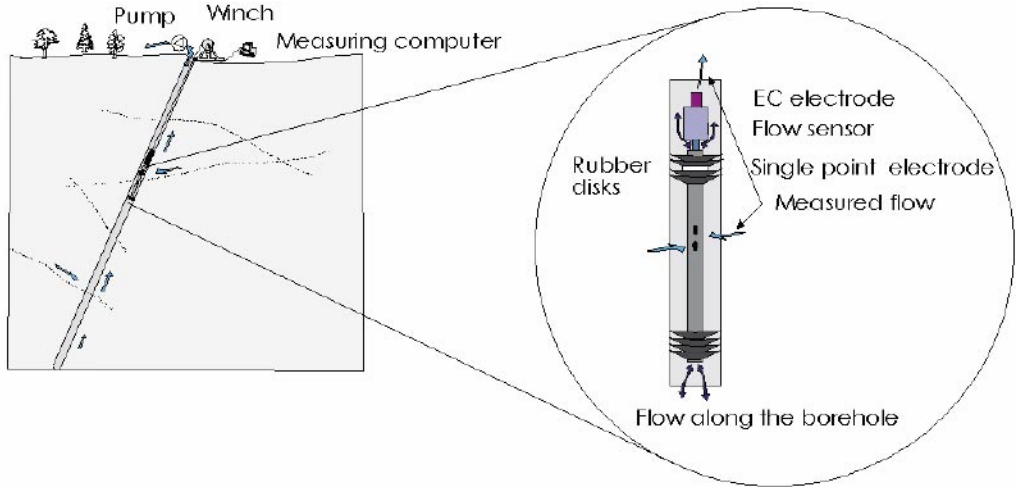

Figure 3-1. *Schematics of the POSIVA difference flow meter.*

When using both the upper and the lower rubber disks, a section around a specific fracture can be sealed off. By pumping at the surface, fracture specific groundwater can be extracted from the section. The electrical conductivity of this groundwater is measured. This was done in KSH02 on a number of fractures between 99.3 and 994.9 m in the borehole. The measurements were performed between the 18th and the 19th of July 2003, and are described in /4/. The quantitative measuring range of the EC electrode of the POSIVA difference flow meter is 0.02–11 S/m. For further details concerning the measurements with the POSIVA difference flow meter please consult the publications mentioned above.

The electrical conductivity, among other entities, of the groundwater coming from fractures in three sections of KSH01A was measured as a part of the hydrogeochemical program. The sections 156.5–167 m, 245–261.5 m, and 548–565 m were sealed off and groundwater was pumped out of the sections to the surface, where the electrical conductivity was measured. The measurements were carried out during 2003 from the 27th of March to the 23rd of April, from the 24th of April to the 20th of May, and from the 23rd of June to the 17th of September in the three sections respectively.

3.3 Location of hydraulically conductive fractures

The POSIVA difference flow meter shown in Figure 3-1 has a flow sensor and the flow from specific fractures in sealed off sections can be measured. When performing these measurements both the upper and the lower rubber disks are used. Measurements can be made both with and without pumping at the surface.

Difference flow measurements were performed in KSH01A between the borehole lengths 100 and 995 m. The measurements were carried out from the 18th of February to the 2nd of March 2003, and are described in /3/. Difference flow measurements were performed in KSH02 between 80 and 997 m. The measurements were carried out from the 7th to the 22nd of July 2003, and are described in /4/. The quantitative measuring range of the flow sensor is 0.1–5,000 mL/min.

3.4 Location of natural fractures

The bore core of KSH01A was logged from 101.68 m to 1,007.28 m between the 17th of March and the 16th of December 2003. The bore core of KSH02 was logged between 79.97 m–1,007.16 m in 2003 and 2004.

In the core log, fractures parting the core are recorded. Fractures parting the core that have not been induced in the drilling or core handling are called natural fractures. Parts of the core that are crushed or lost are also recorded as well as the spatial distribution of different rock types. Data from the core logging of KSH01A and KSH02 are available in SICADA. Information on bore core (boremap) logging can be found in e.g. /5/.

4 Execution

4.1 Theory

4.1.1 The formation factor

The theory needed for obtaining formation factors by electrical methods is described in /6/. The formation factor is the ratio between the diffusivity of the rock matrix to that of free pore water. If the species diffusing through the porous system are much smaller than the characteristic length of the pores and no interactions occur between the mineral surfaces and the species, the formation factor is only a geometrical factor that is defined by the transport porosity, the tortuosity and the constrictivity of the porous system:

$$F_f = \frac{D_e}{D_w} = \varepsilon_t \frac{\delta}{\tau^2} \qquad 4\text{-}1$$

where F_f is the formation factor, D_e (m^2/s) is the effective diffusivity of the rock, D_w (m^2/s) is the diffusivity in the free pore water, ε_t is the transport porosity, τ is the tortuosity, and δ is the constrictivity. When obtaining the formation factor by electrical methods the Einstein relation between diffusivity and ionic mobility is used:

$$D = \frac{\mu RT}{zF} \qquad 4\text{-}2$$

where D (m^2/s) is the diffusivity, μ ($m^2/V\times s$) is the ionic mobility, z the charge number and R, T and F, are the gas constant, temperature, and Faraday constant respectively. From the Einstein relation it is easy to show that the formation factor also is given by the ratio of the pore water resistivity to the resistivity of the saturated rock /7/:

$$F_f = \frac{\rho_w}{\rho_r} \qquad 4\text{-}3$$

where ρ_w (ohm.m) is the pore water resistivity and ρ_r (ohm.m) is the rock resistivity. The resistivity of the saturated rock can easily be obtained by standard geophysical methods.

At present it is not feasible to extract pore water from the rock matrix. Therefore, it is assumed that the pore water is in equilibrium with the free water surrounding the rock and measurements are performed on this free water. The validity of this assumption has to be discussed for every specific site. The resistivity is the reciprocal to electrical conductivity. Traditionally the EC is used when measuring on water and resistivity is used when measuring on rock.

4.1.2 Surface conductivity

In intrusive igneous rock the mineral surfaces are normally negatively charged. As the negative charge often is greater than what can be balanced by cations specifically adsorbed on the mineral surfaces, an electrical double layer with an excess of mobile cations will form at the pore wall. If a potential gradient is placed over the rock, the excess cations in the electrical double layer will move. This process is called surface conduction and this additional conduction may have to be accounted for when obtaining the formation factor

of rock saturated with a pore water of low ionic strength. If the electrical conductivity of the pore water is around 0.5 S/m or above, errors associated with surface conduction are deemed to be acceptable. This criterion is based on laboratory work by /8/ and /7/. The effect of the surface conduction on rock with formation factors below 1×10^{-5} was not investigated in these works. In this report surface conduction has not been accounted for as only the groundwater in the upper 100 or 200 m of the boreholes has a low ionic strength and as more knowledge is needed on surface conduction before performing corrections.

4.1.3 Artefacts

Comparative studies have been performed on a large number of 1–2 cm long samples from Äspö in Sweden /8/. Formation factors obtained with an electrical resistivity method using alternating current were compared to those obtained by a traditional through diffusion method using uranin as the tracer. The results show that formation factors obtained by the electrical resistivity measurements are a factor of about 2 times larger that those obtained by through diffusion measurements. A similar effect was found on granitic samples up to 12 cm long using iodide in tracer experiments /9/ The deviation of a factor 2 between the methods may be explained by anion exclusion of the anionic tracers. Previously performed work suggests that the Nernst-Einstein equation between the diffusivity and electrical conductivity is generally applicable in granitic rock and that no artefacts give rise to major errors.

4.1.4 Fractures in-situ

In-situ rock resistivity measurements are highly disturbed by free water in open fractures. The current sent out from the downhole tool in front of an open fracture will be propagated both in the porous system of the rock matrix and in the free water in open fractures. Due to the low formation factor of the rock matrix, current may be preferentially propagated in a fracture intersecting the borehole even if its aperture is only on the order of 10^{-5} m.

There could be some confusion concerning the terminology of fractures. In order to avoid confusion an organization sketch of different types of fractures is shown in Figure 4-1. The subgroups of fractures that interfere with the rock resistivity measurements are marked with grey.

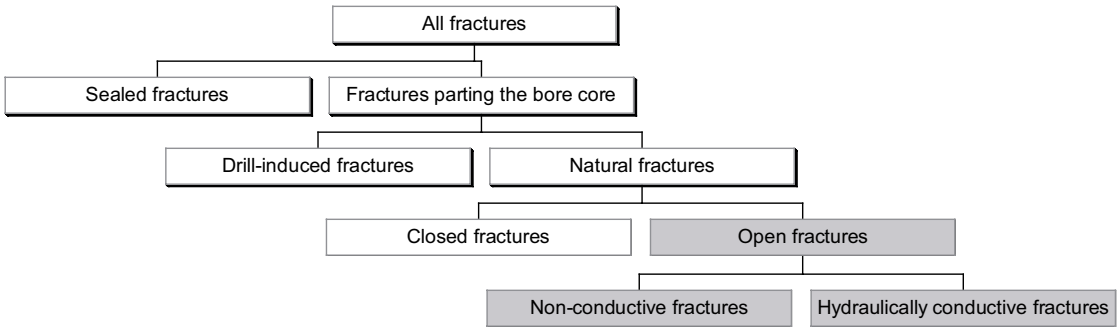

Figure 4-1. *Organization sketch of different types of fractures in-situ.*

The information of different types of fractures in-situ is obtained in the bore core logging and in the hydraulic flow logging. A fracture intersecting the borehole is most likely to part the bore core. In the core log, fractures that part the core are either natural of drill-induced fractures. Sealed fractures that do not part the core are also recorded in the core log. Laboratory results suggest that sealed fractures generally have no major interference on rock resistivity measurements. However, some fractures that are only partly sealed may influence the rock resistivity measurements.

Natural fractures are either open or closed, depending on the aperture. A fracture is closed when its aperture is so small that the amount of water it holds is comparative to that held in the adjacent porous system. In this case the "adjacent porous system" is the porous system of the rock matrix the first few centimetres from the fracture. An open fracture has a larger aperture, may be hydraulically conductive, and holds enough water to interfere with the rock resistivity measurements. Currently there is no way of obtaining the fracture aperture in the bore core log and one cannot separate open from closed fractures. Open fractures could either be hydraulically conductive or non-conducting, depending on how they are connected to the fracture network and on the hydraulic gradients of the system. Figure 4-2 shows different fractures intersecting a borehole.

In this report the rock resistivity is used to obtain formation factors of the rock surrounding the borehole. The obtained formation factors may later be used in models for radionuclide transport in fractured crystalline rock. Different conceptual approaches may be used in the models. This report aims to deliver formation factors that could be used in models based on two different conceptual approaches.

4.1.5 Rock matrix formation factor

In a common conceptual approach used in radionuclide transport modelling, the rock-groundwater system is divided into two main units. The solid and non-fractured rock constitutes one main unit and open fractures, irrespectively of their groundwater flow, constitute the other main unit. Radionuclide transport towards the biosphere will occur in open hydraulically conductive fractures, as the radionuclides are carried by the groundwater. Radionuclide retardation will occur due to diffusion into the rock matrix and interactions with the rock matrix. When modelling according to this conceptual approach the rock matrix formation factor, F_f^{rm}, is needed.

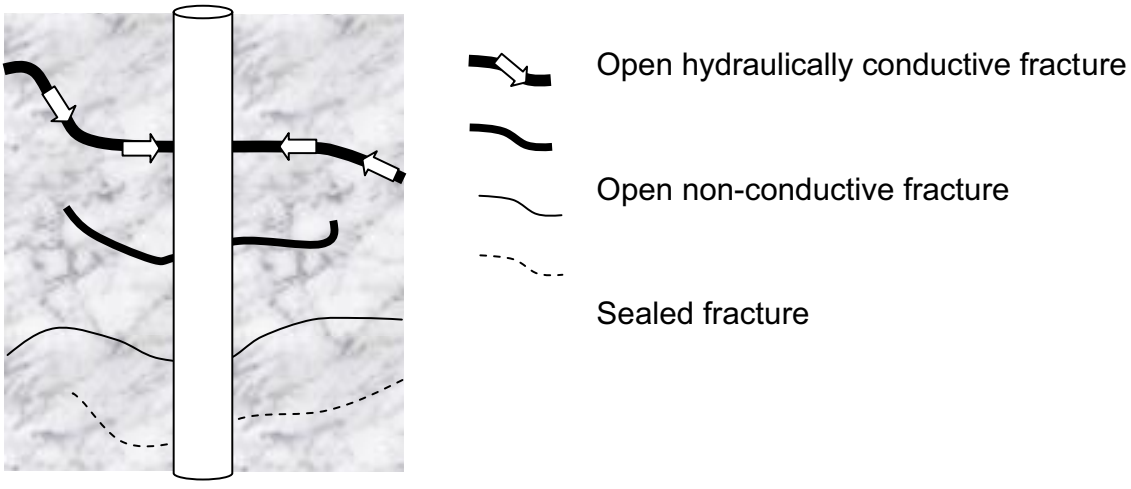

Figure 4-2. *Fractures intersecting a borehole.*

The rock matrix formation factor is obtained from rock matrix resistivity data. When obtaining the rock matrix resistivity from the in-situ measurements, all resistivity data that may have been affected by open fractures have to be sorted out. With present methods one cannot separate open from closed natural fractures in the core logging. By investigating the rock resistivity log at a fracture one could draw conclusions weather it is open or closed. However, for formation factor logging by electrical methods this in not an independent method and cannot be used. Therefore all natural fractures have to be considered as potentially open and all resistivities obtained close to of a natural fracture are sorted out.

As the current beam sent out by the in-situ rock resistivity tool has a certain thickness, a fracture can affect a measurement even if it intersects the borehole at some distance above or below the current electrode. By examining the resistivity logs obtained by the Century 9072 tool it has been found that resistivity values obtained within 0.5 m from a natural fracture generally should be sorted out. This distance includes a safety margin of 0.1–0.2 m. The resistivities remaining after the sorting process constitute a rock matrix resistivity log. In Figure 4-3, fracture subgroups marked in grey are regarded as potentially open fractures when obtaining the in-situ rock matrix formation factor.

4.1.6 Fractured rock formation factor

In an alternative conceptual approach used when modelling radionuclide transport, the rock-groundwater system is divided into two main units based on main transport mechanisms. Open hydraulically conductive fractures, where advective flow is the main transport mechanism, constitute one main unit and the porous system of the bedrock, where diffusion is the main transport mechanism, constitutes the other main unit. Here the porous system of the bedrock includes both open non-conductive fractures, closed fractures, partly sealed fractures, and the microporous network of the rock matrix.

A problem with this approach is to determine to what main unit open fractures having a very low groundwater flow should be sorted. At what water velocity is the advective transport dominant and at what velocity is the diffusive transport dominant? A practical solution to this problem is to base this sorting on the detection limit of the in-situ tool measuring the groundwater flow of specific fractures. If a groundwater flow can be detected, the fracture is hydraulically conductive and advective transport is dominant. If no groundwater flow can be detected the fracture is defined as non-conductive and diffusive transport is assumed to dominate.

The actual flow in fractures where diffusion is the dominating transport process is most likely lower than that which could be measured with current in-situ methods. However, in a performance assessment one can argue that one should only account for the flow-wetted

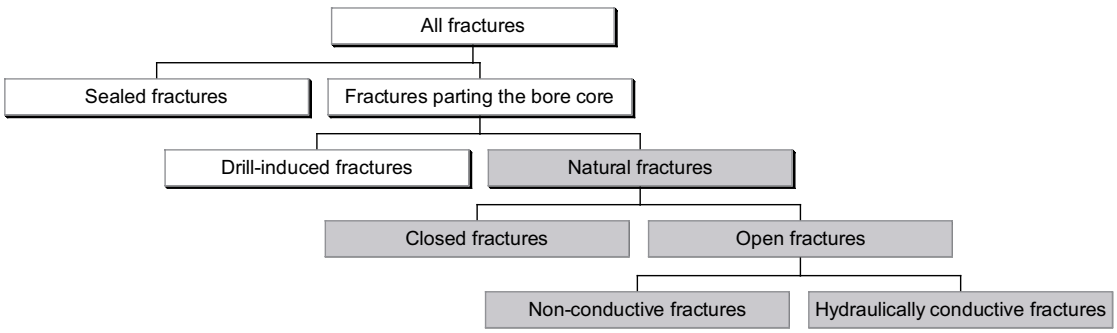

Figure 4-3. *Organization sketch of potentially open fractures in-situ.*

surface of detected hydraulically conductive fractures. The flow wetted surface describes the area of the interface between the rock matrix and hydraulically conductive fractures wherein radionuclides can be transported. It could be considered as non-conservative to include the flow-wetted surface of open fractures that have not been proved to be hydraulically conductive. If fractures where no water-flow has been measured are considered as non-conductive, retardation due to diffusion into these fractures can be accounted for.

When modelling according to this conceptual approach the fractured rock formation factor, F_f^{fr}, is needed. When obtaining the fractured rock formation factor, the fractured rock resistivity is used. Here only rock resistivity values that may have been affected by hydraulically conductive fractures are sorted out. By examining the resistivity logs obtained by the Century 9072 tool it has been found that resistivity values obtained within 0.5 m from a hydraulically conductive fracture generally should be sorted out. This distance includes a safety margin of 0.1–0.2 m.

4.2 Rock resistivity measurements in-situ

4.2.1 Uncertainties related to the equipment used

From laboratory measurements on rock samples taken from the bore cores of KSH01A and KSH02 one can expect in-situ rock matrix resistivities on the order of 10^5–10^6 ohm. m for the more resistive rock. It would not be far fetched to assume that the most resistive rock in-situ has an insignificant porous system with a limited pore connectivity. If this is the case, its resistivity would be close to that of the rock minerals. In granitic rock, mineral resistivities are on the order of 10^8–10^{14} ohm.m. At present there are no available downhole tools that can measure such high resistivities. Therefore one can always expect that a fraction of the rock in-situ has a resistivity outside the quantitative measuring range of the rock resistivity tool.

As long as this fraction is acceptably small this poses no major problem. This can be illustrated by taking an example from the borehole KLX02 in the Oskarshamn site investigation area. In this borehole a total of 15,900 in-situ rock resistivities were obtained in the borehole section 205 m to 1,000 m. Figure 4-4 shows a histogram including all these resistivities. In the histogram the resistivity interval 0–150,000 ohm.m was divided into 30 sections each one spanning over 5,000 ohm.m. This means that 8.9% of all resistivity data were in the 0–5,000 ohm.m region, 11.5% in the 5,000–10,000 ohm.m region and so forth.

The rock resistivity tool used in this campaign was the slimhole Dual-Laterolog from ANTARES Datensysteme GmbH. According to the manufacturer this tool has a high performance range from 0.1 to 50,000 ohm.m and measures resistivities quantitatively up to 200,000 ohm.m with an error not exceeding 20%. Less than 1% of the resistivities measured in the borehole section 205 m to 1,000 m exceeded 150,000 ohm.m and less than 2% exceeded 100,000 ohm.m. In order to examine the accuracy of the slimhole Dual-Laterolog a comparative study was initiated. 100 core samples from KLX02 were taken to the laboratory were resistivity measurements were performed /10/. The conclusion was that the downhole tool worked properly. This is an example of a successful logging where a great majority of the rock resistivities obtained were within the quantitative measuring range of the tool.

According to the logging company, the rock resistivity tools Century 9072 and Century 9030, which were used when logging the in-situ rock resistivity of KSH01A and KSH02,

have the quantitative measuring range 0–50,000 ohm.m. Within this range the accuracy should be within ± 5%. Outside this range the results may quickly become increasingly poor. This may manifests in a non-linear response of the obtained resistivity with increasing true rock resistivity. The highest resistivity value obtained with the Century 9072 when measuring in KSH01A and KSH02 was 78,800 ohm.m. Here the true resistivity could very well be 100,000 or 1,000,000 ohm.m, as expected from the laboratory data. The true resistivity could even be in line with the resistivity of dry rock.

As can be seen in Figure 4-4 a significant fraction of the rock surrounding KLX02 has a resistivity higher than 50,000 ohm.m. About 10% of the resistivities measured in the borehole section 205 m to 1,000 m exceeded 50,000 ohm.m.

The rock resistivity of KLX02 was also measured using the Century 9072 and Century 9030 tools prior to the measurements in KSH01A and KSH02. The result from the Century 9072 tool was not encouraging as the obtained resistivities were one order of magnitude lower than those measured with the slimhole Dual-Laterolog. The Century 9030 tool proved to be unsuited for logging in granitic rock as it suffered from flashover and delivered unreasonable rock resistivities ranging from -3×10^7 to 3×10^7 ohm.m.

The discouraging results in KLX02 lead to a modification of both the Century 9072 and Century 9030 tools. The modifications were not successful for the Century 9030 tool and therefore, it was decided not to use results from the tool in this report. The modifications of the Century 9072 tool were more successful as it started delivering reasonable values. According to the logging company the tool should perform according to specifications after the modifications, with a quantitative measuring range of 0–50,000 ohm.m. However, the same specifications were given before the measurements in KLX02 and until a calibration of the tool is made one can only speculate in the actual quantitative measuring range.

The rock surrounding the borehole section 880 m to 1,000 m of KSH01A is sparsely fractured. On average, only about one natural fracture per meter of bore core was found in the core logging. In this section 39% of the rock matrix resistivities measured by the Century 9072 tool exceeded 50,000 ohm.m. Figure 4-5 shows the resistivity log from this borehole section.

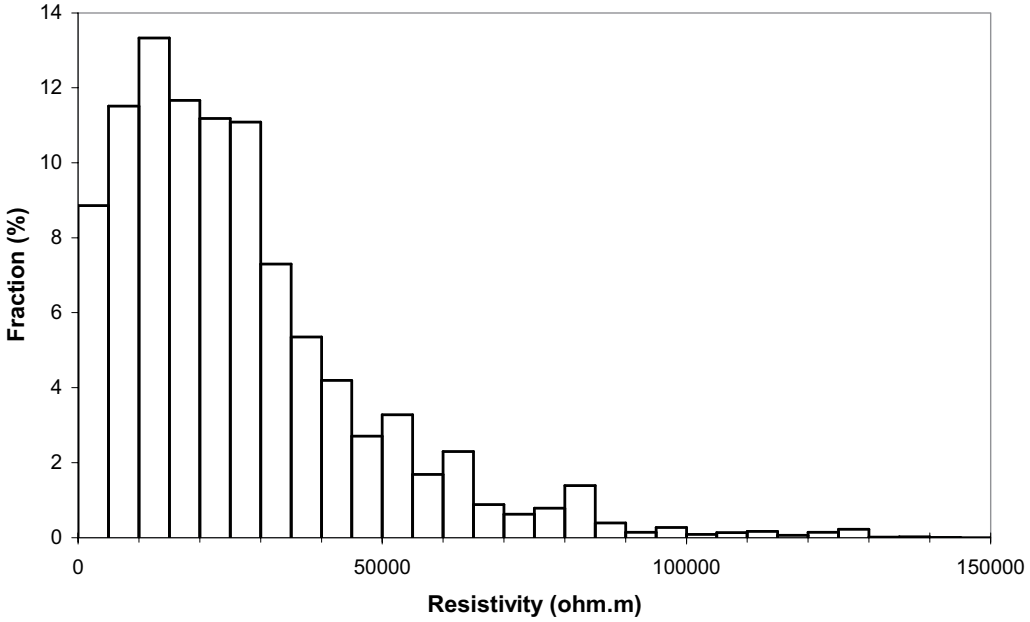

Figure 4-4. *Distribution of rock resistivities in KLX02.*

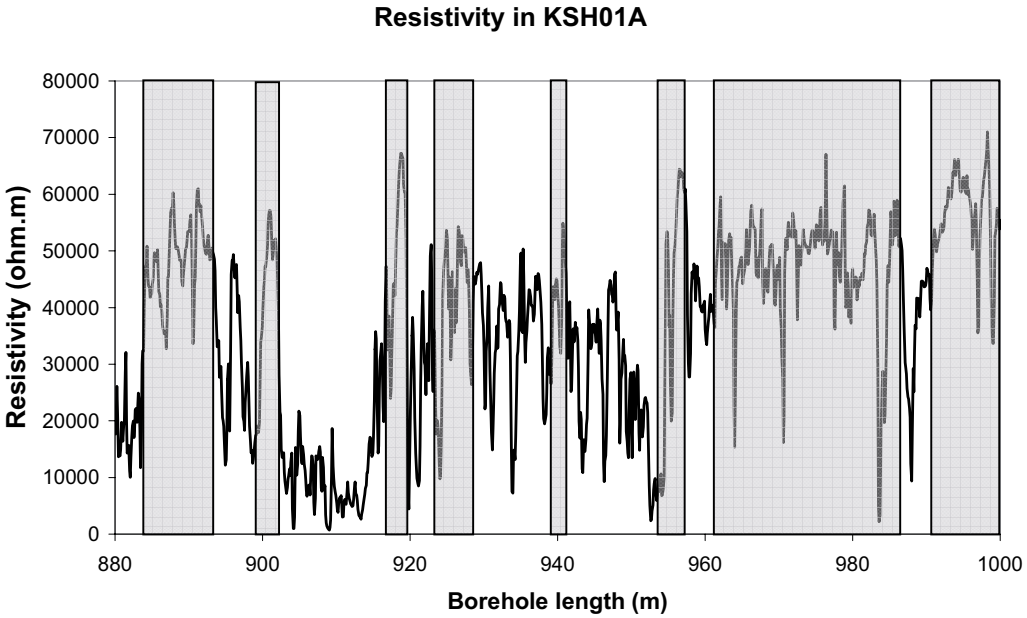

Figure 4-5. *Regions with rock resistivities exceeding 50,000 ohm.m (KSH01A).*

Here regions with rock having a resistivity around or over 50,000 ohm.m is marked with semi-transparent grey fields. It could be questioned if the tool is suitable for measurements in this type of rock.

In the remainder of this report it is assumed that the upper quantitative measuring limit of the Century 9072 tool is 50,000 ohm.m. There has been no attempt to correct or sort out rock resistivities that are higher than 50,000 ohm.m.

4.2.2 Rock resistivity log KSH01A

Rock resistivities were taken from SICADA. The resistivities were obtained in a campaign described in /1/ with the focused tool Century 9072. The borehole was logged between 0.3 and 1,002.9 m. In order to obtain an exact depth calibration the track marks made in the borehole were used. According to /1/ an exact depth calibration was not obtained. The following deviations in the calibration with depth are reported.

Table 4-1. Deviation in borehole lengths. Data from /1/.

Reference mark (m)	110	150	200	250	300	350	400	450	500
Deviation (m)	0.00	0.01	0.03	0.05	0.08	0.12	0.14	0.15	0.20
Reference mark (m)	550	600	650	700	750	800	850	899	950
Deviation (m)	0.20	0.25	0.28	0.26	0.28	0.34	0.35	0.39	0.42

The deviation is fairly linear with the borehole length. The borehole length reported in /1/ was corrected between 110–1,002.9 m by subtracting the deviations obtained by the linear equation shown in Figure 4-6.

In Figure 4-6 the borehole length is according to the reference marks. No correction in reported borehole length was made between 0–110 m.

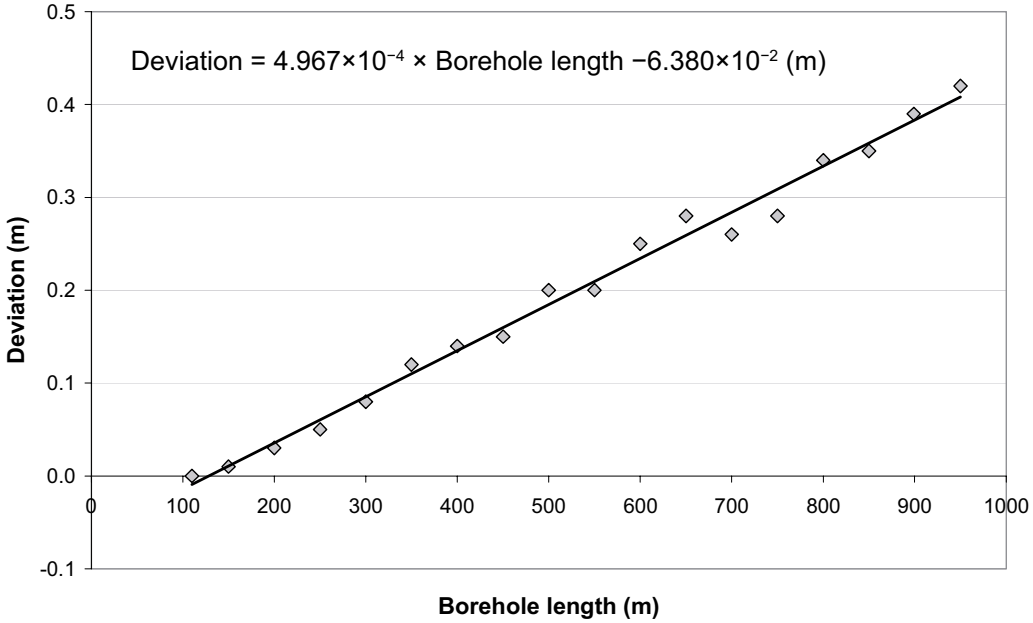

Figure 4-6. *Deviations in borehole length in KSH01A.*

4.2.3 Rock matrix resistivity log KSH01A

After adjusting the borehole length of the rock resistivity log, all resistivity data obtained within 0.5 m from a natural fracture detected in the core log were sorted out. For the core log, no correction in the reported borehole length was needed. In the core log a total of 3,046 natural fractures are recorded. In addition 7 crush zones and one zone where the core is lost are recorded. A total of 2.6 m of the core is crushed or lost. Natural fractures can potentially intersect the borehole in zones where the core is crushed of lost. Therefore, a natural fracture every decimetre was assumed in these zones. The locations of natural fractures in KSH01A are shown in Appendix B1. A total of 1,290 rock matrix resistivities were obtained between 103–1,001 m, where 1,037 values (80%) were within the quantitative measuring range of the Century 9072 tool. The rock matrix resistivity log between 103–1,001 m is shown in Appendix B1.

Figure 4-7 shows a histogram of the rock matrix resistivities obtained between 103–1,001 m in KSH01A. The histogram range from 0–100,000 ohm.m and is divided into sections of 5,000 ohm.m.

4.2.4 Fractured rock resistivity log KSH01A

After adjusting the borehole length of the rock resistivity log, all resistivity data obtained within 0.5 m from a hydraulically conductive fracture detected in the difference flow logging /3/ were sorted out. For the difference flow log, no correction in the reported borehole length was needed. A total of 82 hydraulically conductive fractures were detected in KSH01A. The locations of hydraulically conductive fractures in KSH01A are shown in Appendix B1. A total of 8,271 fractured rock resistivities were obtained between 103–1,001 m where 7,707 values (93%) were within the quantitative measuring range of the Century 9072 tool. The fractured rock resistivity log between 103–1,001 m is shown in Appendix B1.

Figure 4-8 shows a histogram of the fractured rock resistivities obtained between 103–1,001 m in KSH01A. The histogram range from 0–100,000 ohm.m and is divided into sections of 5,000 ohm.m.

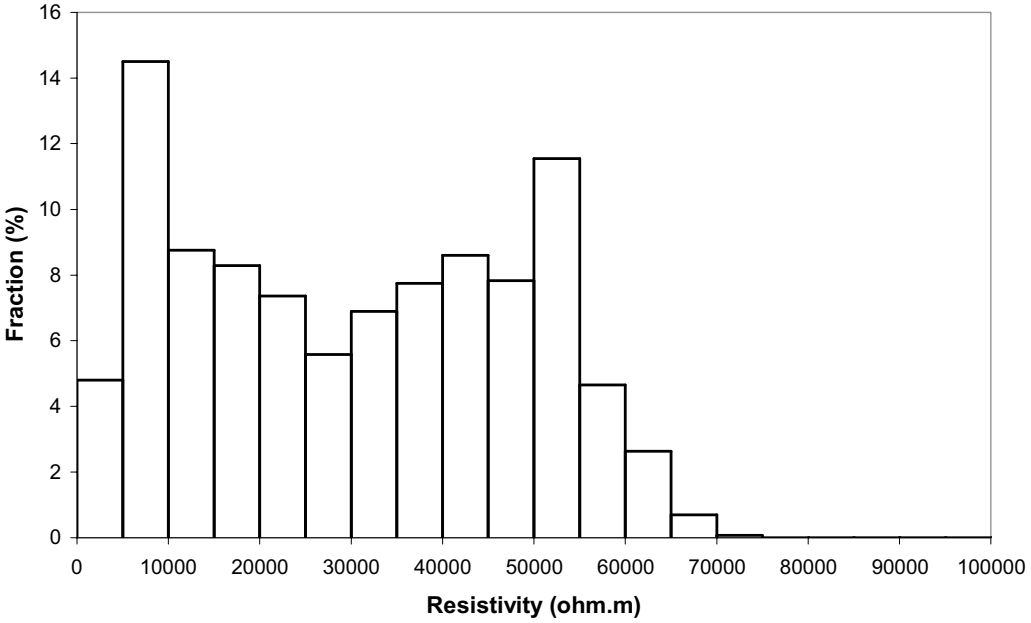

Figure 4-7. *Histogram of rock matrix resistivities in KSH01A.*

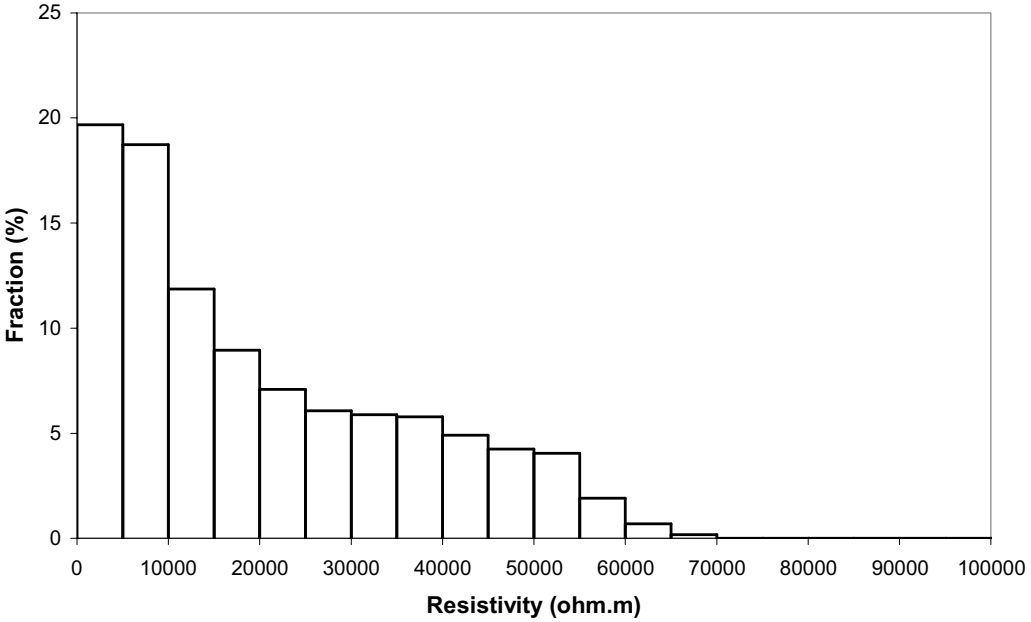

Figure 4-8. *Histogram of fractured rock resistivities in KSH01A.*

4.2.5 Rock resistivity KSH02

Rock resistivities were taken from SICADA. The resistivities were obtained in a campaign described in /2/ with the focused tool Century 9072. The borehole was logged between 78.1 and 1,001.7 m. In order to obtain an exact depth calibration, the track marks made in the borehole were used. According to /2/ an exact depth calibration was not obtained. The following deviations in the calibration with depth are reported.

Table 4-2. Deviation in borehole lengths. Data from /2/.

Reference mark (m)	105	153	203	256	317	362	415	468	519
Deviation (m)	0.00	0.01	0.07	0.09	0.14	0.17	0.19	0.24	0.28
Reference mark (m)	571	624	674	727	780	830	852	900	950
Deviation (m)	0.28	0.39	0.40	0.43	0.46	0.50	0.55	0.56	0.61

The deviation is fairly linear with the borehole length. The borehole length reported by /2/ was corrected between 105–1,001.7 m by subtracting the deviations obtained by the linear equation shown in Figure 4-9:

In Figure 4-9 the borehole length is according to the reference marks. No correction in the reported borehole length was made between 0–105 m.

4.2.6 Rock matrix resistivity log KSH02

After adjusting the borehole length of the rock resistivity log, all resistivity data obtained within 0.5 m from a natural fracture detected in the core log were sorted out. For the core log no correction in the reported borehole length was needed. In the core log a total of 4,971 natural fractures are recorded. In addition 37 crush zones and 12 zones where the core is lost are recorded. A total of 21 m of the core is crushed or lost. Natural fractures can potentially intersect the borehole in zones where the core is crushed of lost. Therefore, a natural fracture was assumed every decimetre in these zones. The locations of natural fractures in KSH02 are shown in Appendix B2. A total of 577 rock matrix resistivities were obtained between 81–999 m. All values were within the quantitative response limits of the Century 9072 tool. The rock matrix resistivity log between 81–999 m is shown in Appendix B2.

Figure 4-10 shows a histogram of the rock matrix resistivities obtained between 81–999 m in KSH02. The histogram range from 0–100,000 ohm.m and is divided into sections of 5,000 ohm.m.

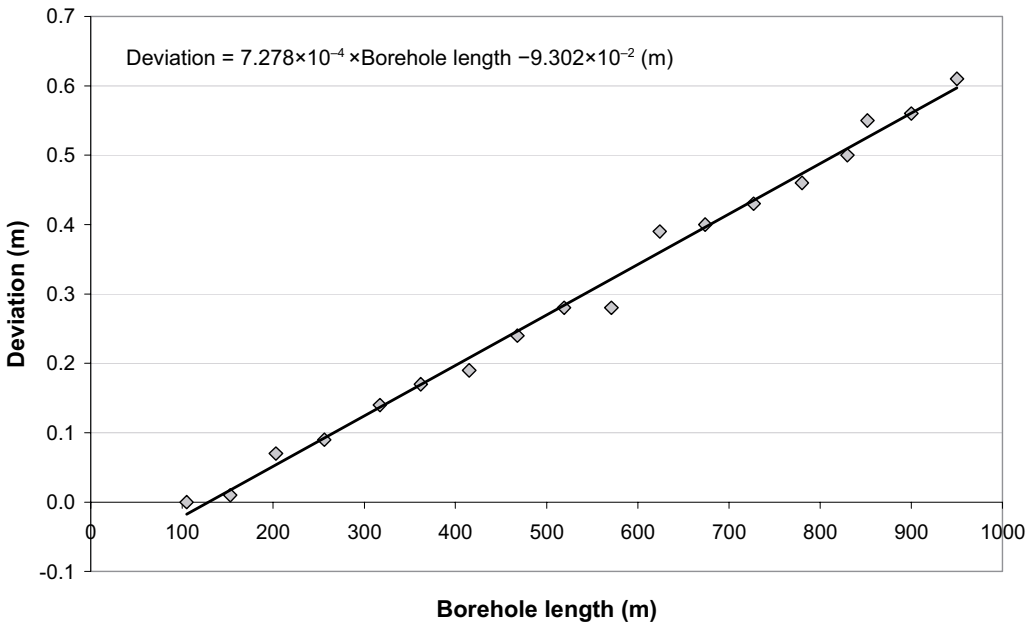

Figure 4-9. *Deviations in borehole length in KSH02.*

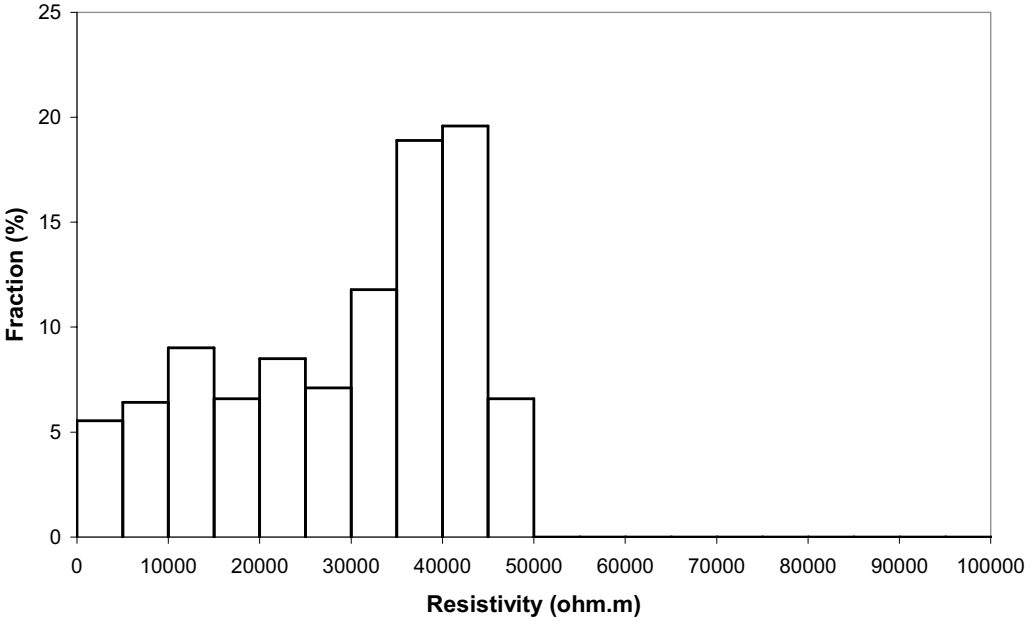

Figure 4-10. *Histogram of rock matrix resistivities in KSH02.*

4.2.7 Fractured rock resistivity log KSH02

After adjusting the borehole length of the rock resistivity log, all resistivity data obtained within 0.5 m from a hydraulically conductive fracture detected in the difference flow logging /4/ were sorted out. For the difference flow log, no correction in the reported borehole length was needed. A total of 82 hydraulically conductive fractures were detected in KSH02. The locations of hydraulically conductive fractures in KSH02 are shown in Appendix B2. A total of 8,494 fractured rock resistivities were obtained between 81–999 m, where 8,476 values (99.8%) were within the quantitative measuring range of the Century 9072 tool. The fractured rock resistivity log between 81–999 m is shown in Appendix B2.

Figure 4-11 shows the distribution of the fractured rock resistivities obtained between 81–999 m in KSH02. The histogram range from 0–100,000 ohm.m and is divided into sections of 5,000 ohm.m.

4.3 Groundwater EC measurements in-situ

4.3.1 EC measurements in KSH01A

The EC (electrical conductivity) of groundwater extracted from fractures was measured in the hydrogeochemical program. In the first run of measurements, the borehole section 156.5 to 167 m was sealed off. By pumping at the surface, groundwater could be extracted from the fractures in this section. Figure 4-12 shows the EC obtained. A number of measurements were made each day. Initially the section was filled with borehole fluid, which explains the increase in EC the first few days of the pumping as the section was increasingly filled with groundwater from the fractures. A fairly stable value around 1.56 S/m was obtained. It was assumed that the EC of the groundwater at 161.75 m was 1.56 S/m.

In the second run of measurements the borehole section 245 to 261.5 m was sealed off. A fairly stable value around 1.79 S/m was obtained (Figure 4-13). It was assumed that the EC of the groundwater at 253.25 m was 1.79 S/m.

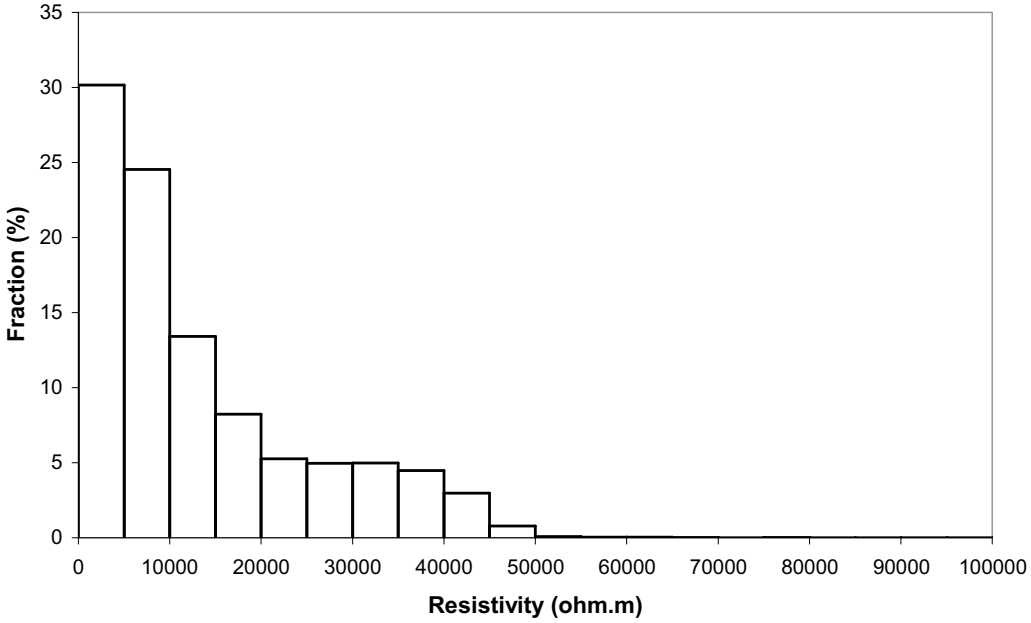

Figure 4-11. *Histogram of fractured rock resistivities in KSH02.*

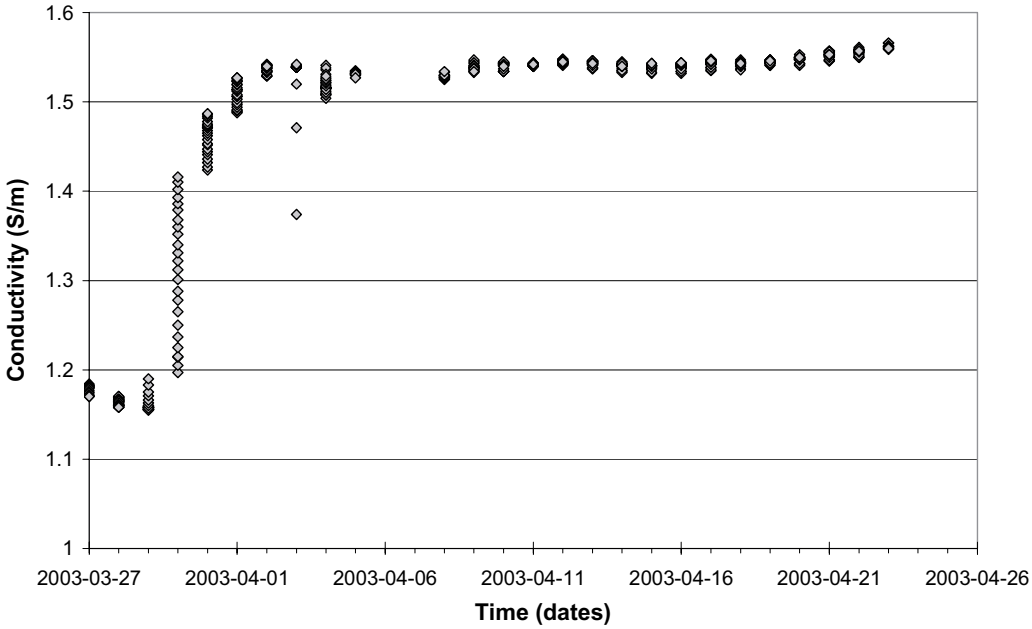

Figure 4-12. *EC obtained in the hydrogeochemical program in section 156.5 to 167 m in KSH01A.*

In the third run of measurements the borehole section 548 to 656 m was sealed off. However, due to problem with leakage of borehole fluid into the section the only conclusion that could be drawn from this experiment is that the groundwater had an EC of at least 1 S/m.

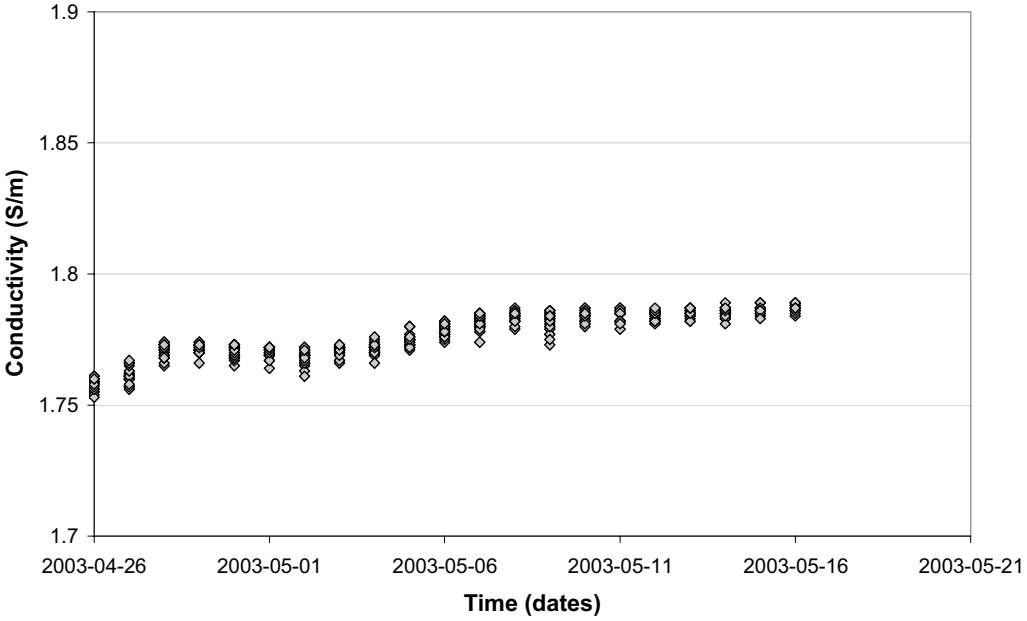

Figure 4-13. *EC obtained in the hydrogeochemical program in section 245 to 261.5 m in KSH01A.*

The EC of the borehole fluid in KSH01A was logged between the borehole lengths 22.9 and 998.2 m using the POSIVA difference flow meter /3/. The borehole fluid was first logged before beginning extensive pumping associated with the flow-logging and this borehole fluid EC is shown in Figure 4-14 as the black solid line. The borehole fluid EC was also logged after the extensive pumping that is shown as the solid grey line in Figure 4-14.

The borehole fluid EC is decreasing at the end of the borehole. This is due to the fact that very little groundwater flows in or out of fractures in this section and that cooling water from the drilling still remains in the borehole. The two diamonds in Figure 4-14 is the obtained groundwater ECs from the hydrogeochemical campaign. The triangles shows the groundwater flow from specific fractures obtained in the difference flow measurements using a drawdown /3/. The groundwater flow axis is on the right in Figure 4-14. In the lower 275 m of the borehole there is virtually no flow of groundwater from fractures. The peak in the solid grey line at 688 m therefore indicate that groundwater flowing out of the fractures at this depth has an EC of at least 1.31 S/m. As can be seen from Figure 4-14 the flow out of the fractures in this section of the borehole is not that great. Therefore the cooling water from the drilling might to some extent influence this value. The peaks at 553 and 593 indicate groundwater ECs of at least 1.74 and 1.59 S/m respectively. The flow out from fractures in this section of the borehole is greater and therefore, the cooling water from the drilling probably influences the obtained groundwater ECs less. The five EC values indicated in Figure 4-14 by circles were used when predicting a groundwater EC profile in KSH01A.

4.3.2 EC measurements in KSH02

A number of fracture specific groundwater ECs were obtained from KSH02 by extracting water from specific fractures using the POSIVA difference flow meter /4/. The tool is lowered down to a specific fracture and the fracture specific EC is measured. By also measuring the groundwater flow out of the fracture it is calculated how long time it will take to fill up the sealed off borehole section three times. After this time it is assumed

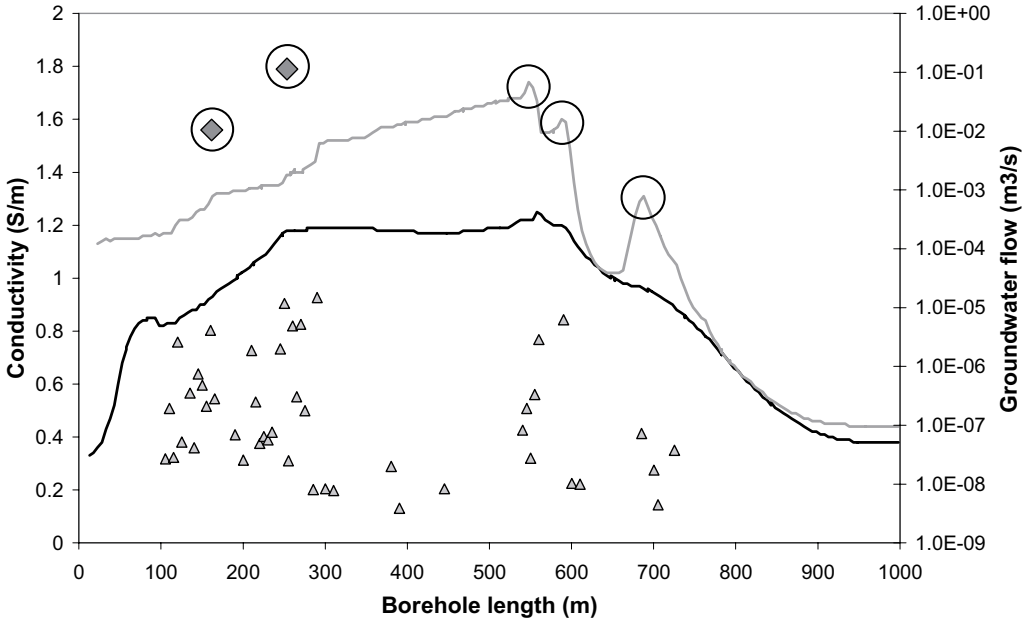

Figure 4-14. *Groundwater EC in KSH01A.*

that the measured EC is representative for the groundwater coming out of the fracture. Figure 4-15 shows the transient EC profile obtained at a fracture located at the borehole length of 99.3 m.

The dashed line represents the borehole fluid EC obtained with the difference flow meter after extensive pumping. When moving the tool borehole fluid usually leaks into the sealed off section. Therefore, one can expect that the initial water in the section is a mixture of borehole fluid and fracture specific ground water from the latest measurement. The profile in Figure 4-15 indicates that the measurement was successful.

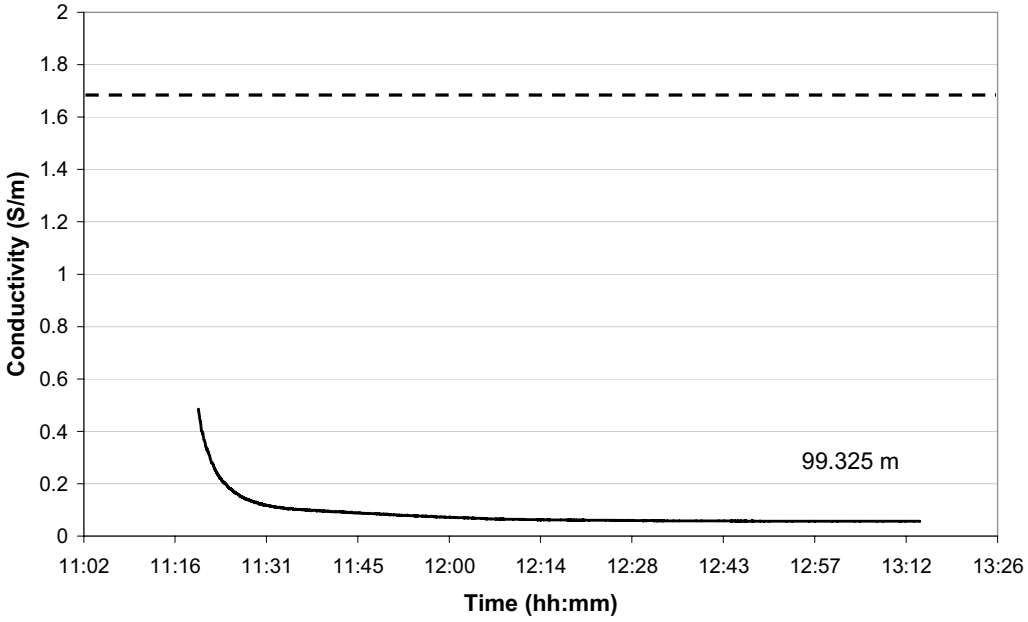

Figure 4-15. *Transient fracture specific EC profile.*

A major leakage of borehole fluid into the section is indicated by an obtained fracture specific EC close to the borehole fluid EC. A small leakage that varies with time is indicated by peaks and dips in the transient profile. Development of gas due to the pressure drop at the borehole-rock interface is indicated by a transient profile that fluctuates. A small constant leakage into the sealed off section can be hard to detect. On the other hand such a small leakage is not of major significance. Still it is a somewhat subjective and difficult task of obtaining the fracture specific EC.

The profiles and interpretations of 15 transient fracture specific EC profiles are presented in Appendix B3. The borehole fluid after extensive pumping in KSH02 is shown in Appendix B4. Figure 4-16 shows the suggested groundwater EC profiles for KSH01A and KSH02. For comparison the groundwater EC profile for KLX02 taken from /10/ is shown.

It could be questioned if the true groundwater EC profile of KSH01A decreases with depth. A constant EC or an EC profile that is slightly increasing with borehole depth would maybe have been more reasonable. However, comparing with the variation in rock resistivities, which range over three orders of magnitude, the variations of the groundwater ECs are small. It was assumed that the groundwater EC profile of KSH01A could be described by the linear equation:

$$EC\ (S/m) = -3.96\times10^{-4} \times \text{Borehole length (m)} + 1.78 \qquad 4\text{-}4$$

within the borehole region 103–1,001 m. Furthermore it was assumed that the groundwater EC profile of KSH02 could be described by the linear equation:

$$EC\ (S/m) = -6.25\times10^{-3} \times \text{Borehole length (m)} + -5.09\times10^{-1} \qquad 4\text{-}5$$

within the borehole region 100–999 m. The borehole EC in the region 81–100 m of KSH02 was assumed to be constant at 0.057 S/m. Down to about 180 m in KSH02 one can expect to have problems with surface conduction when obtaining formation factors by electrical methods, as the groundwater has a low ionic strength.

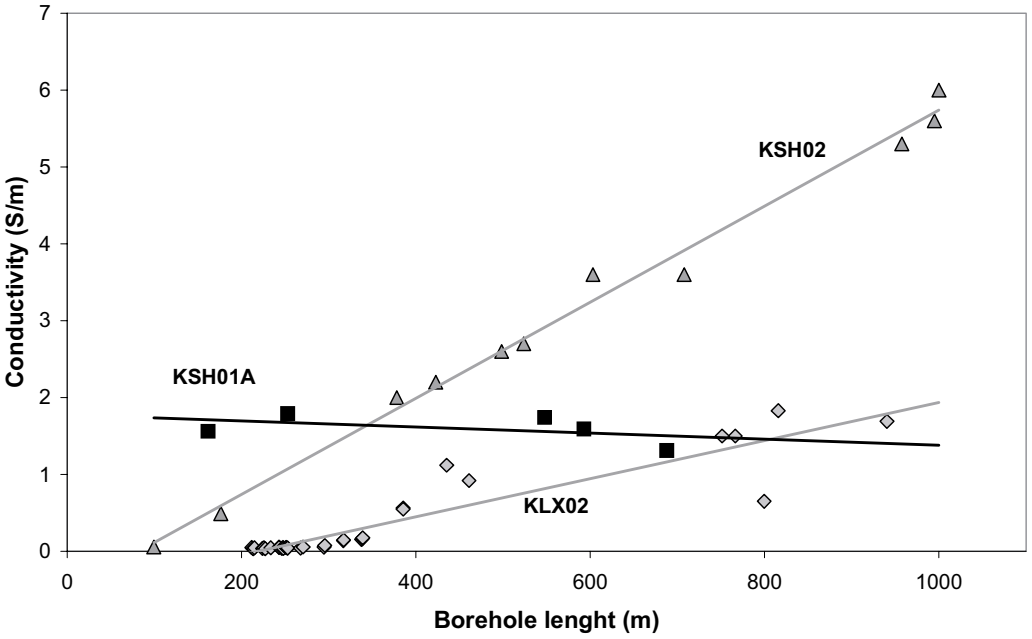

Figure 4-16. *Groundwater EC profiles in the Oskarshamn site investigation area.*

4.3.3 Electrical conductivity of the pore water

The rock surrounding KSH01A and KSH02 is very fractured. On average four natural fractures part every meter of bore core. From the rock resistivity log one can see that a substantial fraction of the natural fractures are open. If assuming that only 10% of the natural fractures are open a typical block of solid rock would be 2–3 m wide. Even the centre of such a block would be fairly well equilibrated with non-sorbing solutes in a 1,000 years perspective. The rock resistivity log suggests that most of the blocks are smaller. A one-meter wide block could be fairly well equilibrated in a 100 years perspective.

At depth, groundwater in fairly large hydraulically conductive fractures or fracture zones is thought to have a flow velocity of a few meters per year /11/. However, the amount of water that is held by hydraulically conductive fractures is very small comparing to amount of water in the pores. Therefore, this water soon becomes equilibrated with the pore water of the surrounding rock. For this reason one can expect to find an EC profile of the groundwater that is slowly and continuously increasing or decreasing with borehole length. One can also expect that this profile would not undergo major changes in a 1,000 years perspective, except during special events such as certain phases of a glacial period.

As the EC profiles of the groundwater of KSH01A and KSH02 are slowly and continuously increasing or decreasing with borehole length, it is reasonable to assume that the pore water generally is fairly well equilibrated with the free groundwater surrounding the rock.

4.4 Formation factor measurements in the laboratory

The laboratory work was performed by Chemical Engineering and Technology at the Royal Institute of Technology in Stockholm, Sweden, during the time period from the 12th of January to the 24th of May 2004.

4.4.1 Samples

The formation factors of 45 and 38 rock samples from KSH01A and KSH02 respectively were obtained by electrical methods in the laboratory. The sample lengths and diameters were measured with a Vernier caliper and the results are shown in Appendix A2 and A4. Generally the sample length was 30 mm and the diameter 50 mm. The sample taken from the bore core of KSH01A with the upper borehole length 420.77 m was damaged, as some of the rock was chipped off. It was assessed that this influenced the results by about 5% and this was corrected for. The other samples were intact even though some were intersected by small fractures.

4.4.2 Sample preparation

The samples were dried for 24 hours at a temperature of 110°C. When the samples had cooled to room temperature their cylinder surfaces were covered with silicon polymer sealant. This is to prevent the pore water from evaporating during the measurements and to prevent short-circuiting in a solution film on the sample edges. The silicon polymer sealant was allowed to dry for a few days.

4.4.3 Sample saturation

The samples were saturated with a 1.00 M NaCl solution by the vacuum method described in e.g. /8/. The samples were placed in a desiccator above the NaCl solution. The air was evacuated. The gas in the pore was allowed to equilibrate for 3 hours and after this period water vapour at a low pressure had diffused into the porous system. The samples were then shaken down in the NaCl solution. After at least 3 hours the pressure was increased. The pressure increase had duration of at least 30 minutes. The samples were then stored in a 1.00 M NaCl solution for up to 15 weeks for further saturation and equilibration at atmospheric pressure. The desiccator only allowed for saturation of maximum 12 samples in each run. The dates of saturation for the samples are shown in Appendix A1.

4.4.4 Resistivity measurements

The rock resistivity was measured by connecting copper electrodes to the exposed ends of the saturated samples. To ensure good contact, porous filters soaked in electrolyte were placed between the rock and the electrodes. When measuring the rock resistivity, alternating current with a frequency of 94 Hz was used. To be correct the resistance of the rock was measured. The resistivity was then obtained from the resistance and the dimensions of the sample. Each measurement had duration of about 1 minute. Each sample was measured two times with an hour passing between the measurements.

To investigate the degree of saturation, the resistivities of the samples were measured on more than one occasion. The resistivities of the samples from KSH01A were measured after approximately 7, 10 and, 15 weeks of saturation and equilibration at atmospheric pressure. The resistivities of the samples from KSH02 were measured after approximately 7 and 10 weeks of saturation and equilibration at atmospheric pressure. The resistances obtained in the measurements are shown in Appendix A2 and A4. Figure 4-17 shows the degree of saturation of the samples from KSH01A after 7 and 10 weeks. Here it is assumed that the samples were fully saturated after 15 weeks. This assumption could be questioned. On the x-axis of Figure 4-17, the formation factor obtained after 15 weeks of saturation and equilibration at atmospheric pressure is shown.

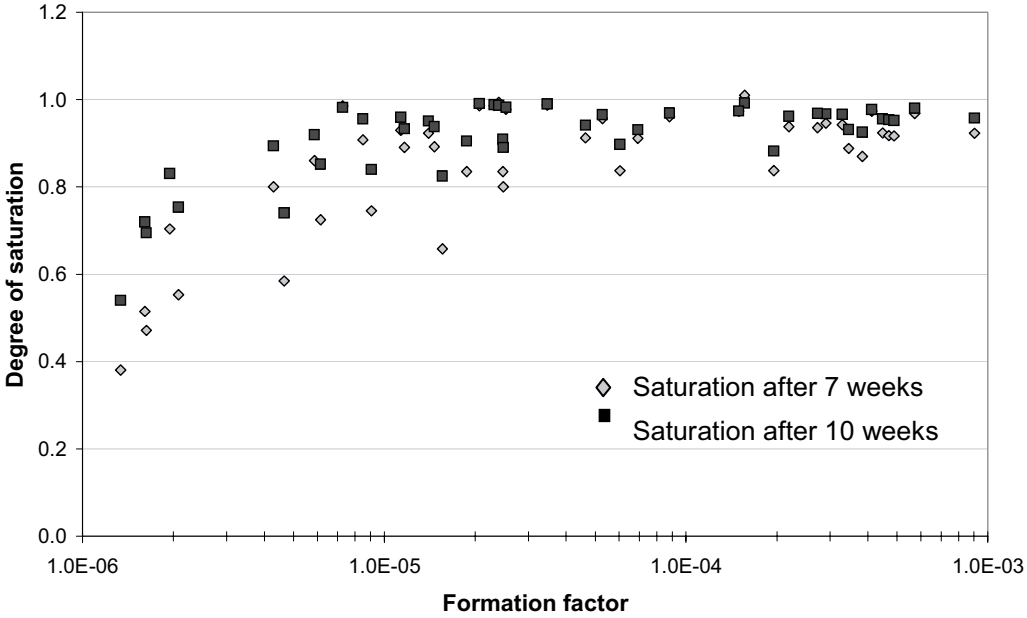

Figure 4-17. *Degree of saturation and equilibration of samples from KSH01A.*

In Figure 4-17 one can see that it is difficult to saturate rock with a very low formation factor. Also the saturation and equilibration at atmospheric pressure is a quite slow process. For future work it is recommended to increase the time of raising the pressure in the vacuum saturation and to decrease the time for saturation and equilibration at atmospheric pressure.

The electrical conductivity and temperature of the 1.00 M NaCl saturation and equilibration solutions were measured when measuring the rock resistivities. The electrical conductivities were quite stable but varied with temperature. The results are shown in Appendix A3 and A5.

4.4.5 Laboratory formation factors

The formation factors were obtained after 15 and 10 weeks of saturation and equilibration at atmospheric pressure for the samples from KSH01A and KSH02 respectively. It was assumed that the samples were fully saturated and that the pore water was in equilibrium with the surrounding 1.00 M NaCl solution. It was also assumed that the samples held the same temperature as the surrounding 1.00 M NaCl solution.

5 Results

5.1 General comments

During the review process it was discovered that the nomenclature for fractures had been changed, and that the evaluation of the in-situ formation factor was based on "old" nomenclature (cores had also been remapped). This could imply minor uncertainties in the statistics of the reported "rock matrix formation factors", since data have been excluded. However, since the data still are judged useful (e.g. as indications of spatial variability) and a re-analysis will take some time, it was decided to publish this report and then evaluate the effects as a separate activity

5.2 Laboratory formation factor

The formation factors obtained in the laboratory are tabulated in Appendix A6 and A7 for KSH01A and KSH02 respectively. Figure 5-1 shows the distributions of the formation factor in KSH01A (upper graph) and KSH02 (lower graph). The $\log_{10}$-normal distribution is used.

As can be seen in Figure 5-1 the obtained formation factors range over three to four orders of magnitude and are fairly well log-normally distributed. The mean values and standard deviations of the curves are shown in Table 5-1 and Table 5-2. The laboratory formation factor logs of KSH01A and KSH02 are shown in Appendix C1 and C2 respectively, as compared to the in-situ formation factor logs.

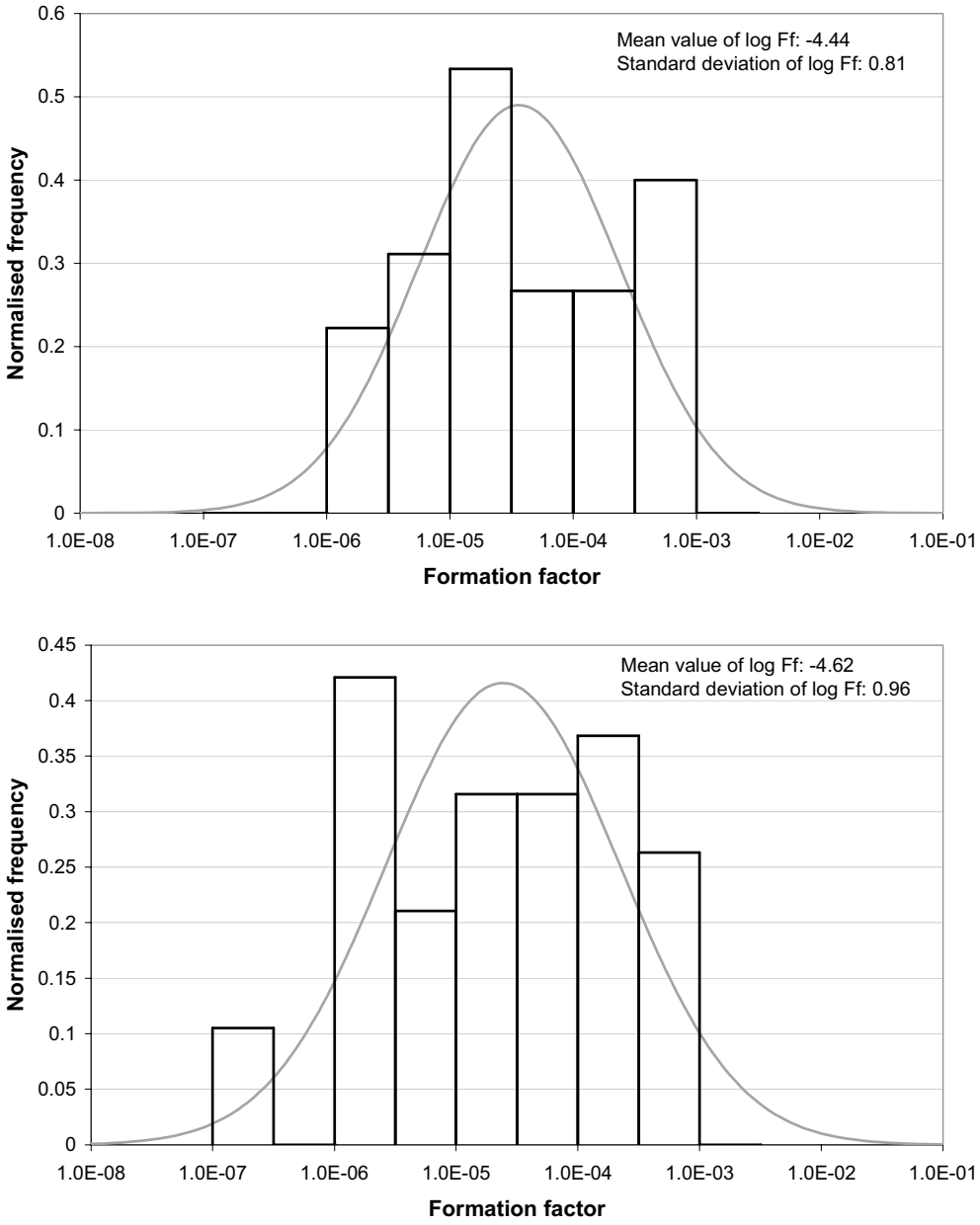

Figure 5-1. *Distribution of laboratory formation factors in KSH01A and KSH02.*

5.3 In-situ rock matrix formation factor

Figure 5-2 shows the distributions of the rock matrix formation factor obtained in-situ in KSH01A (upper graph) and KSH02 (lower graph). The $\log_{10}$-normal distribution is used.

As discussed previously, the results are non-conservative for the lower formation factors due to limitations in the quantitative measuring range of the in-situ rock resistivity tool. By using the normal-score method, as described in /12/, to determine the likelihood that a set of data is normally distributed, the median value and standard deviation of the logarithm of the formation factors could be obtained. In doing this, formation factors affected by the limitations in the in-situ rock resistivity measurements were not used. The median values and standard deviations of the curves are shown in Table 5-1 and Table 5-2. The in-situ rock matrix formation factor logs of KSH01A and KSH02 are shown in Appendix C1 and C2 respectively. Rock type specific histograms of the rock matrix formation factor are shown in Appendix D1 and D3 for KSH01A and KSH02 respectively.

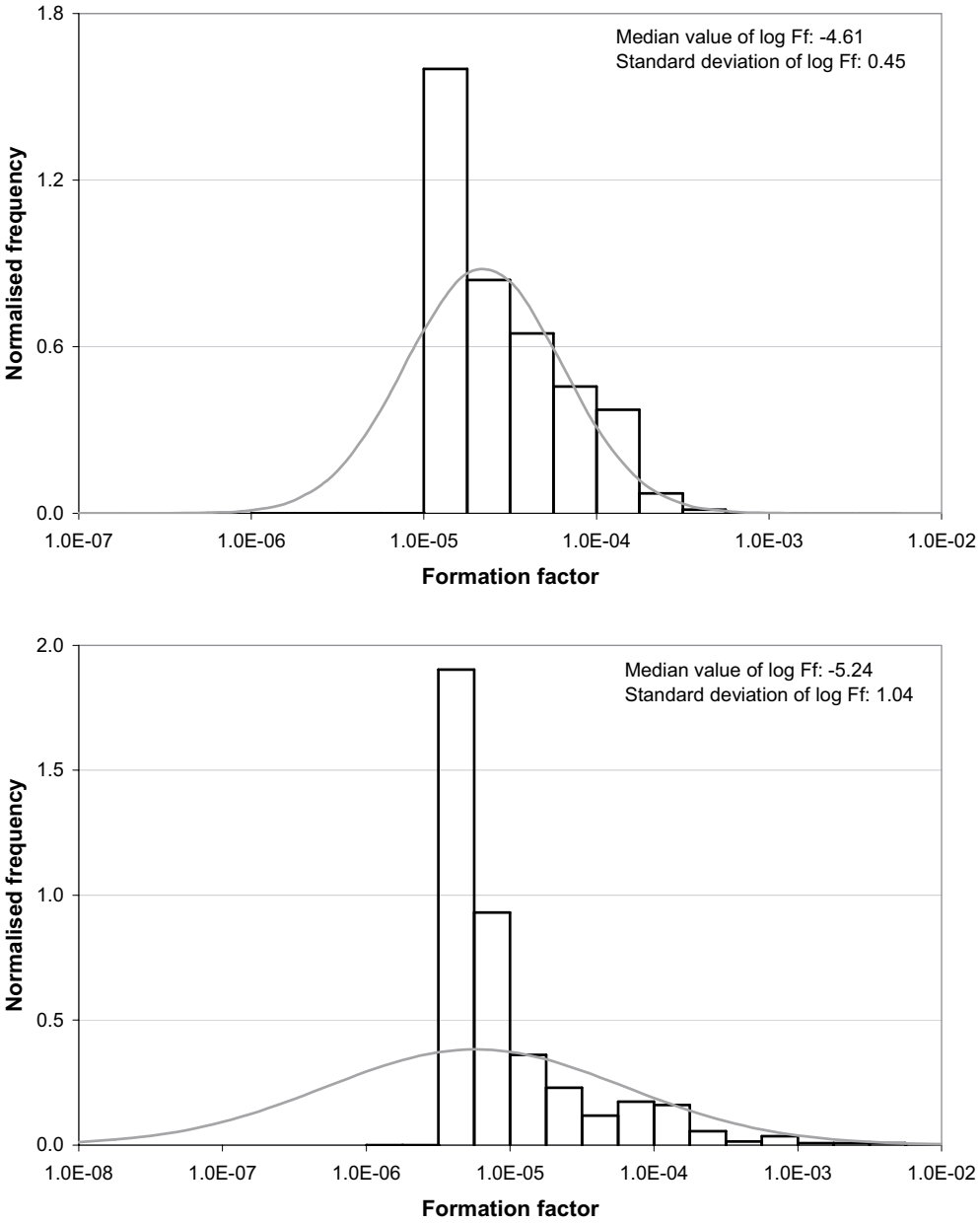

Figure 5-2. *Distribution of in-situ rock matrix formation factors in KSH01A and KSH02.*

5.4 In-situ fractured rock formation factor

Figure 5-3 shows the distributions of the fractured rock formation factor obtained in-situ in KSH01A (upper graph) and KSH02 (lower graph). The $\log_{10}$-normal distribution is used.

The normal-score method was used to determine the likelihood that the logarithms of the formation factors were normally distributed. The median values and standard deviations of the curves are shown in Table 5-1 and Table 5-2. The in-situ fractured rock formation factor logs of KSH01A and KSH02 are shown in Appendix C1 and C2 respectively. Rock type specific histograms of the fractured rock formation factor are shown in Appendix D2 and D4 for KSH01A and KSH02 respectively.

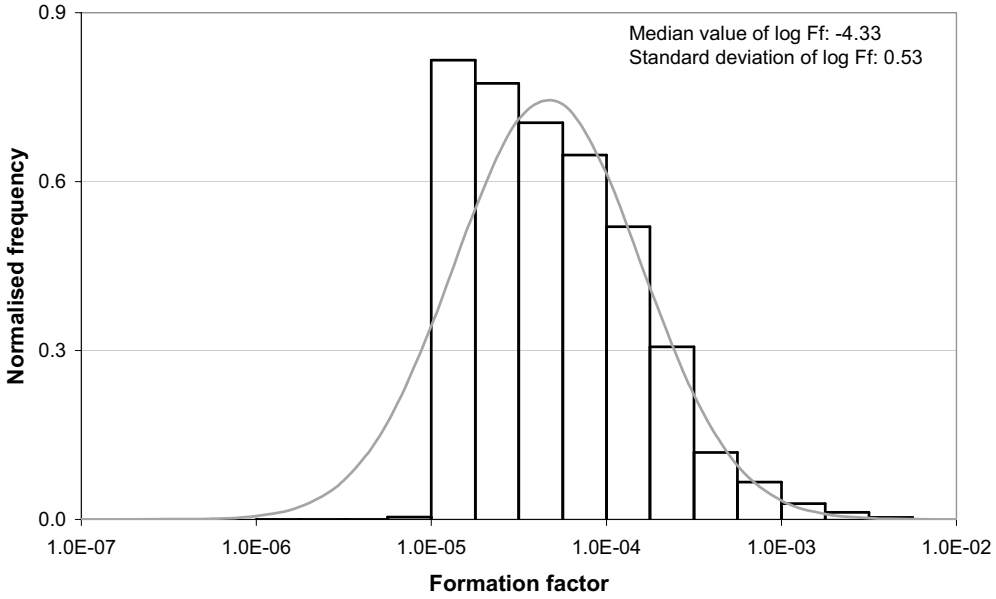

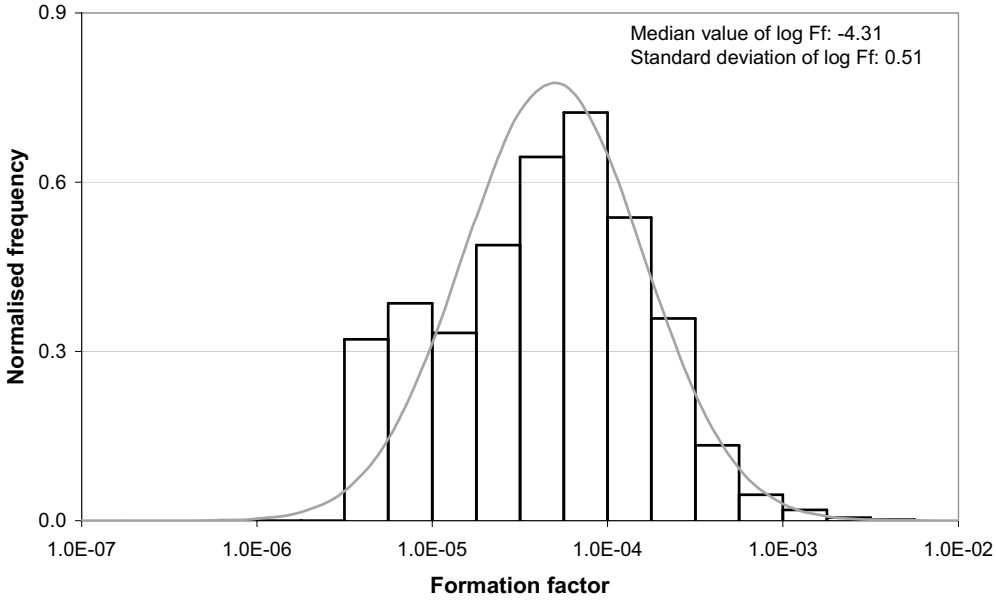

Figure 5-3. *Distribution of in-situ fractured rock formation factors in KSH01A and KSH02.*

5.5 Comparison of formation factors of KSH01A

Figure 5-4 shows the histograms of the laboratory formation factor, in-situ rock matrix formation factor, and in-situ fractured rock formation factor obtained in KSH01A.

In Figure 5-4 one can see the effect of the limited quantitative measuring range of the rock resistivity tool used. Practically no in-situ formation factors below 1.0×10^{-5} could be obtained. The effect is clearly visible, as the electrical conductivity of the groundwater in KSH01A was fairly constant.

Table 5-1 shows mean or median values and the standard deviations of the log-normal distributions for KSH01A. Median values are used when formation factors have been excluded when obtaining the distributions.

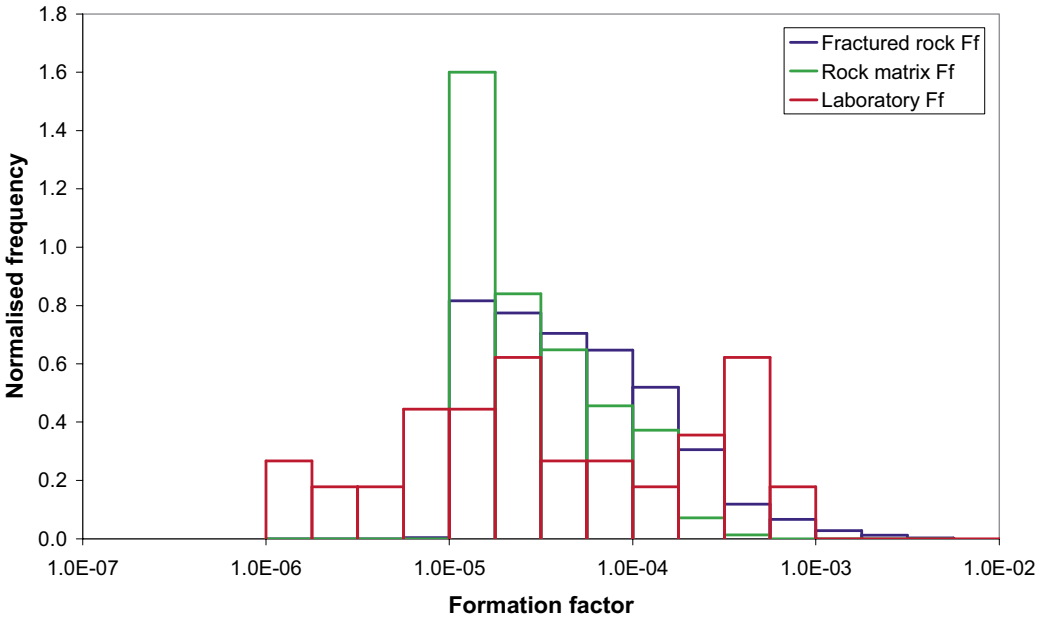

Figure 5-4. *Histograms of formation factors in KSH01A.*

Table 5-1. Data for log-normal distribution, KSH01A.

	Mean log (Ff)	Median log (Ff)	Standard deviation log (Ff)
Laboratory Ff	–4.44		0.81
In-situ Rock matrix Ff		–4.61	0.45
In-situ Fractured rock Ff		–4.33	0.53

Table 5-1 shows that the log-normal distribution obtained from the laboratory data corresponds well with those obtained from the in-situ data. It is recommended to base a comparison of the laboratory and in-situ methods on such data as shown in Table 5-1. An alternative comparison could be made if comparing each laboratory formation factor with the in-situ rock matrix formation factor obtained at a corresponding depth. Such a comparison is tabulated in Appendix C3. The laboratory formation factor from a certain borehole length was compared to the mean value of the in-situ rock matrix formation factors taken from within 0.5 m of that borehole length. However, it is hard to evaluate the result, as the samples sizes differs that much and the rock on the Simpevarp peninsula is so lithologically inhomogeneous. The laboratory sample size is on the order of 10^{-5} m^3 while the in-situ samples size is on the order of 10^{0} m^3.

5.6 Comparison of formation factors of KSH02

Figure 5-5 shows the distributions of laboratory formation factor, in-situ rock matrix formation factor, and in-situ fractured rock formation factor obtained in KSH02.

Table 5-2 shows mean or median values and the standard deviations of the log-normal distributions for KSH02.

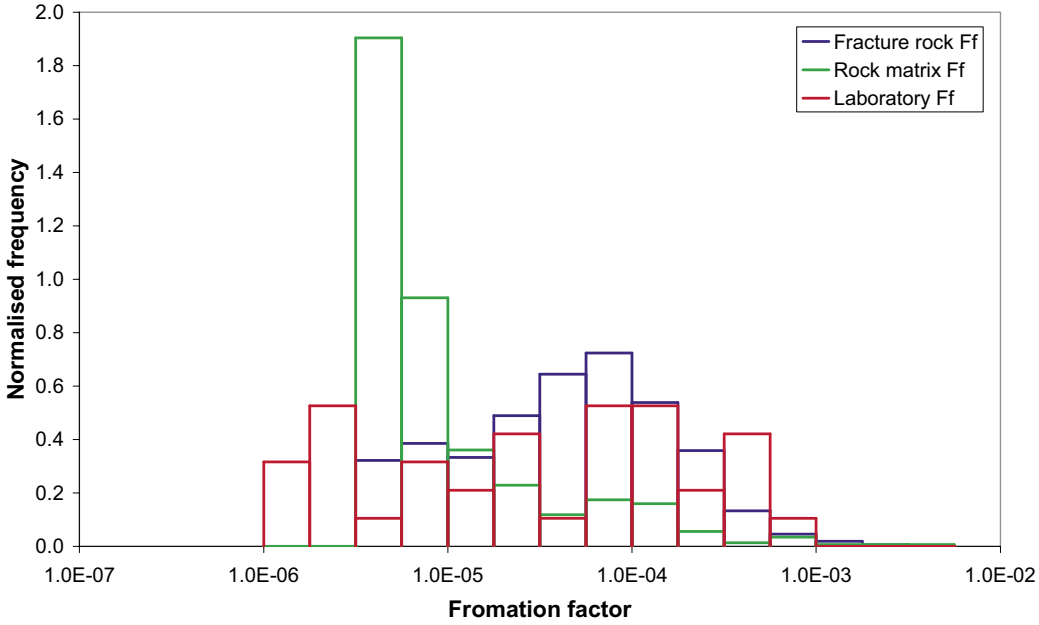

Figure 5-5. *Histograms of formation factors in KSH02.*

Table 5-2. Data for log-normal distribution, KSH02.

	Mean log (Ff)	Median log (Ff)	Standard deviation log (Ff)
Laboratory Ff	–4.62		0.96
In-situ Rock matrix Ff		–5.24	1.04
In-situ Fractured rock Ff		–4.31	0.51

The data of Table 5-2 show that the obtained log-normal distribution of the laboratory data corresponds well with that of the in-situ fractured rock formation factor. The in-situ rock matrix formation factor distribution was based on few data that were poorly distributed in space. The laboratory for mation factor from a certain borehole length was compared to the mean value of the in-situ rock matrix formation factors taken from within 0.5 m of that borehole length. The comparison is tabulated in Appendix C4. As mentioned previously it is recommended to base a comparison of the laboratory and in-situ methods on the data shown in Table 5-2.

6 Summary and discussions

This campaign has answered three important questions. Firstly it seems like in-situ formation factor logging by electrical methods is a workable method that delivers reliable data. It has been shown that the method works well both in theory and in practice and from this campaign one can suggest that formation factors obtained in-situ should be treated with the same dignity as formation factors obtained in the laboratory. In-situ and laboratory investigations nicely complement each other. It should be noted, however, that it requires a lot of experience and insight in a multitude of disciplines, such as transport phenomena, geophysics, hydrology, chemistry and geology, when interpreting the in-situ data and compiling the formation factor logs.

The second answer is that the magnitude of the formation factors vary over a wider range than was expected, also within a specific rock type. This indicates that formation factor distributions may have to be used in future safety assessments. For this purpose it is recommended to use the log-normal distribution.

The third answer is that rock samples brought to the laboratory may be more disturbed than expected. Especially samples from a great depth displayed unexpectedly high formation factors in the laboratory. One can speculate that small fractures were induced in these rock samples in the major stress release when they were taken to the laboratory.

For future work it is recommended to use an in-situ rock resistivity tool with a larger quantitative measuring range. The quantitative measuring range must be large enough so that only an acceptable fraction of the rock is more resistive than that which could be measured. The rock in this remaining fraction may have to be considered as impermeable for diffusion in the safety assessment. In the section 880 m–1,000 m of KSH01A the fraction of rock matrix resistivity data having a resistivity that exceeds 50,000 ohm.m is 39%. In this section the average fracture frequency, about one natural fracture per meter of bore core, is comparable with the average fracture frequency within the Forsmark site investigation area in Sweden.

It is also recommended to slightly change the process of saturating rock samples in the laboratory using the vacuum method. It is recommended to increase the time of raising the pressure in the desiccator when the samples are in the saturation solution. The pressure raise may be continuously or stepwise but should be performed during a workday or if possible a 24 hour period. If doing this the time for saturation and equilibrium under atmospheric pressure may be cut in half.

References

/1/ **Nielsen U T, Ringgaard J, 2003.** Geophysical borehole logging in borehole KSH01A, KSH01B and part of KSH02. Site investigation report SKB P-03-16, Svensk Kärnbränslehantering AB.

/2/ **Nielsen U T, Ringgaard J, Horn F, 2003.** Geophysical borehole logging in borehole KSH02 and KLX02. Site investigation report SKB P-03-111, Svensk Kärnbränslehantering AB.

/3/ **Rouhiainen P, Pöllänen J, 2003.** Difference flow measurements in borehole KSH01A at Simpevarp. Site investigation report SKB, P-03-70, Svensk Kärnbränslehantering AB.

/4/ **Rouhiainen P, Pöllänen J, 2003.** Difference flow measurements in borehole KSH02 at Simpevarp. Site investigation report P-03-110, Svensk Kärnbränslehantering AB.

/5/ **Persson J, Wängnerud A, 2003.** Boremap mapping of telescopic drilled borehole KFM01A. Site investigation report P-03-23, Svensk Kärnbränslehantering AB.

/6/ **Löfgren M, Neretnieks I, 2002.** Formation factor logging in-situ by electrical methods. Background and methodology. SKB TR 02-27, Svensk Kärnbränslehantering AB.

/7/ **Löfgren M, 2001.** Formation factor logging in igneous rock by electrical methods. Licentiate thesis at the Royal Institute of Technology, Stockholm, Sweden. ISBN 91-7283-207-x.

/8/ **Ohlsson Y, 2000.** Studies of Ionic Diffusion in Crystalline Rock. Doctoral thesis at the Royal Institute of Technology, Stockholm, Sweden. ISBN 91-7283-025-5.

/9/ **Löfgren M, Neretnieks I, 2004.** Through electromigration: A new method of obtaining formation factors and investigating connectivity. Submitted for publication in May 2004.

/10/ **Löfgren M, Neretnieks I, 2003.** Formation factor logging by electrical methods. Comparison of formation factor logs obtained in-situ and in the laboratory. J. Contaminant Hydrology, Vol. 61, pp 107–115.

/11/ **SKB SR-97, 1999.** Deep repository for spent nuclear fuel: SR 97 – Post-closure safety. SKB TR-99-06, Svensk Kärnbränslehantering AB.

/12/ **Johnson RA, 1994.** Miller and Freund's probability & statistics for engineers, 5^{ed}. Prentice-Hall Inc, ISBN 0-13-721408-1.

Appendix A

Appendix A1: Date of saturation of rock samples from KSH01A and KSH02

Borehole	Secup (m)	Saturation date	Borehole	Secup (m)	Saturation date
KSH01	19.95	2004-01-26	KSH01	559.90	2004-01-28
KSH01	59.11	2004-01-26	KSH01	580.87	2004-01-28
KSH01	79.64	2004-01-26	KSH01	598.65	2004-01-28
KSH01	99.70	2004-01-26	KSH01	620.22	2004-01-28
KSH01	121.40	2004-01-26	KSH01	640.55	2004-01-28
KSH01	160.71	2004-01-26	KSH01	661.06	2004-01-28
KSH01	181.46	2004-01-26	KSH01	680.20	2004-01-28
KSH01	200.10	2004-01-26	KSH01	699.00	2004-01-28
KSH01	239.95	2004-01-26	KSH01	720.24	2004-01-28
KSH01	261.07	2004-01-26	KSH01	740.53	2004-01-28
KSH01	295.40	2004-01-26	KSH01	760.75	2004-01-29
KSH01	317.77	2004-01-27	KSH01	779.19	2004-01-29
KSH01	340.87	2004-01-27	KSH01	800.40	2004-01-29
KSH01	362.54	2004-01-27	KSH01	820.08	2004-01-29
KSH01	378.97	2004-01-27	KSH01	840.70	2004-01-29
KSH01	398.74	2004-01-27	KSH01	859.15	2004-01-29
KSH01	420.77	2004-01-27	KSH01	880.50	2004-01-29
KSH01	440.22	2004-01-27	KSH01	898.60	2004-01-29
KSH01	460.00	2004-01-27	KSH01	919.65	2004-01-29
KSH01	478.20	2004-01-27	KSH01	960.77	2004-01-29
KSH01	500.30	2004-01-27	KSH01	980.40	2004-01-29
KSH01	520.75	2004-01-27	KSH01	999.45	2004-01-29
KSH01	539.00	2004-01-28			

Secup = upper position of sample in borehole

Borehole	Secup (m)	Saturation date
KSH02	19.95	2004-03-08
KSH02	39.95	2004-03-08
KSH02	60.17	2004-03-08
KSH02	80.00	2004-03-08
KSH02	99.90	2004-03-08
KSH02	119.95	2004-03-08
KSH02	140.15	2004-03-08
KSH02	159.95	2004-03-08
KSH02	179.95	2004-03-08
KSH02	219.65	2004-03-09
KSH02	239.15	2004-03-09
KSH02	259.82	2004-03-09
KSH02	280.00	2004-03-09
KSH02	360.05	2004-03-09
KSH02	399.95	2004-03-09
KSH02	419.95	2004-03-09
KSH02	439.95	2004-03-09
KSH02	459.68	2004-03-09
KSH02	500.37	2004-03-10
KSH02	539.85	2004-03-10
KSH02	560.05	2004-03-10
KSH02	580.10	2004-03-10
KSH02	639.88	2004-03-10
KSH02	680.15	2004-03-10
KSH02	700.00	2004-03-10
KSH02	720.00	2004-03-10
KSH02	740.00	2004-03-10
KSH02	760.16	2004-03-10
KSH02	779.81	2004-03-11
KSH02	819.90	2004-03-11
KSH02	840.00	2004-03-11
KSH02	859.95	2004-03-11
KSH02	880.00	2004-03-11
KSH02	900.00	2004-03-11
KSH02	920.00	2004-03-11
KSH02	940.00	2004-03-11
KSH02	959.95	2004-03-11
KSH02	979.95	2004-03-11

Secup = upper position of sample in borehole

Appendix A2: Laboratory data for rock samples from KSH01A

Secup (m)	Sample length (mm)	Sample ∅ (mm)	Res 1 (ohm)	Res 2 (ohm)	Res 3 (ohm)	Res 4 (ohm)	Res 5 (ohm)	Res 6 (ohm)
19.95	30.7	50.1	13,530	13,390	13,490	13,480	13,350	13,470
59.11	30.3	50.2	102,400	100,500	10,1100	100,000	99,100	100,900
79.64	30.3	50.2	91,500	89,800	90,000	90,200	89000	89,800
99.70	30.4	50.2	87,200	86,700	86,800	87,600	86,200	86,600
121.40	30.5	50.0	294,900	289,500	291,800	292,200	286,700	289,100
160.71	30.6	50.0	274,600	270,500	255,500	260,200	247,000	247,800
181.46	30.6	50.2	41,400	41,200	40,800	40,700	39,300	39,700
200.10	30.5	50.1	1,792,000	1,834,000	1,340,000	1,310,000	1,009,000	996,000
239.95	30.4	50.0	469,000	468,000	395,000	399,000	338,000	341,000
261.07	29.5	50.1	5,060	5,000	4,970	5,010	4,880	4,910
295.40	30.3	50.2	60,600	60,000	59,600	60,300	59,400	59,700
317.77	30.0	50.2	32,500	32,300	31,600	31,600	29,460	29,600
340.87	30.1	50.1	2,533,000	2,437,000	1,779,000	1,763,000	1,286,000	1,272,000
362.54	30.3	50.2	196,300	194,900	188,900	188,600	181,100	182,500
378.97	30.3	50.0	162,400	159,500	156,600	154,500	147,600	149,400
398.74	30.4	50.2	200,600	198,300	189,100	190,000	177,100	178,100
420.77	21.4	50.0	71,400	71,100	64,800	65,600	59,300	59,700
440.22	22.5	50.1	5,020	5,000	4,760	4,760	4,440	4,460
460.00	30.3	50.1	5,120	4,910	4,860	4,790	4,610	4,650
478.20	30.5	50.1	2,839,000	2,609,000	1,829,000	1,844,000	1,268,000	1,295,000
500.30	30.0	50.0	83,800	82,800	82,500	82,600	81,400	81,400
520.75	30.3	50.0	609,000	603,000	542,000	539,000	482,000	48,8000
539.00	30.4	50.0	1,497,000	1,553,000	1,250,000	1,325,000	1,058,000	1,088,000
559.90	30.4	51.1	4,196,000	3,689,000	2,727,000	2,785,000	1,436,000	1,558,000
580.87	30.4	50.0	775,000	760,000	597,000	610,000	445,000	452,000
598.65	30.2	50.2	104,100	103,400	92,400	93,500	82,600	83,500
620.22	30.3	50.0	12,640	12,830	12,030	12,060	10,650	10,680
640.55	30.5	50.2	49,300	48,800	47,400	47,300	44,600	44,900
661.06	30.5	50.1	133,700	133,100	121,900	123,200	111,300	111,400
680.20	30.4	50.1	413,000	411,000	384,000	384,000	351,000	358,000
699.00	30.5	50.1	311,000	307,000	273,300	273,000	229,000	231,500
720.24	30.5	50.1	24,740	24,510	24,310	24,340	23,600	23,720
740.53	30.4	50.1	203,700	201,700	161,700	160,700	132,700	134,200
760.75	30.4	50.0	160,800	159,100	150,900	152,000	142,500	142,800
779.19	30.4	50.0	41,500	41,200	38,500	38,300	34,500	34,700
800.40	30.2	40.9	21,460	21,160	21,210	21,210	20,670	20,800
820.08	30.3	50.2	2,496	2,456	2,369	2,385	2,282	2,287
840.70	30.3	50.2	4,830	4,750	4,570	4,610	4,390	4,400
859.15	30.4	50.2	4,640	4,610	4,430	4,440	4,230	4,250
880.50	30.3	50.0	6,260	6,210	5,850	5,830	5,420	5,430
898.60	29.4	50.0	6,530	6,480	6,300	6,340	6,110	6,150
919.65	30.3	49.9	7,620	7,580	7,370	7,430	7,170	7,200
960.77	30.5	50.0	3,790	3,770	3,710	3,730	3,660	3,660
980.40	30.4	50.1	8,190	8,120	7,850	7,850	7,600	7,660
999.45	30.3	50.1	1,0130	10,040	9,810	9,790	9,450	9,470

Secup = upper position in borehole, Sample ∅ = diameter of sample, Res 1 = measured resistance in first run 2004-03-18, Res 2 = measured resistance in second run 2004-03-18, Res 3 = measured resistance in first run 2004-04-08, Res 4 = measured resistance in second run 2004-04-08. Res 5 = measured resistance in first run 2004-05-18, Res 6 = measured resistance in second run 2004-05-18.

Appendix A3: Laboratory data for the solutions used for samples from KSH01A

1.00 M NaCl	Conductivity (S/m)	Temperature (°C)
Saturation solution 2004-01-27	7.56	21.4
Saturation solution 2004-01-29	7.68	22.0
Equilibration solution 2004-01-27	7.26	19.5
Equilibration solution 2004-01-29	7.55	21.1
Equilibration solution 2004-03-09	7.42	20.4
Equilibration solution 2004-03-18[a]	7.34	20.1
Equilibration solution 2004-03-18[b]	7.34	20.1
Equilibration solution 2004-04-08[a]	7.48	21.2
Equilibration solution 2004-04-08[b]	7.44	20.7
Equilibration solution 2004-05-18[a]	7.55	21.8
Equilibration solution 2004-05-18[b]	7.55	21.2

a = conductivity and temperature measured before first run, b = conductivity and temperature measured after second run.

Appendix A4: Laboratory data for rock samples from KSH02

Secup (m)	Sample length (mm)	Sample ∅ (mm)	Res 1 (ohm)	Res 2 (ohm)	Res 3 (ohm)	Res 4 (ohm)
19.95	30.4	50.2	8,640,000	9,330,000	733,0000	7,000,000
39.95	30.4	50.0	1,027,000	991,000	961,000	931,000
60.17	30.6	50.1	88,600	88,400	88,100	88,500
80.00	30.6	50.2	27,020	26,870	25,220	25,270
99.90	21.9	50.2	8,880	8,880	8,440	8,470
119.95	30.5	50.2	666,000	659,000	551,000	550,000
140.15	30.5	50.2	1,285,000	1,330,000	1,262,000	1,274,000
159.95	30.6	50.2	89,700	89,300	89,600	89,900
179.95	30.4	50.3	264,800	264,000	260,100	263,000
219.65	30.4	50.2	2,097,000	2,242,000	1,895,000	1,794,000
239.15	30.3	50.2	817,000	825,000	708,000	71,3000
259.82	30.4	50.2	304,000	309,000	295,200	299,500
280.00	30.1	50.2	977,000	988,000	881,000	887,000
360.05	30.0	50.1	4,070	4,080	3,870	3,890
399.95	30.2	50.1	204,600	204,200	193,000	194,100
419.95	30.3	50.0	9,470	9,470	9,170	9,120
439.95	30.0	50.0	742,000	722,000	648,000	692,000
459.68	30.3	50.2	13,160	12,980	11,810	12,020
500.37	28.0	50.0	2,433	2,443	2,271	2,284
539.85	30.0	50.0	89,700	89,500	87,900	88,400
560.05	29.9	50.0	128,600	128,300	124,400	124,300

580.10	30.3	50.0	8,070,000	10,980,000	8,590,000	10,790,000
639.88	29.3	50.2	10,300	10,300	10,270	10,290
680.15	29.4	50.1	66,000	65,600	63,200	63,400
700.00	29.7	50.1	11800	11840	11530	11600
720.00	30.4	50.0	1501000	1574000	1330000	1327000
740.00	30.1	50.0	5700	5670	5610	5630
760.16	29.8	49.4	241400	240200	222100	222400
779.81	28.2	50.1	5700	5660	5560	5550
819.90	30.0	50.2	5360	5300	5000	5010
840.00	30.1	50.1	1110000	1110000	1096000	1094000
859.95	30.4	50.1	40600	40700	40600	40700
880.00	30.4	49.9	17210	17240	16460	16450
900.00	30.4	50.2	23250	23180	22470	22470
920.00	30.3	50.1	29080	29090	27840	27910
940.00	30.3	50.2	14700	14700	13810	13910
959.95	30.4	50.2	22020	22070	22030	22040
979.95	30.1	50.1	28360	28410	27630	27700

Secup = upper position in borehole, Sample ∅ = diameter of sample, Res 1= measured resistance in first run 2004-05-04, Res 2 = measured resistance in second run 2004-05-04, Res 3 = measured resistance in first run 2004-05-24, Res 4 = measured resistance in second run 2004-05-24.

Appendix A5: Laboratory data for the solutions used for samples from KSH02

1.00 M NaCl	Conductivity (S/m)	Temperature (°C)
Saturation solution 2004-03-09	7.48	21.6
Saturation solution 2004-03-12	7.64	21.6
Equilibration solution 2004-03-09	7.09	18.9
Equilibration solution 2004-03-12	7.32	20.6
Equilibration solution 2004-05-04[a]	7.45	21.1
Equilibration solution 2004-05-04[b]	7.46	21.1
Equilibration solution 2004-05-24[a]	7.46	21.3
Equilibration solution 2004-05-24[b]	7.45	21.0

a = conductivity and temperature measured before first run, b = conductivity and temperature measured after second run.

Appendix A6: Laboratory formation factor for rock samples from KSH01A

Secup (m)	Formation factor	Secup (m)	Formation factor
19.95	1.56×10^{-4}	559.90	1.34×10^{-6}
59.11	2.06×10^{-5}	580.87	4.66×10^{-6}
79.64	2.31×10^{-5}	598.65	2.48×10^{-5}
99.70	2.40×10^{-5}	620.22	1.95×10^{-4}
121.40	7.28×10^{-6}	640.55	4.64×10^{-5}
160.71	8.49×10^{-6}	661.06	1.87×10^{-5}
181.46	5.28×10^{-5}	680.20	5.87×10^{-6}
200.10	2.08×10^{-6}	699.00	9.06×10^{-6}
239.95	6.15×10^{-6}	720.24	8.82×10^{-5}
261.07	4.12×10^{-4}	740.53	1.56×10^{-5}
295.40	3.47×10^{-5}	760.75	1.46×10^{-5}
317.77	6.92×10^{-5}	779.19	6.03×10^{-5}
340.87	1.61×10^{-6}	800.40	1.49×10^{-4}
362.54	1.14×10^{-5}	820.08	9.04×10^{-4}
378.97	1.40×10^{-5}	840.70	4.70×10^{-4}
398.74	1.17×10^{-5}	859.15	4.88×10^{-4}
420.77	$^{*}2.72\times10^{-5}$	880.50	3.84×10^{-4}
440.22	3.46×10^{-4}	898.60	3.29×10^{-4}
460.00	4.48×10^{-4}	919.65	2.91×10^{-4}
478.20	1.63×10^{-6}	960.77	5.72×10^{-4}
500.30	2.53×10^{-5}	980.40	2.73×10^{-4}
520.75	4.29×10^{-6}	999.45	2.19×10^{-4}
539.00	1.95×10^{-6}		

Secup = upper position in borehole. Formation factor = mean value of formation factors taken in first and second run 2004-05-18. The samples had been equilibrated for 110–112 days. * Corrected for defect in sample.

Appendix A7: Laboratory formation factor for rock samples from KSH02

Secup (m)	Formation factor	Secup (m)	Formation factor
19.95	*2.88×10^{-7}	539.85	2.33×10^{-5}
39.95	2.20×10^{-6}	560.05	1.64×10^{-5}
60.17	2.36×10^{-5}	580.10	*2.17×10^{-7}
80.00	8.22×10^{-5}	639.88	1.93×10^{-4}
99.90	1.76×10^{-4}	680.15	3.16×10^{-5}
119.95	3.76×10^{-6}	700.00	1.75×10^{-4}
140.15	1.63×10^{-6}	720.00	1.56×10^{-6}
159.95	2.31×10^{-5}	740.00	3.66×10^{-4}
179.95	7.85×10^{-6}	760.16	9.39×10^{-6}
219.65	1.12×10^{-6}	779.81	3.46×10^{-4}
239.15	2.89×10^{-6}	819.90	4.06×10^{-4}
259.82	6.93×10^{-6}	840.00	1.87×10^{-6}
280.00	2.31×10^{-6}	859.95	5.09×10^{-5}
360.05	5.26×10^{-4}	880.00	1.27×10^{-4}
399.95	1.06×10^{-5}	900.00	9.17×10^{-5}
419.95	2.26×10^{-4}	920.00	7.40×10^{-5}
439.95	3.06×10^{-6}	940.00	1.48×10^{-4}
459.68	1.72×10^{-4}	959.95	9.35×10^{-5}
500.37	8.40×10^{-4}	979.95	7.41×10^{-5}

Secup = upper position in borehole. Formation factor = mean value of formation factors taken in first and second run 2004-05-24. The samples had been equilibrated for 73–76 days. *Possibly outside quantitative measuring range of the rock resistivity meter.

Appendix B

Appendix B1: In-situ rock resistivities and fractures KSH01A

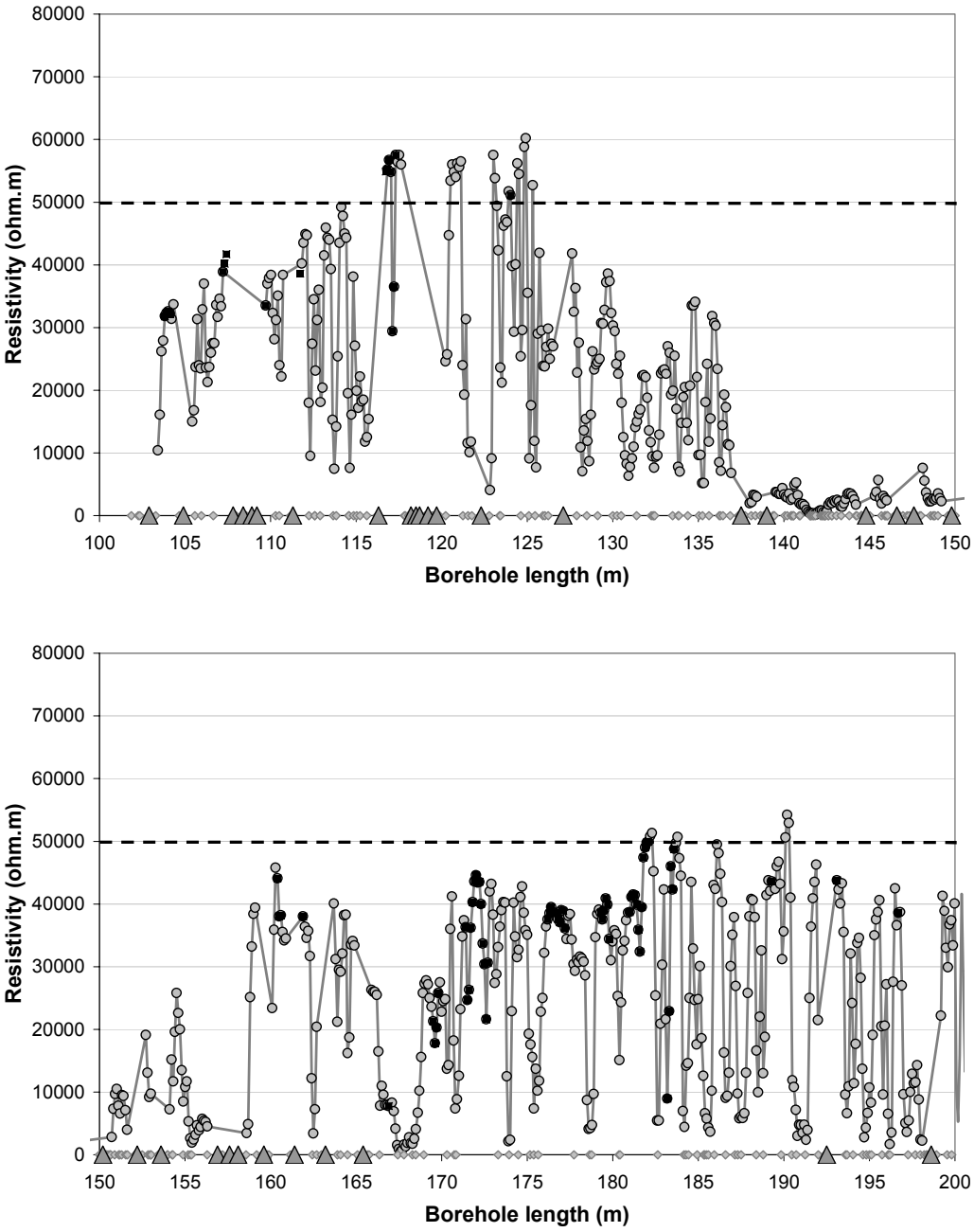

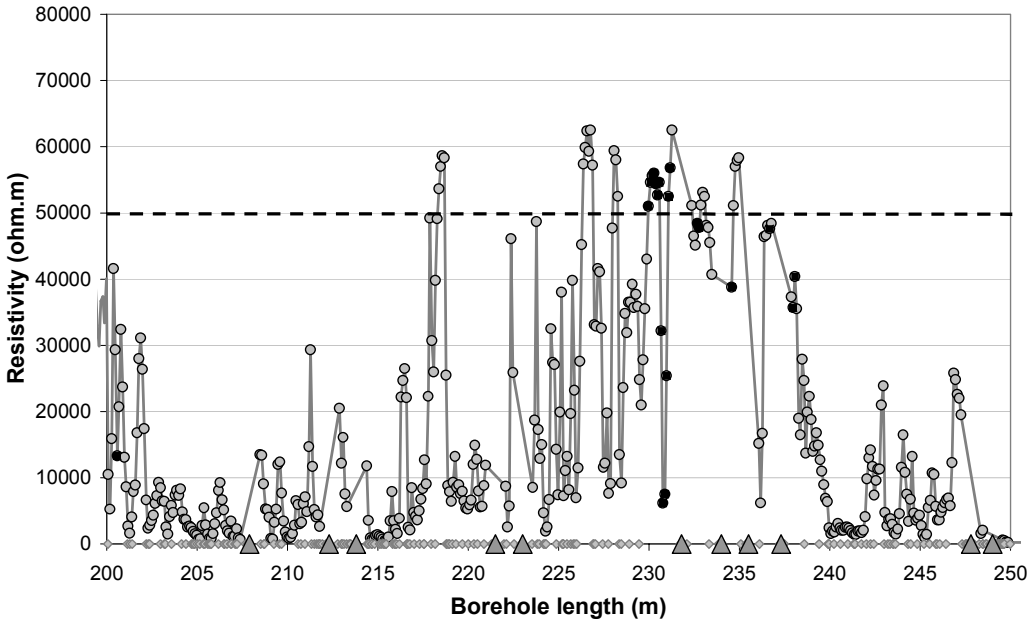

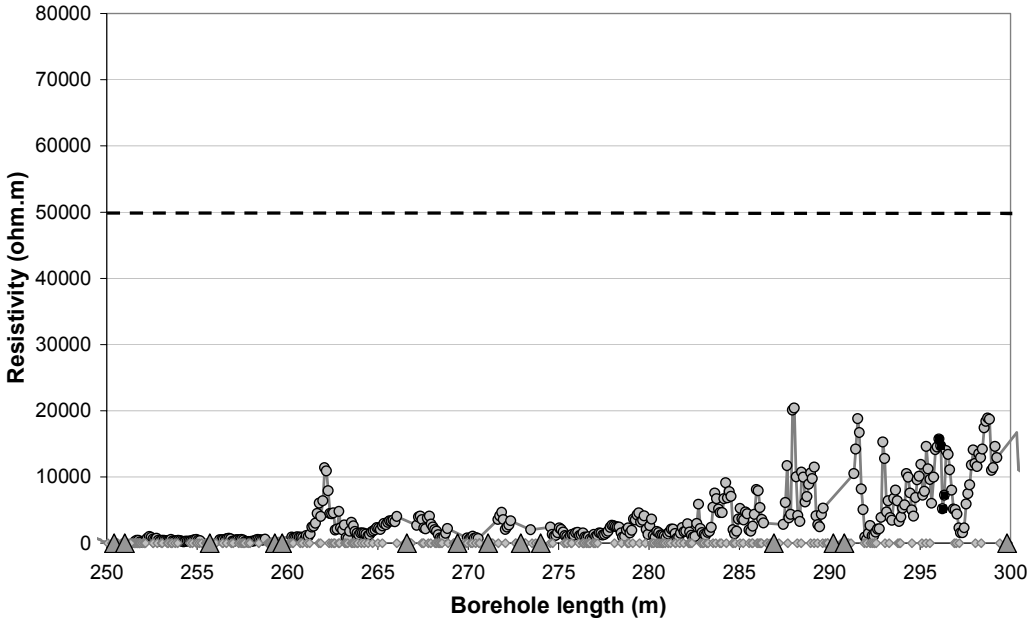

Fractured rock resistivity
Rock matrix resistivity
Location of natural fracture parting the bore core
Location of hydraulically conductive fracture detected in the difference flow logging
Upper limit of quantitative measuring range

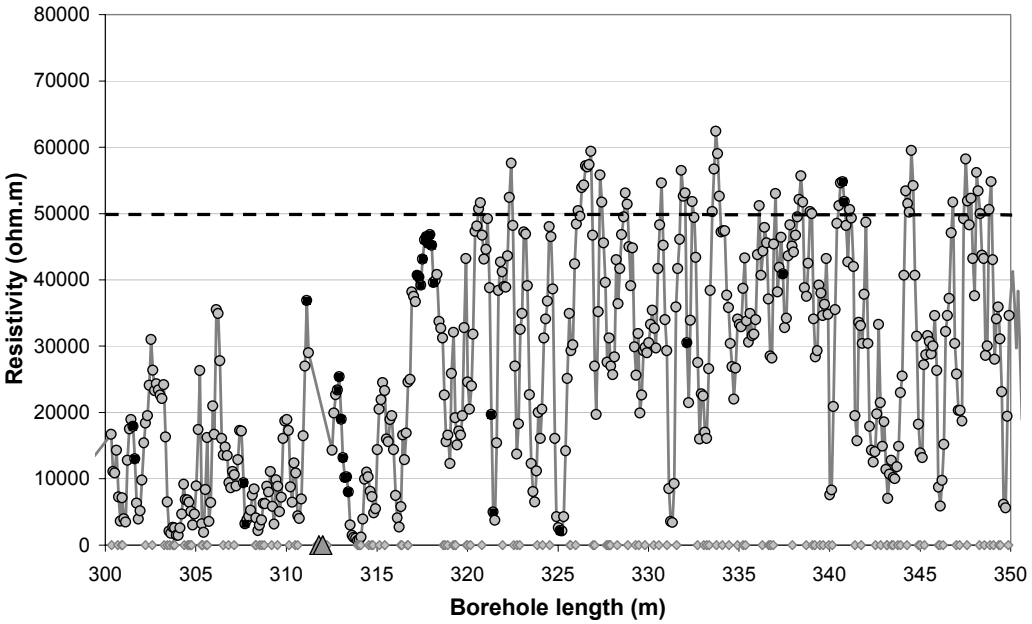

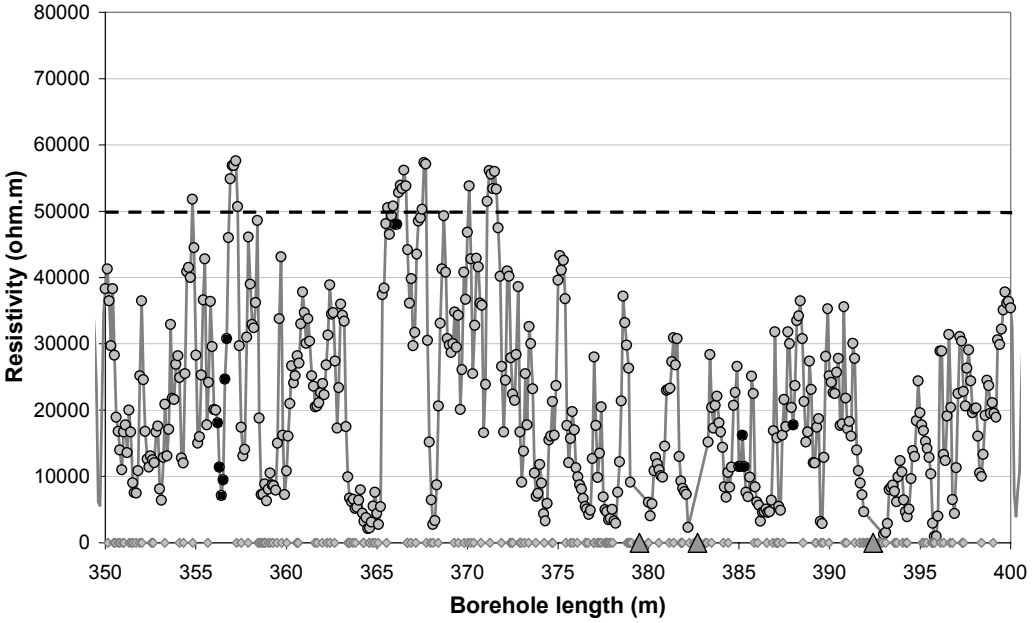

Fractured rock resistivity
Rock matrix resistivity
Location of natural fracture parting the bore core
Location of hydraulically conductive fracture detected in the difference flow logging
Upper limit of quantitative measuring range

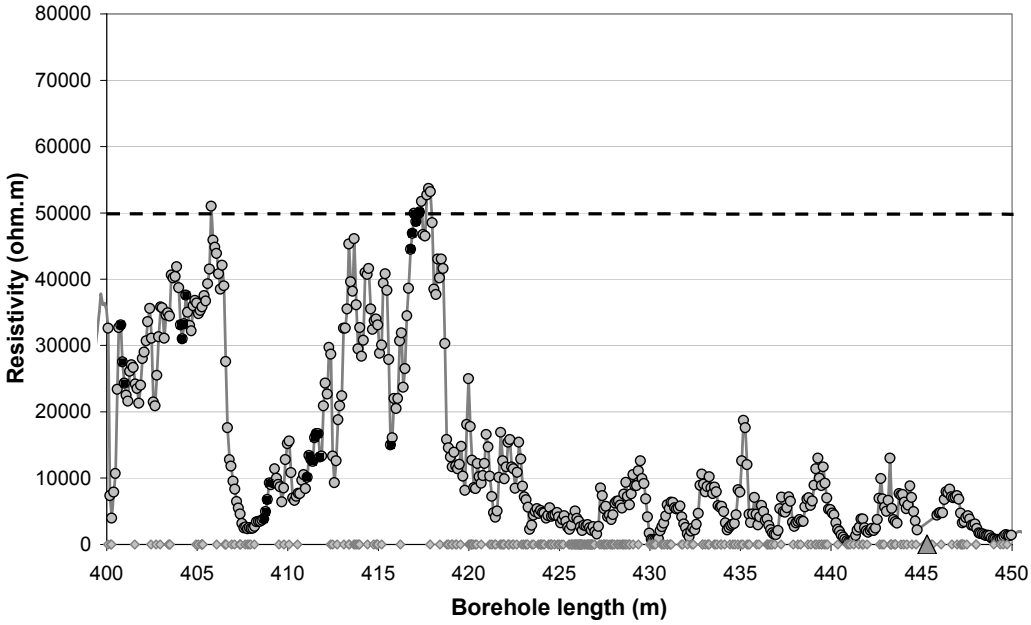

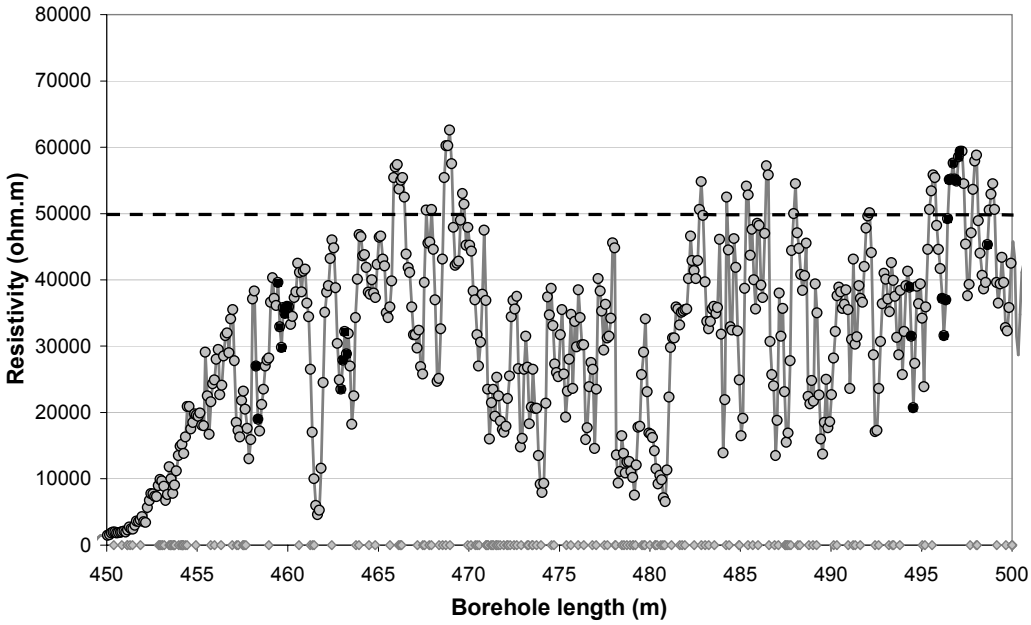

Fractured rock resistivity
Rock matrix resistivity
Location of natural fracture parting the bore core
Location of hydraulically conductive fracture detected in the difference flow logging
Upper limit of quantitative measuring range

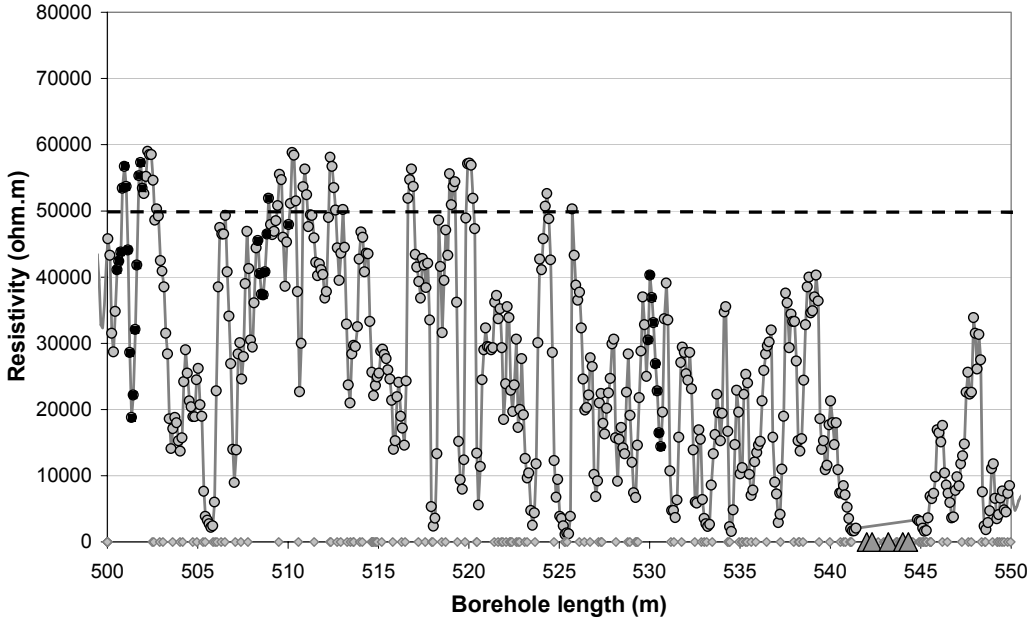

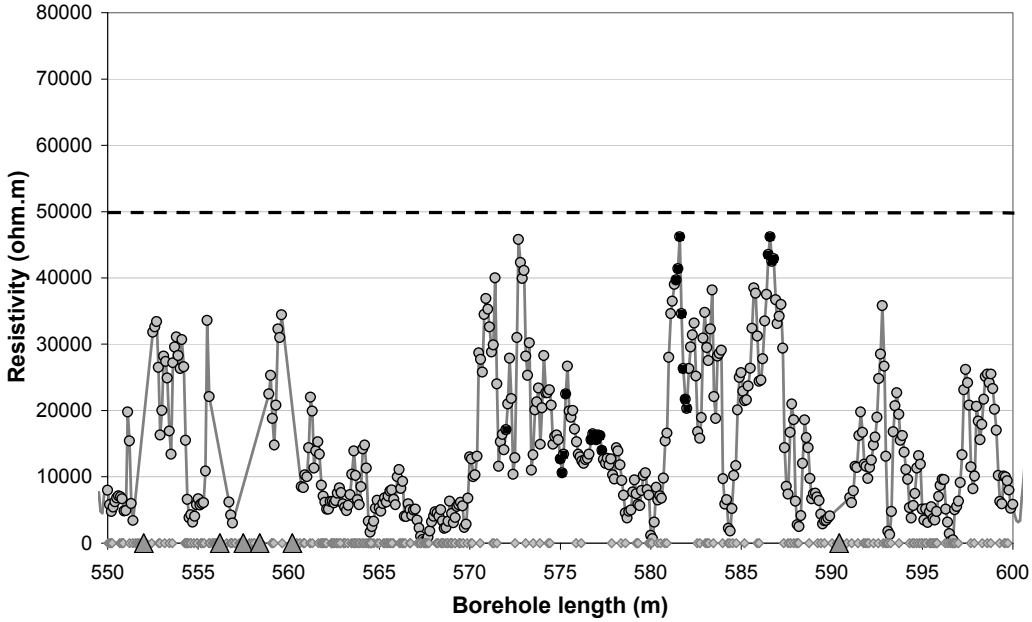

Fractured rock resistivity
Rock matrix resistivity
Location of natural fracture parting the bore core
Location of hydraulically conductive fracture detected in the difference flow logging
Upper limit of quantitative measuring range

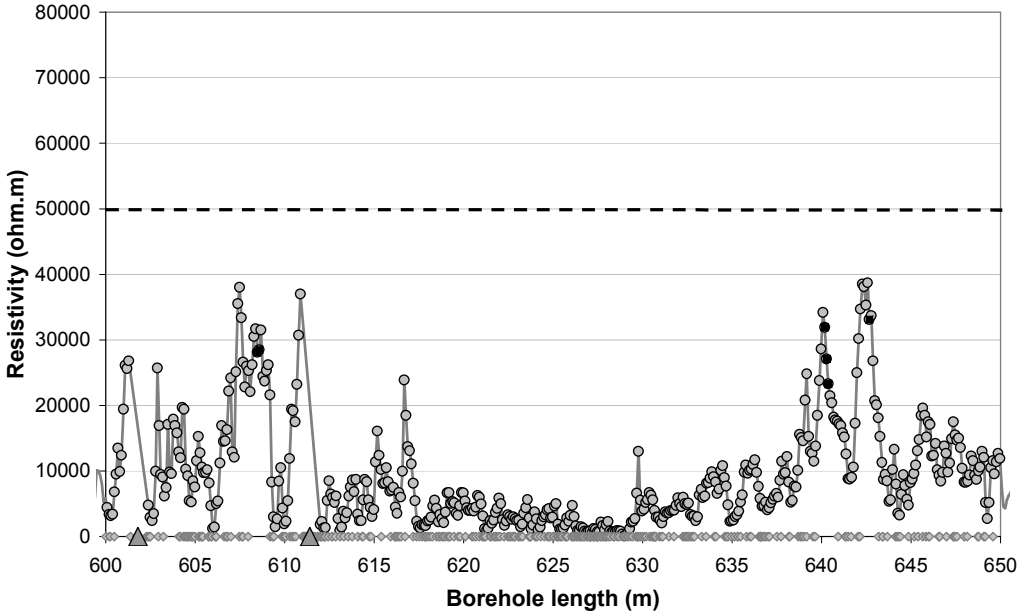

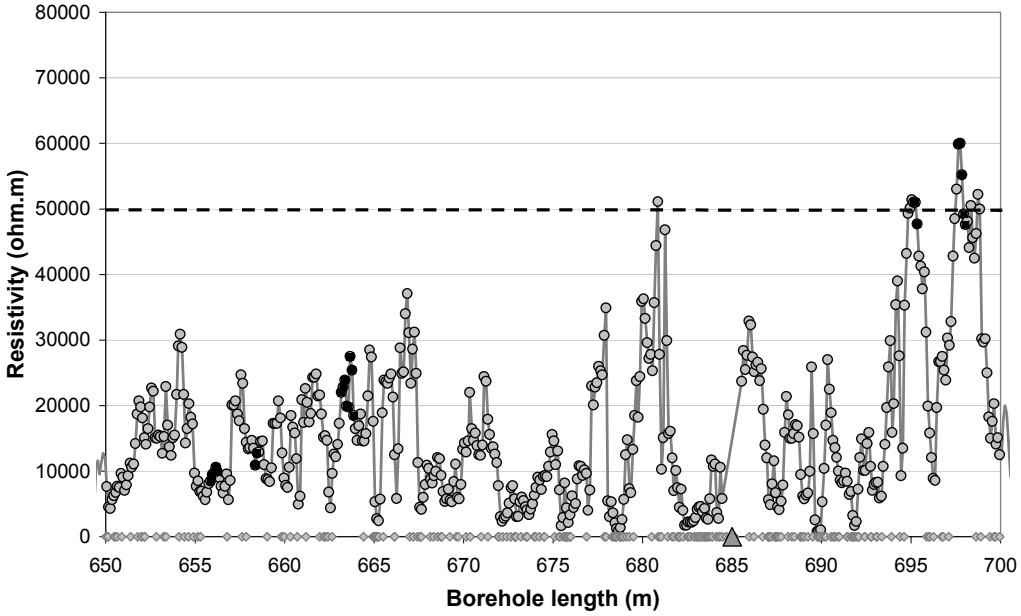

Fractured rock resistivity
Rock matrix resistivity
Location of natural fracture parting the bore core
Location of hydraulically conductive fracture detected in the difference flow logging
Upper limit of quantitative measuring range

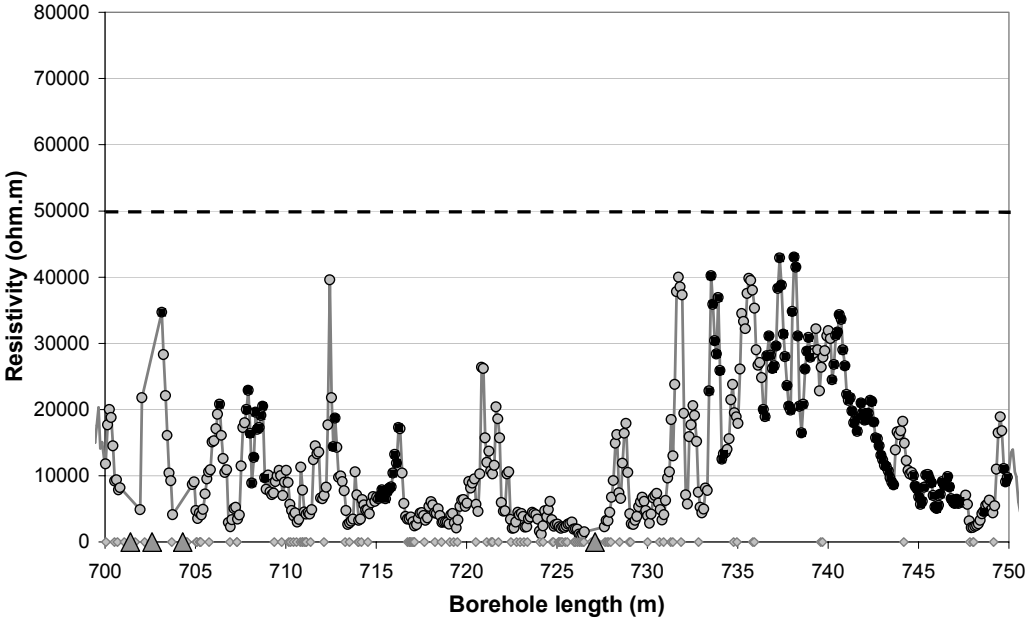

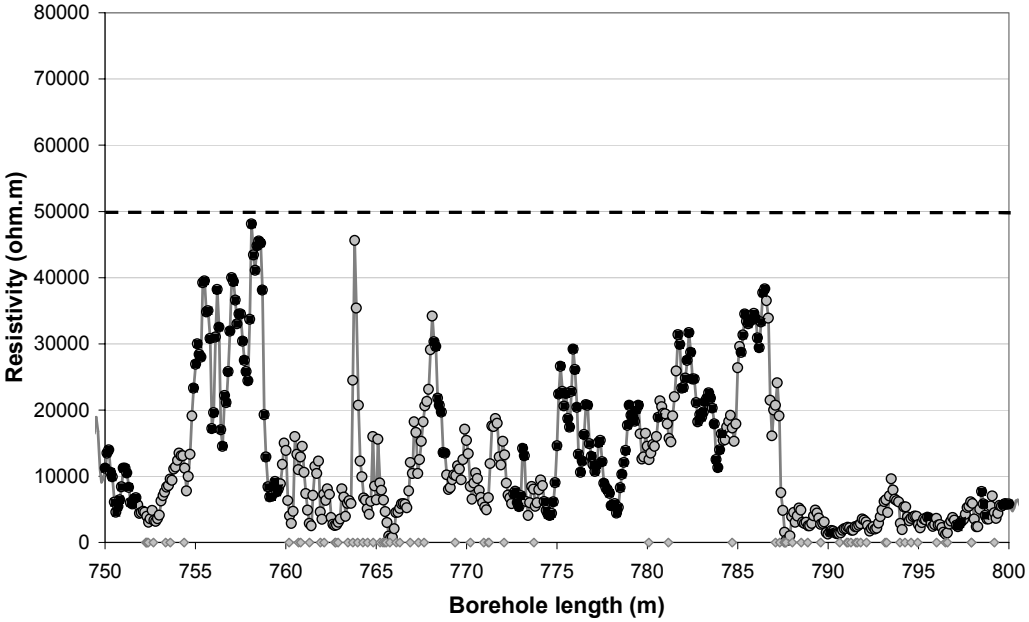

Fractured rock resistivity
Rock matrix resistivity
Location of natural fracture parting the bore core
Location of hydraulically conductive fracture detected in the difference flow logging
Upper limit of quantitative measuring range

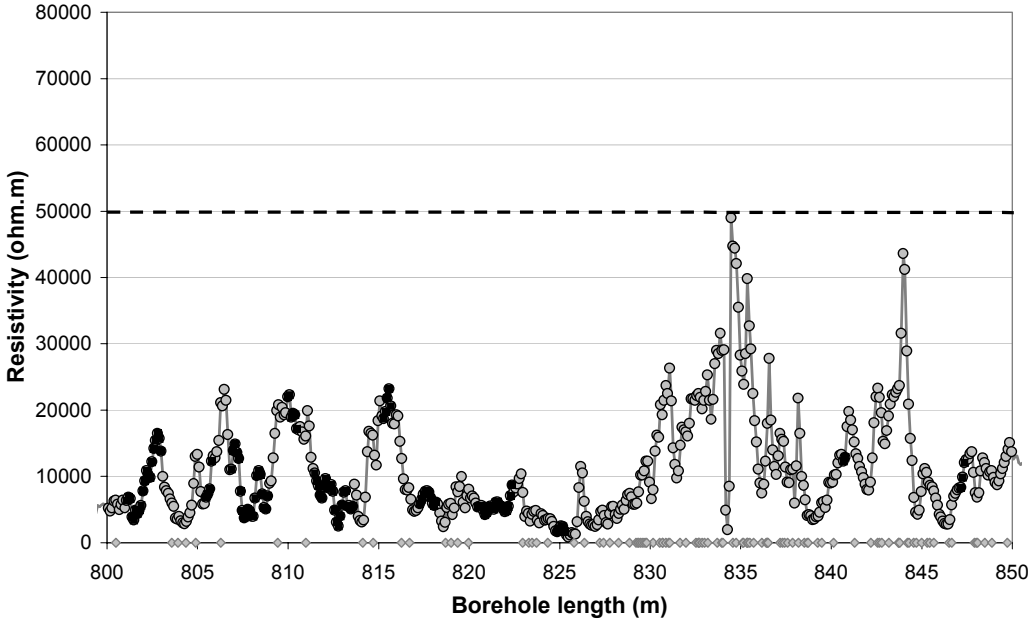

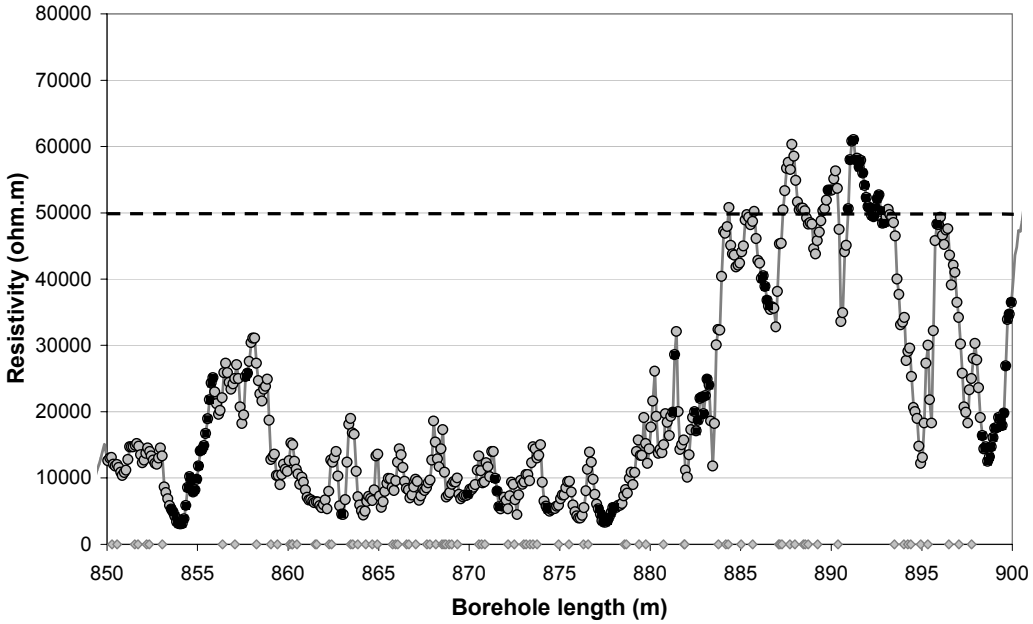

Fractured rock resistivity
Rock matrix resistivity
Location of natural fracture parting the bore core
Location of hydraulically conductive fracture detected in the difference flow logging
Upper limit of quantitative measuring range

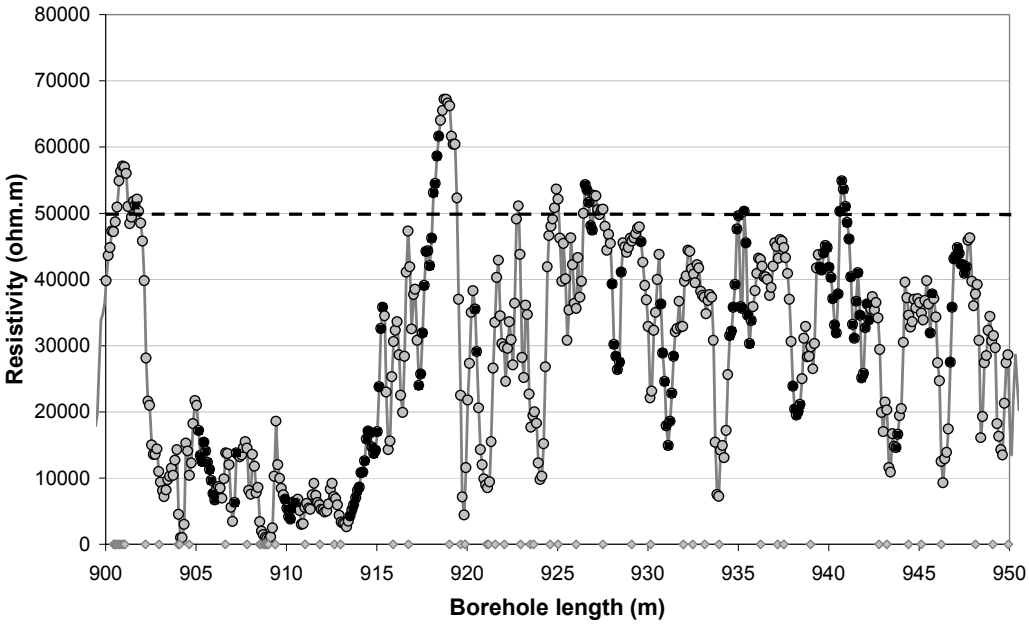

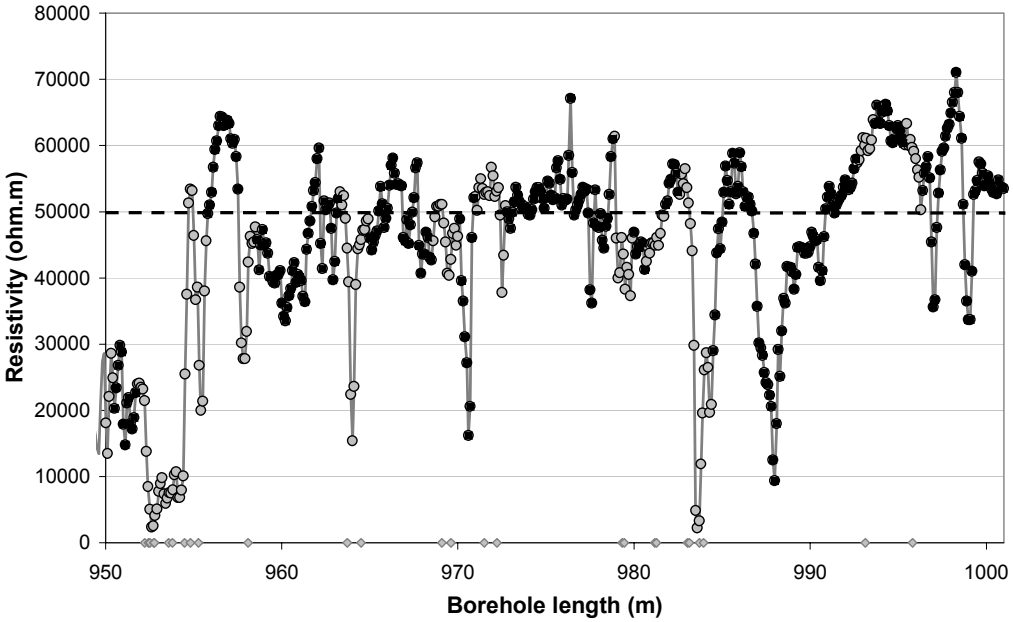

Fractured rock resistivity
Rock matrix resistivity
Location of natural fracture parting the bore core
Location of hydraulically conductive fracture detected in the difference flow logging
Upper limit of quantitative measuring range

Appendix B2: In-situ rock resistivities and fractures KSH02

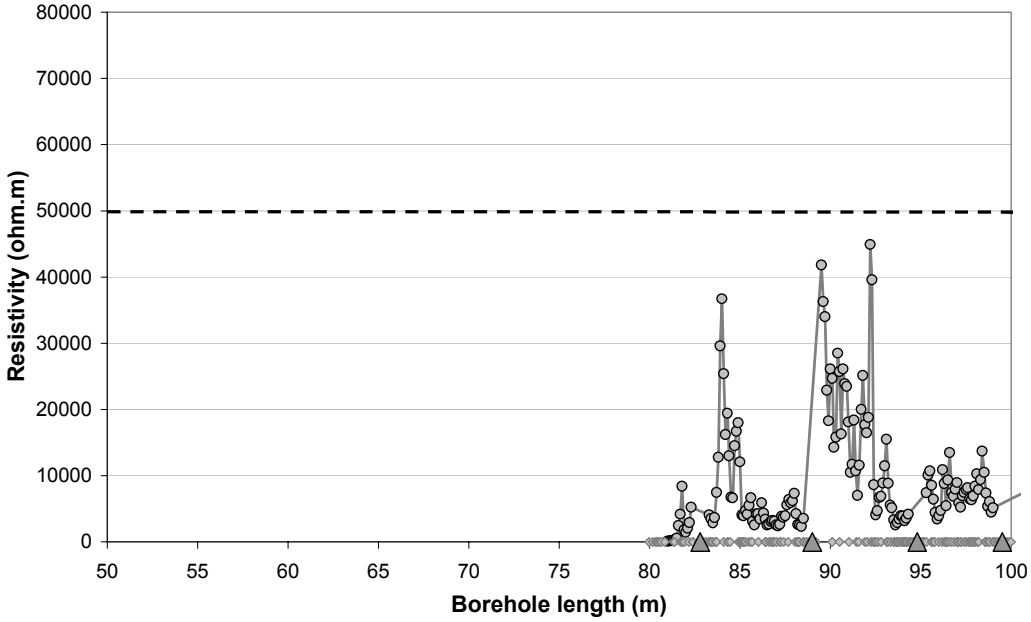

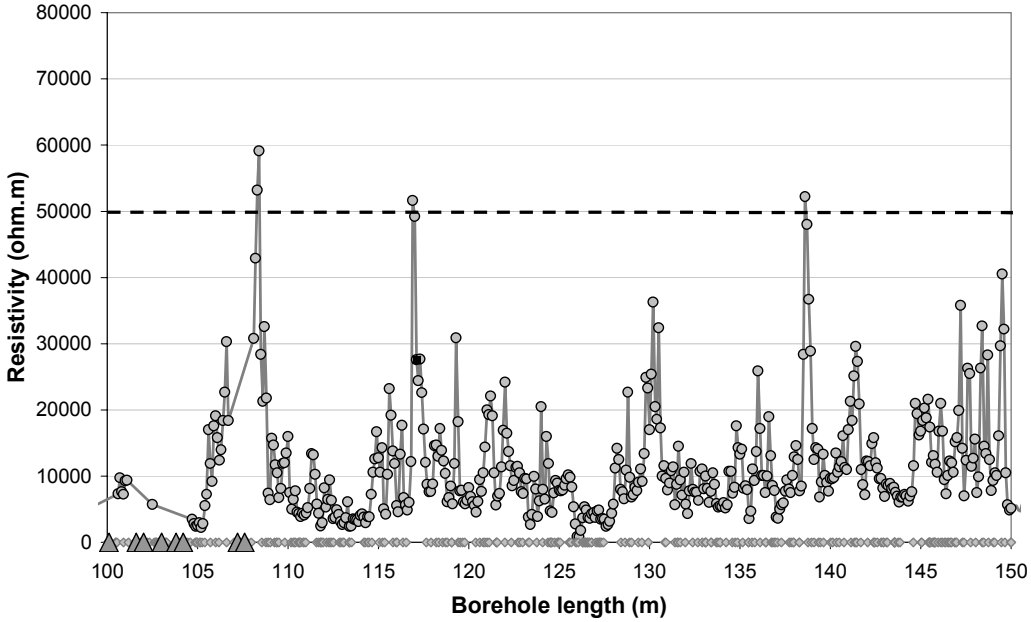

Fractured rock resistivity
Rock matrix resistivity
Location of natural fracture parting the bore core
Location of hydraulically conductive fracture detected in the difference flow logging
Upper limit of quantitative measuring range

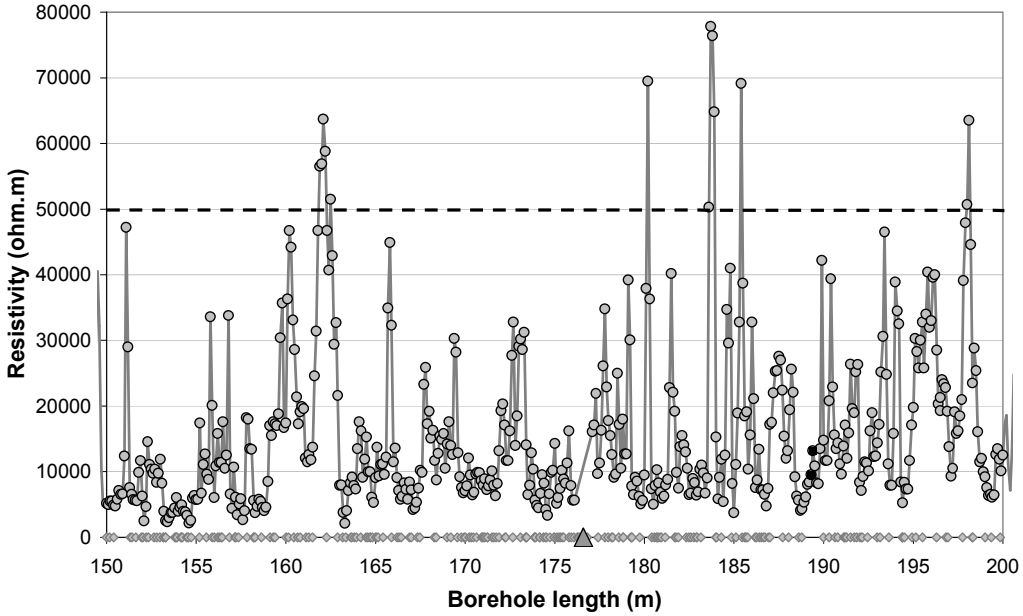

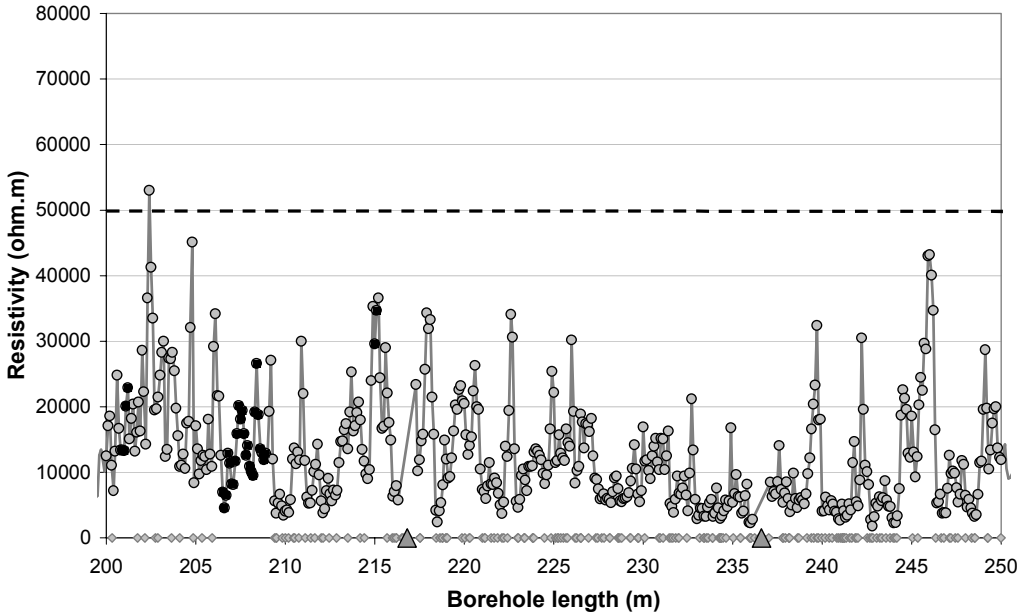

Fractured rock resistivity
Rock matrix resistivity
Location of natural fracture parting the bore core
Location of hydraulically conductive fracture detected in the difference flow logging
Upper limit of quantitative measuring range

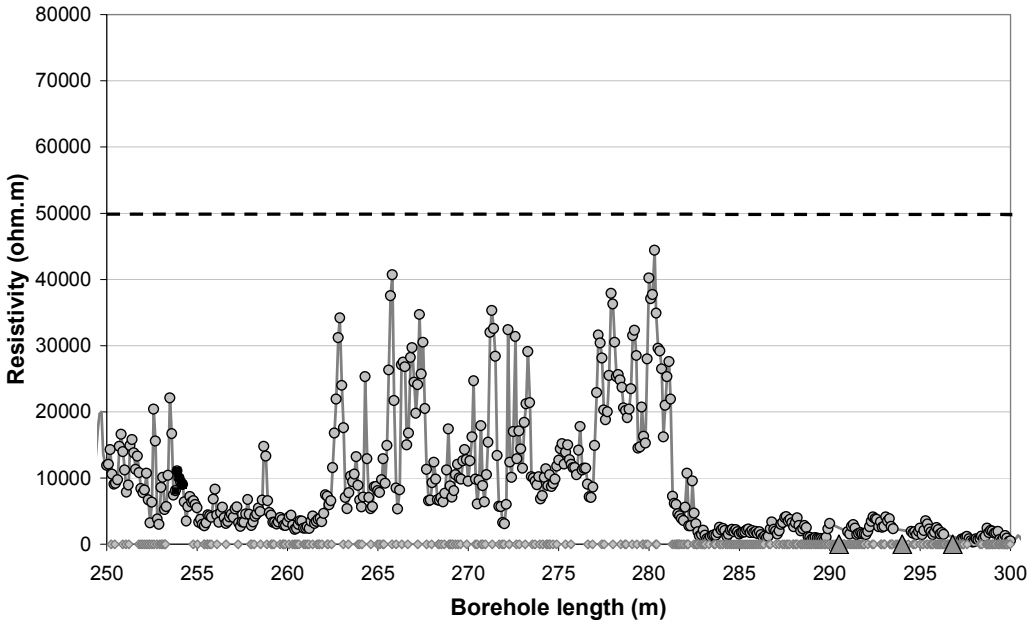

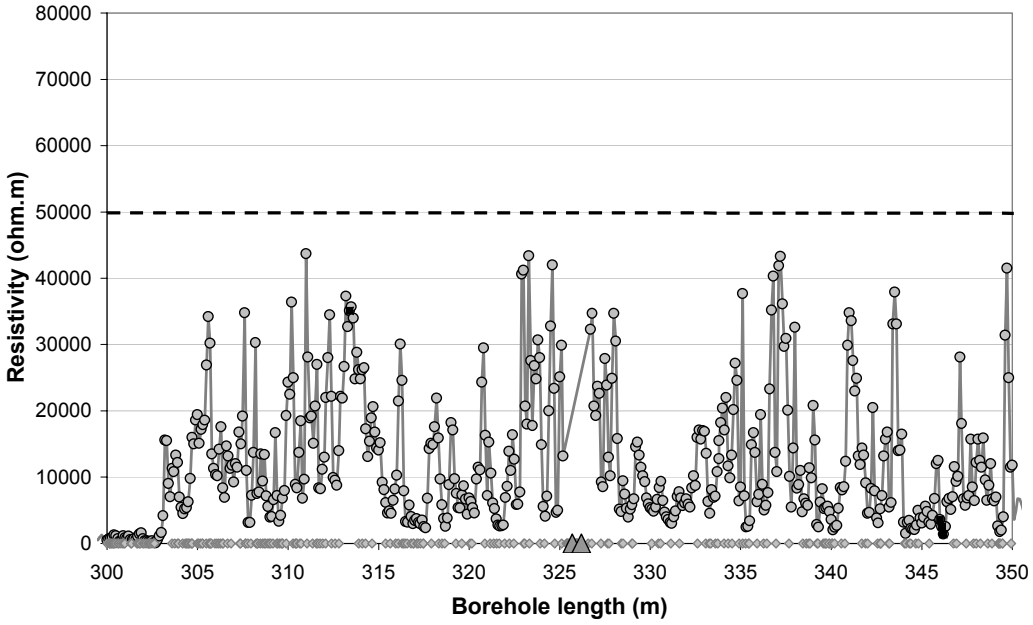

Fractured rock resistivity
Rock matrix resistivity
Location of natural fracture parting the bore core
Location of hydraulically conductive fracture detected in the difference flow logging
Upper limit of quantitative measuring range

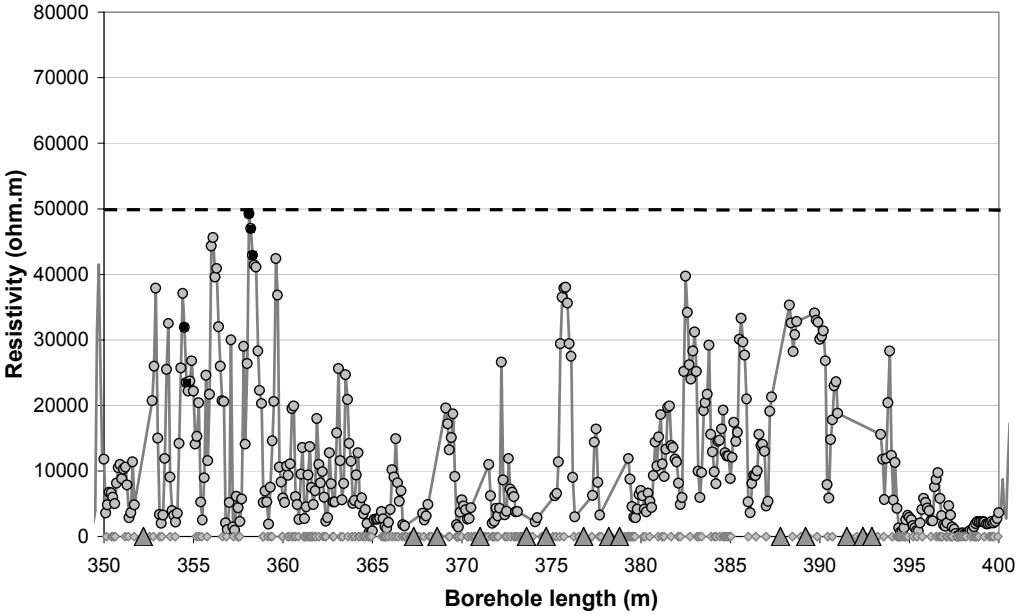

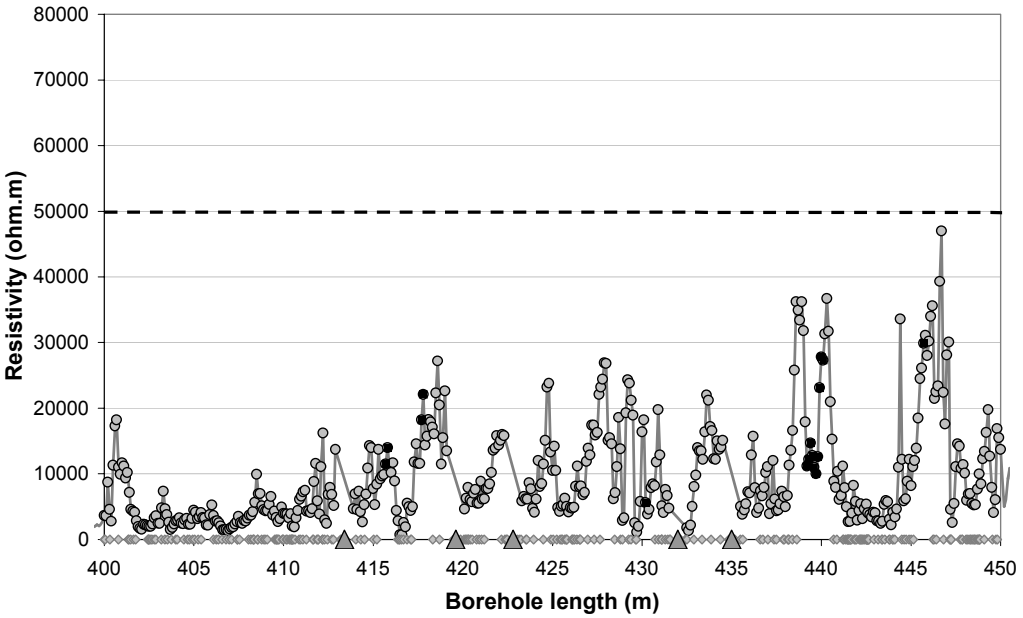

Fractured rock resistivity
Rock matrix resistivity
Location of natural fracture parting the bore core
Location of hydraulically conductive fracture detected in the difference flow logging
Upper limit of quantitative measuring range

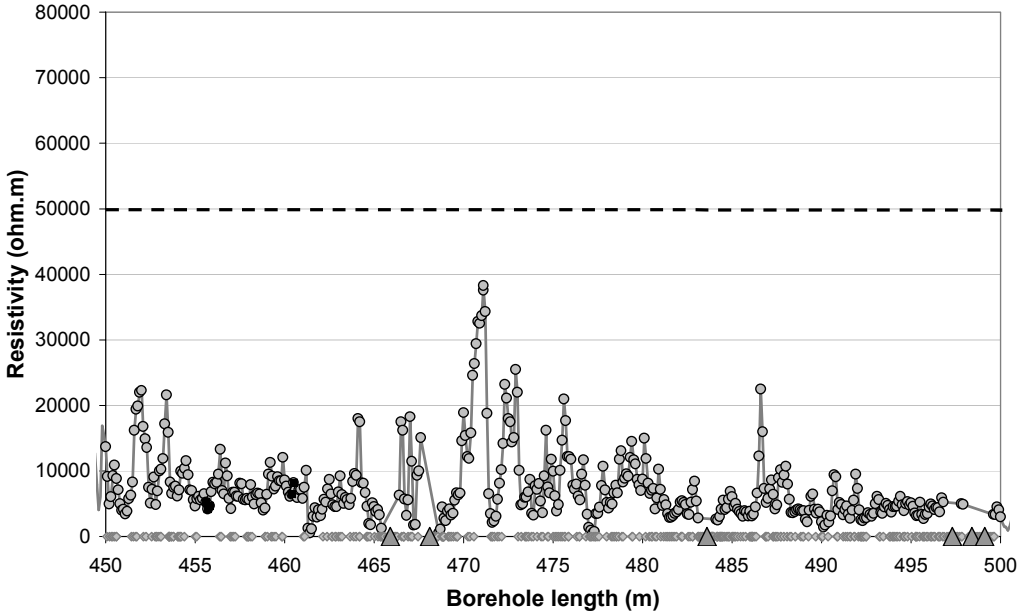

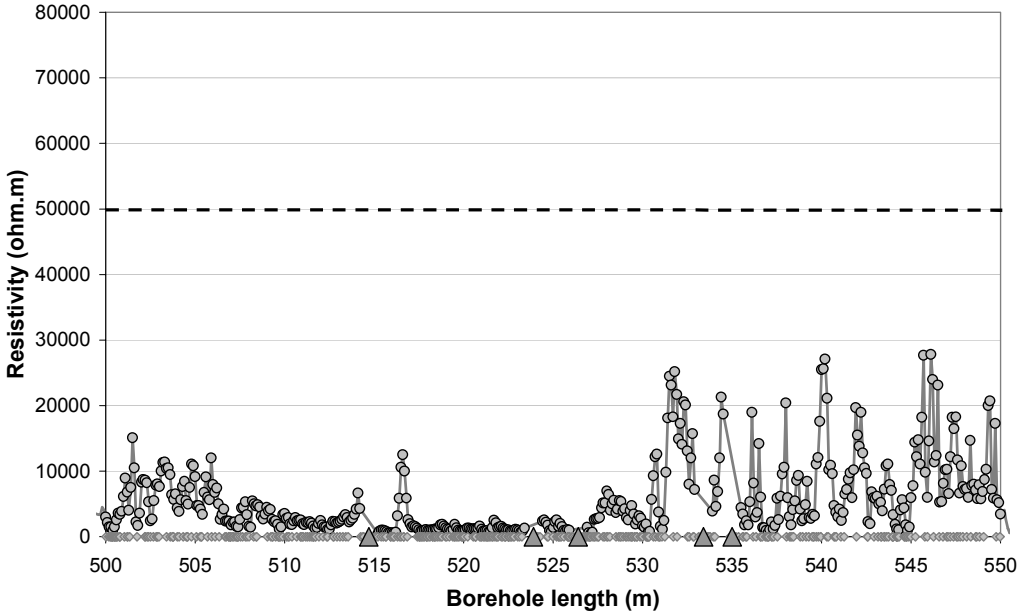

Fractured rock resistivity
Rock matrix resistivity
Location of natural fracture parting the bore core
Location of hydraulically conductive fracture detected in the difference flow logging
Upper limit of quantitative measuring range

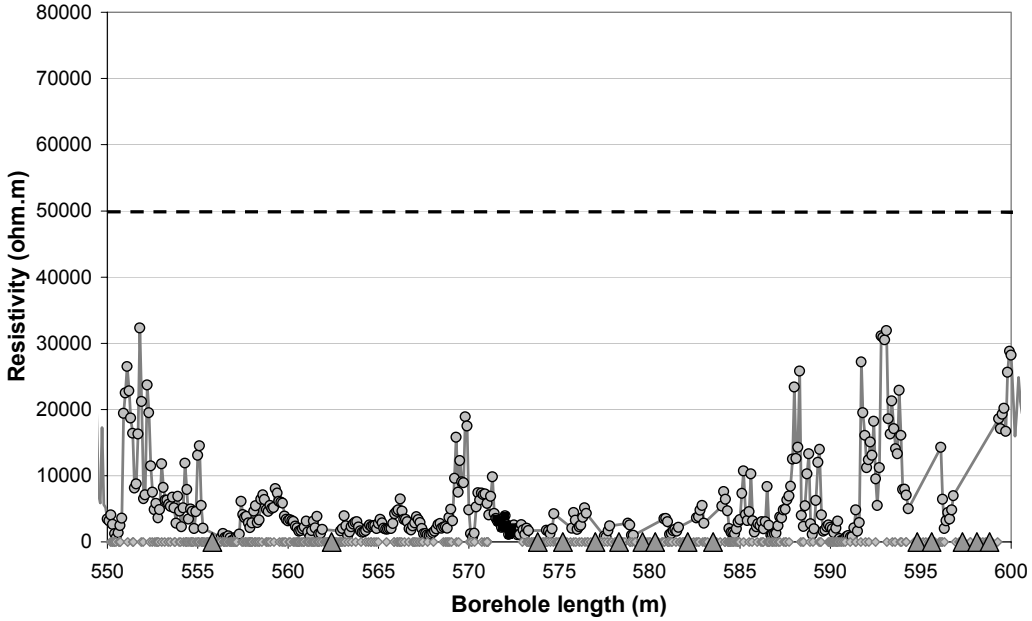

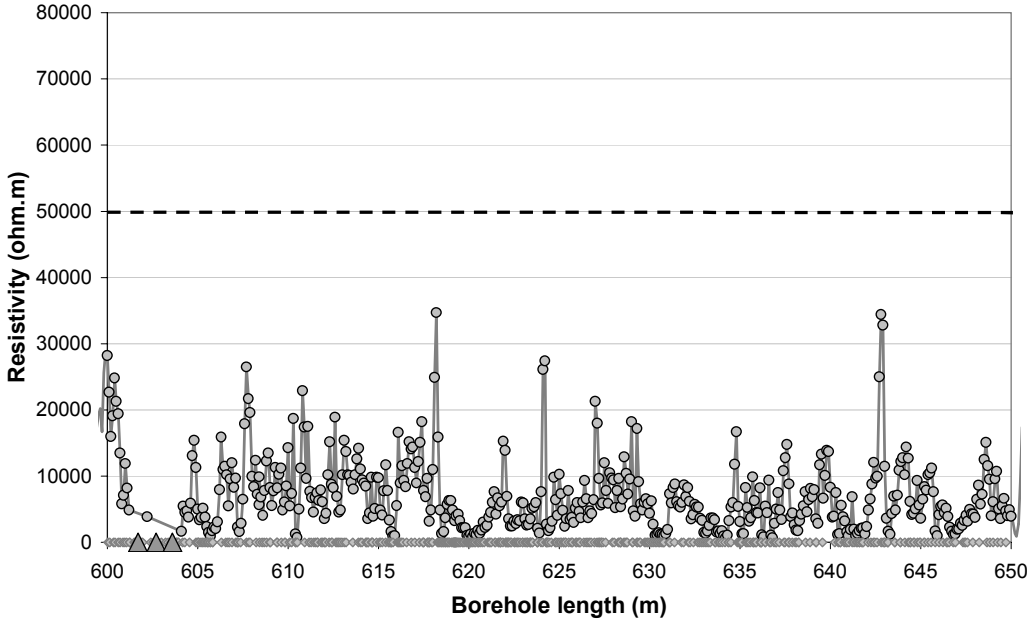

Fractured rock resistivity
Rock matrix resistivity
Location of natural fracture parting the bore core
Location of hydraulically conductive fracture detected in the difference flow logging
Upper limit of quantitative measuring range

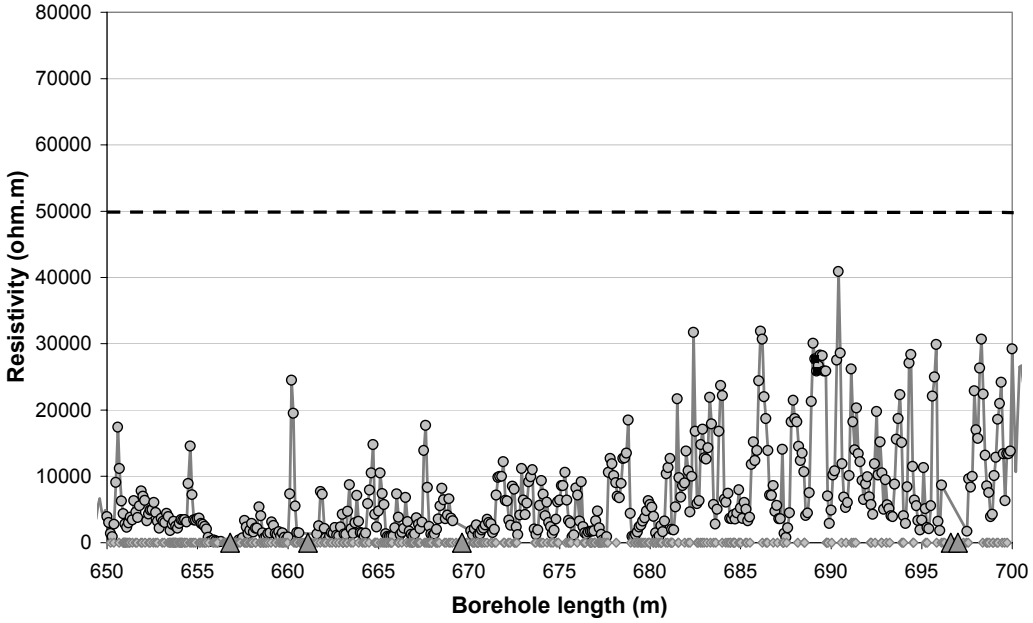

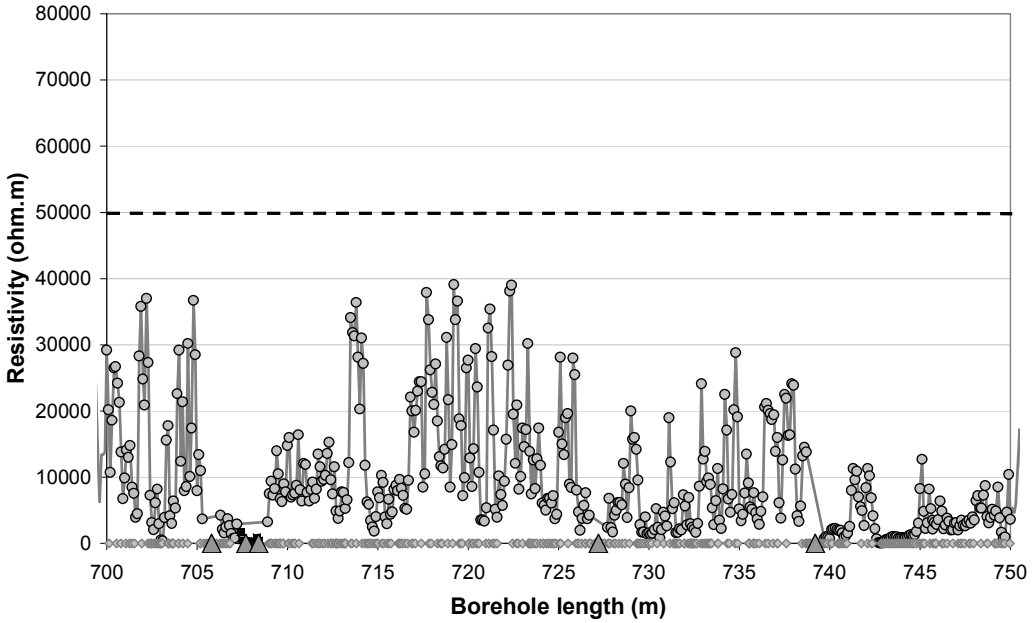

Fractured rock resistivity
Rock matrix resistivity
Location of natural fracture parting the bore core
Location of hydraulically conductive fracture detected in the difference flow logging
Upper limit of quantitative measuring range

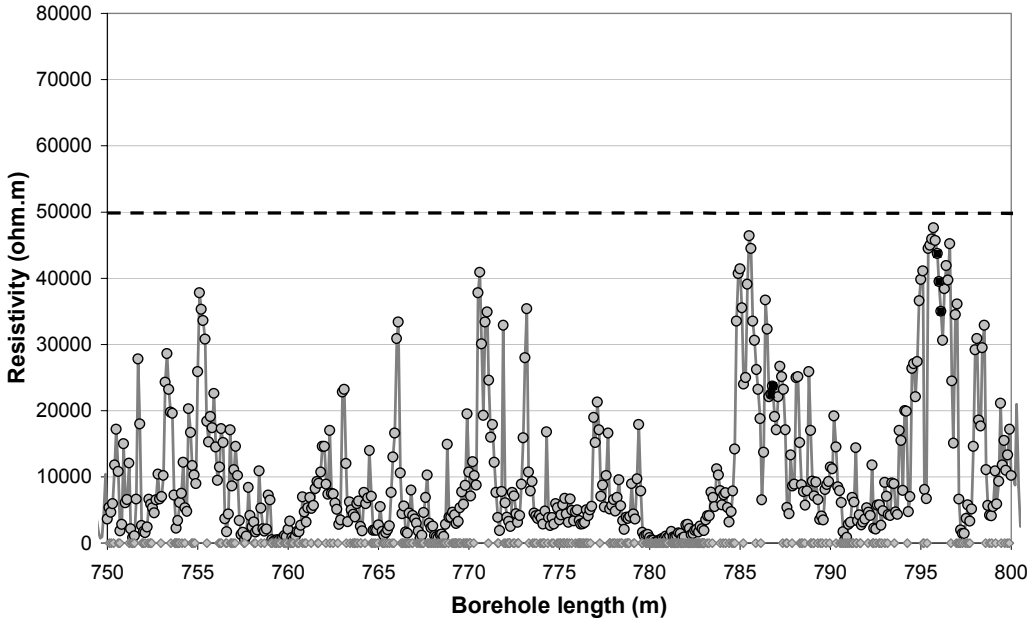

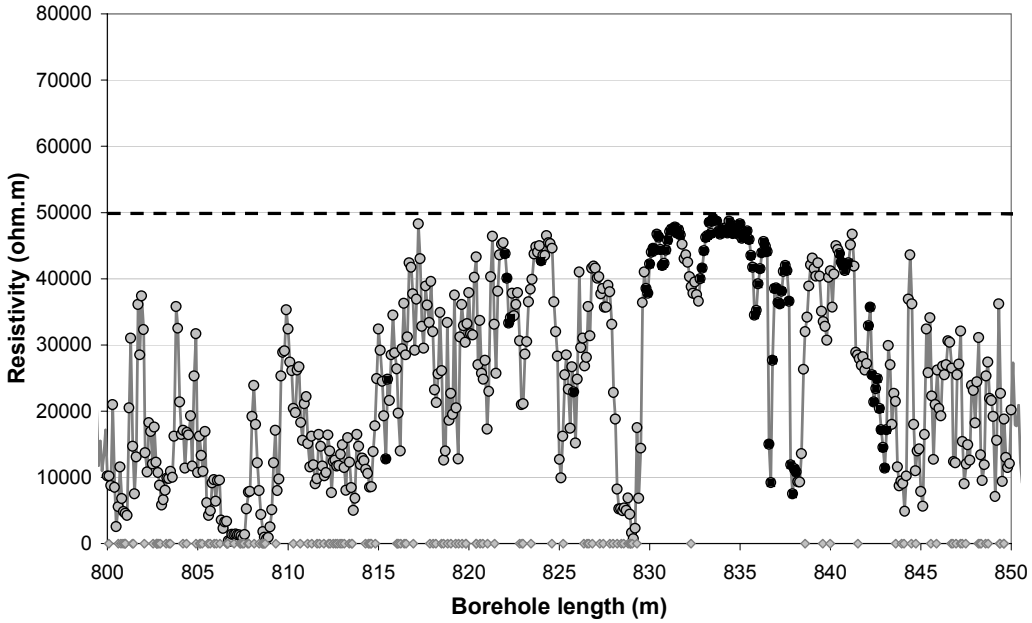

Fractured rock resistivity
Rock matrix resistivity
Location of natural fracture parting the bore core
Location of hydraulically conductive fracture detected in the difference flow logging
Upper limit of quantitative measuring range

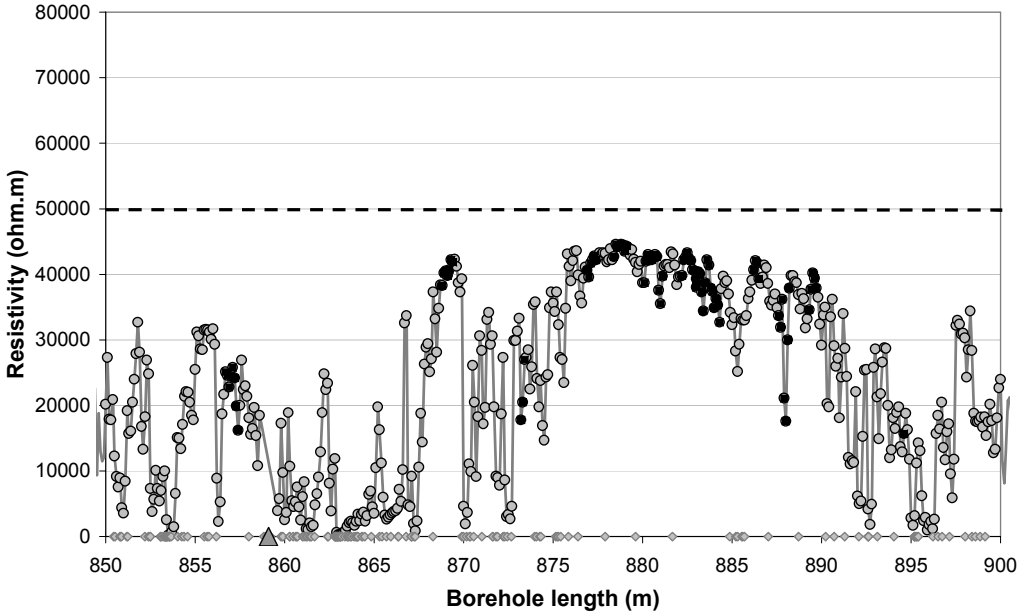

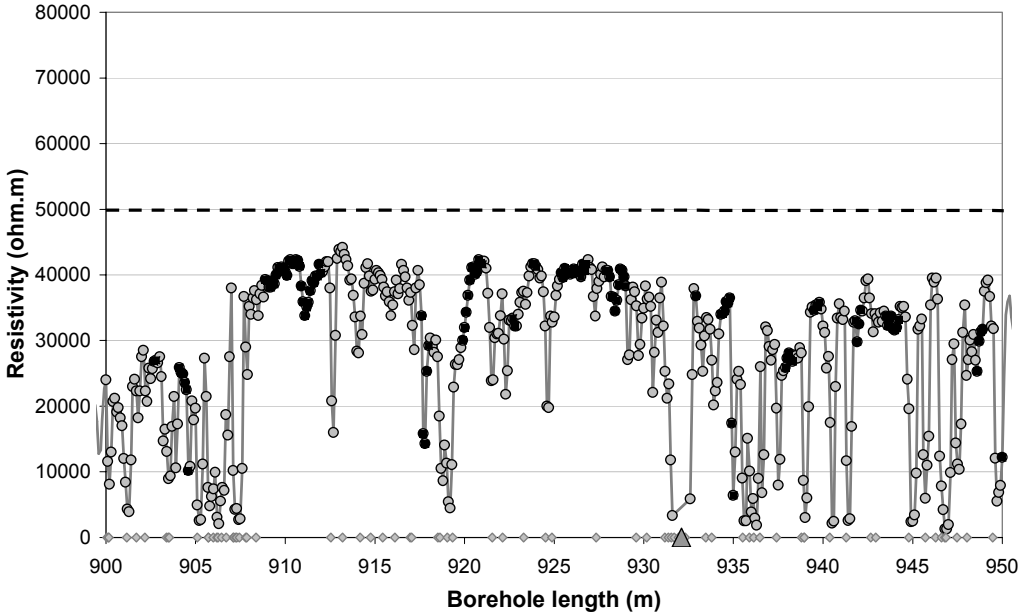

Fractured rock resistivity
Rock matrix resistivity
Location of natural fracture parting the bore core
Location of hydraulically conductive fracture detected in the difference flow logging
Upper limit of quantitative measuring range

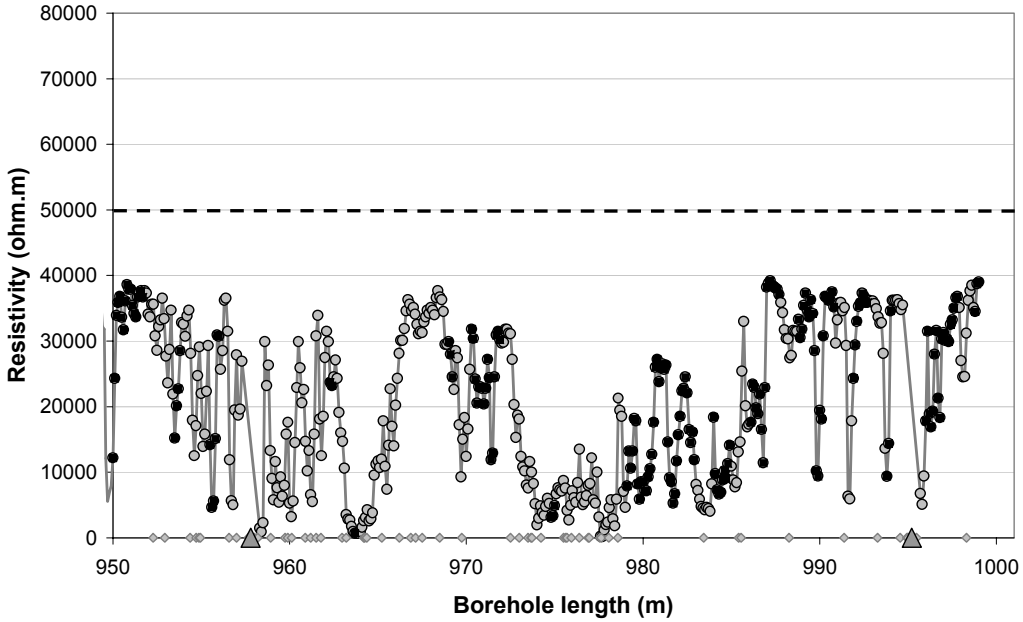

Fractured rock resistivity
Rock matrix resistivity
Location of natural fracture parting the bore core
Location of hydraulically conductive fracture detected in the difference flow logging
Upper limit of quantitative measuring range

Appendix B3: In-situ fracture specific EC in KSH02

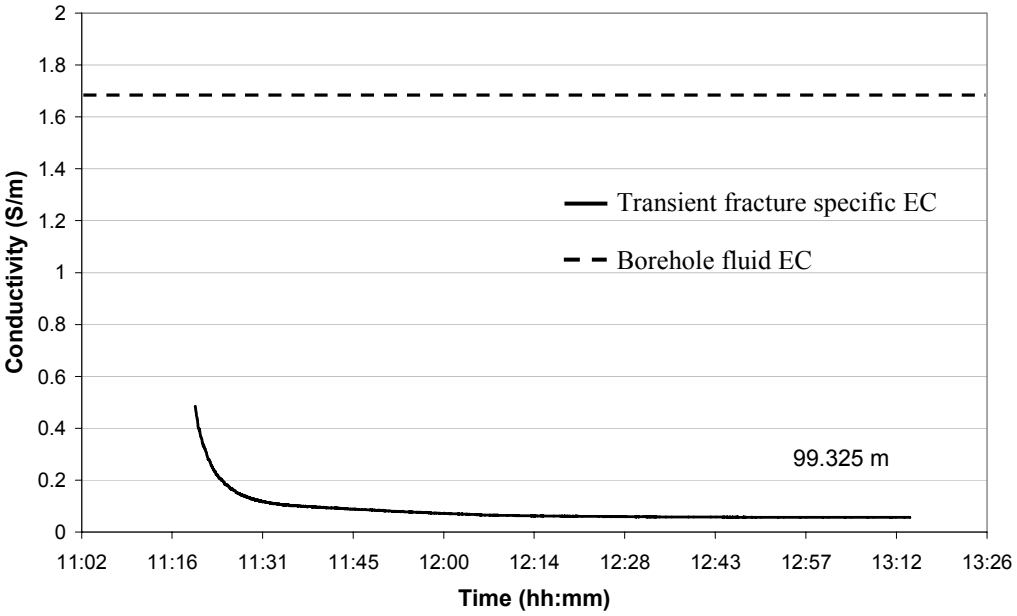

Borehole length: 99.325 m, fracture specific EC: 0.057 S/m
Comment: The obtained conductivity clearly deviates from that of the borehole fluid and there is no sign of leakage. The curve is non-fluctuating and there is no sign of gas formation or of other problems.

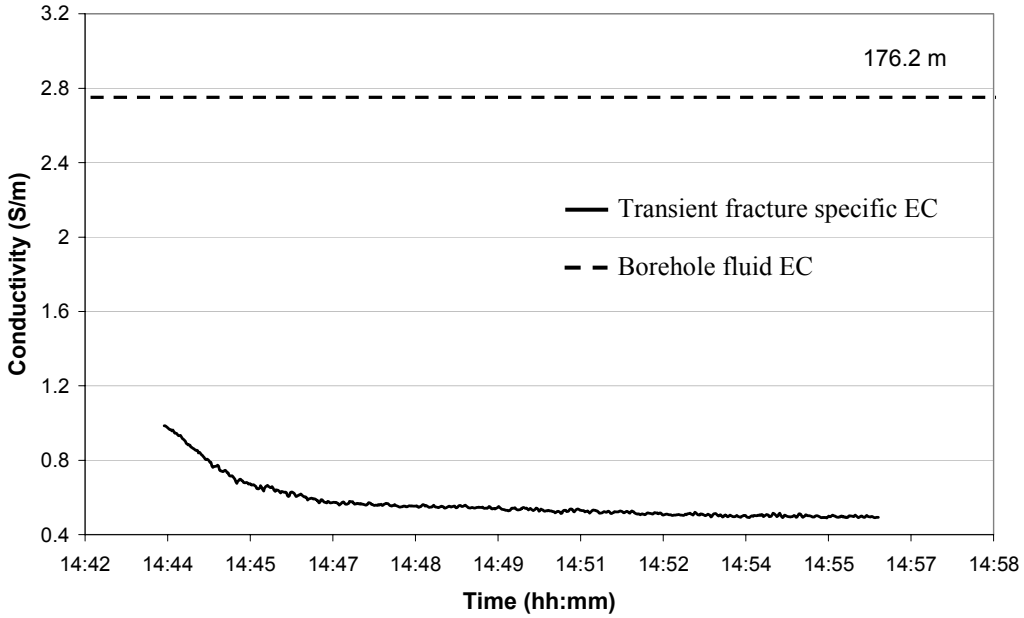

Borehole length: 176.2 m, fracture specific EC: 0.49 S/m
Comment: The obtained conductivity clearly deviates from that of the borehole fluid and there is no sign of leakage. The curve is non-fluctuating and there is no sign of gas formation or of other problems.

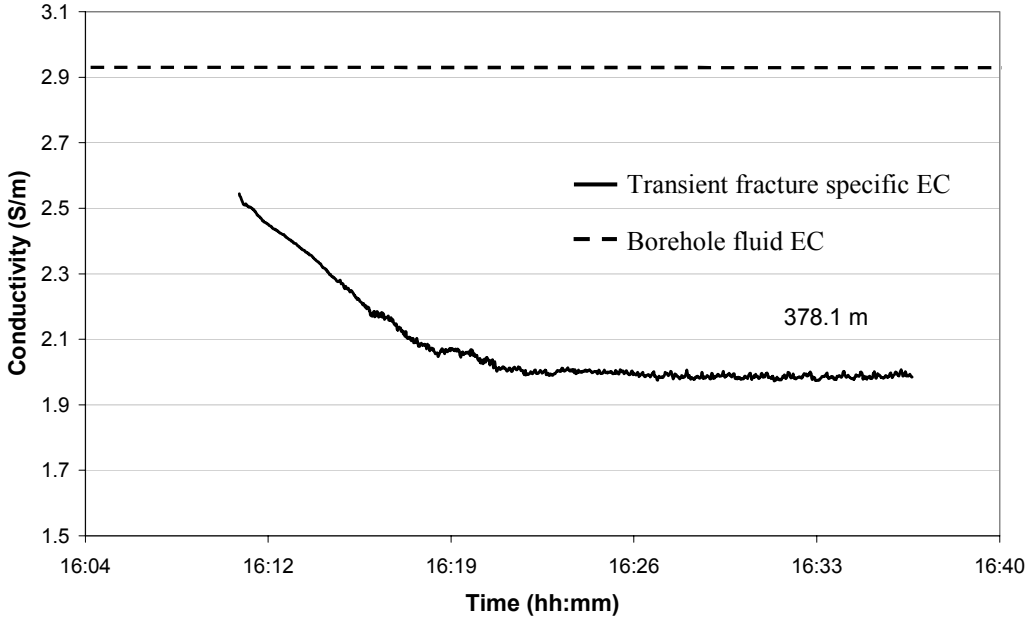

Borehole length: 378.1 m, fracture specific EC: 2.0 S/m
Comment: The obtained conductivity clearly deviates from that of the borehole fluid and there is no sign of leakage. The curve is non-fluctuating and there is no sign of gas formation or of other problems.

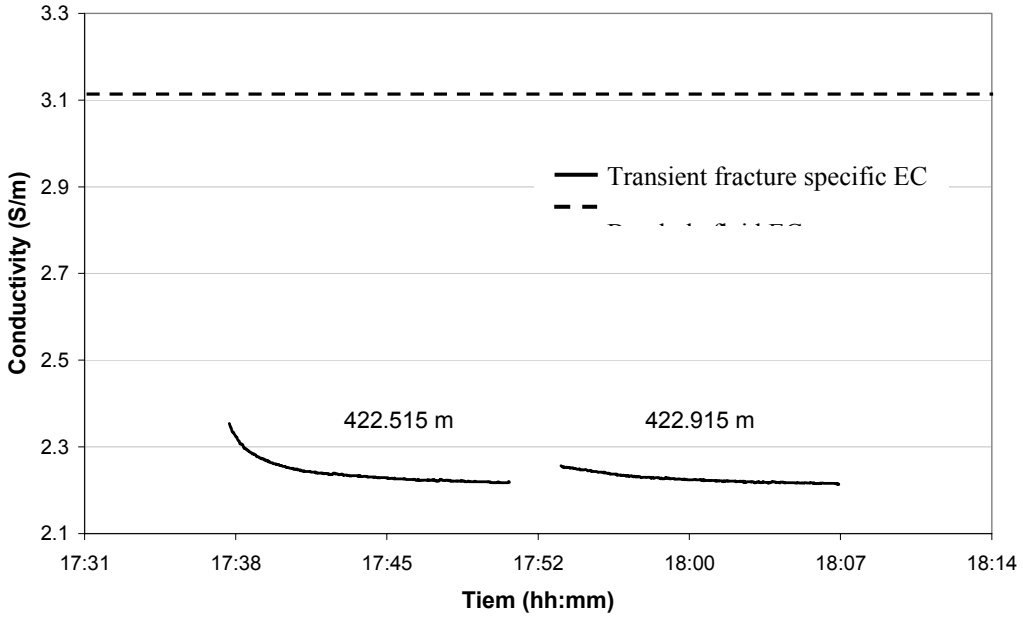

Borehole length: 422.715 m (422.515 and 422.915 m), fracture specific EC: 2.2 S/m
Comment: Two curves were obtained from two nearby fractures. The obtained conductivity clearly deviates from that of the borehole fluid and there is no sign of leakage. The curves are non-fluctuating and there is no sign of gas formation or of other problems. As it is likely that the fractures are interconnected, a single value was chosen at the borehole length 422.715.

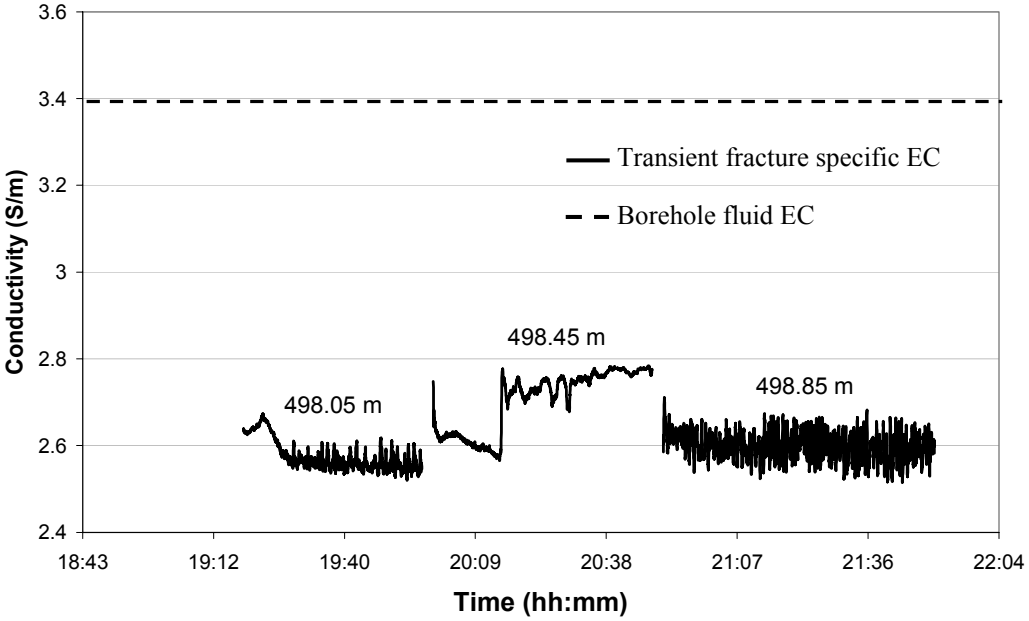

Borehole length: 498.45 m (498.05 and 498.85 m), fracture specific EC: 2.6 S/m
Comment: Three curves were obtained from three nearby fractures. The curve taken at 498.45 m indicates that a leakage occurred at the time 20:15. Therefore this curve was dismissed. The curves taken at 498.05 and 498.85 fluctuate and this may indicate formation of gas or some leakage. However the fluctuations are small enough to obtain a reasonable stable conductivity. The obtained resistivity deviates clearly from that of the borehole fluid so possible a leakage would have to be a minor leakage. As it is likely that the fractures are interconnected a single value was chosen at the borehole length 498.45.

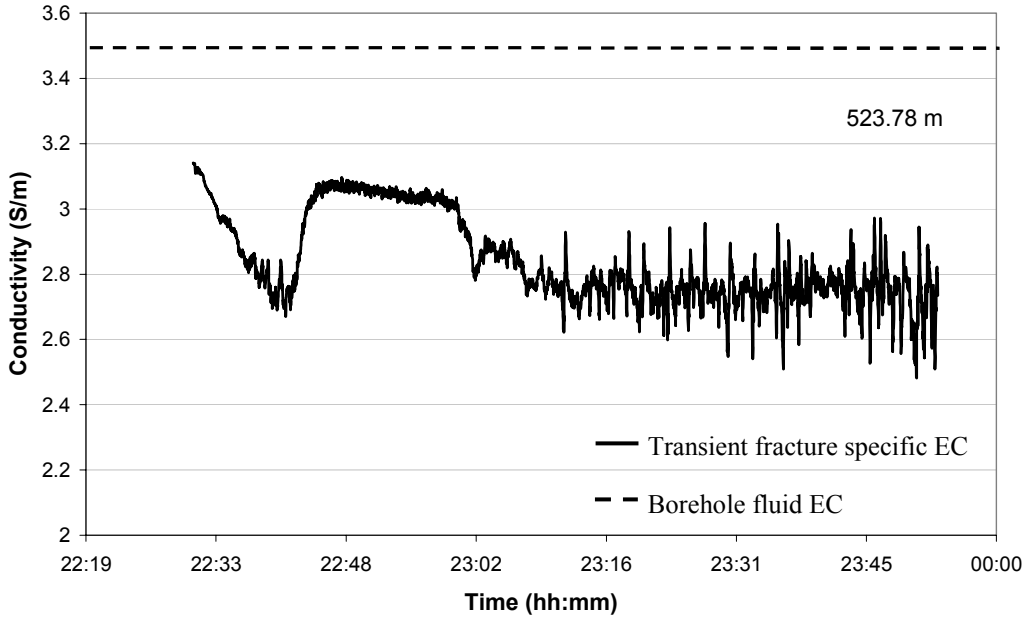

Borehole length: 523.78 m, fracture specific EC: 2.7 S/m
Comment: The curve taken at 498.45 m indicates that a leakage occurred at the time 22:42 for about 15 minutes. Thereafter the curve does not seem to be influenced by a major leakage. The curve fluctuates and this may indicate formation of gas or a minor leakage. However the fluctuations are small enough to obtain a reasonable stable conductivity. This conductivity deviates significantly from that of the borehole fluid.

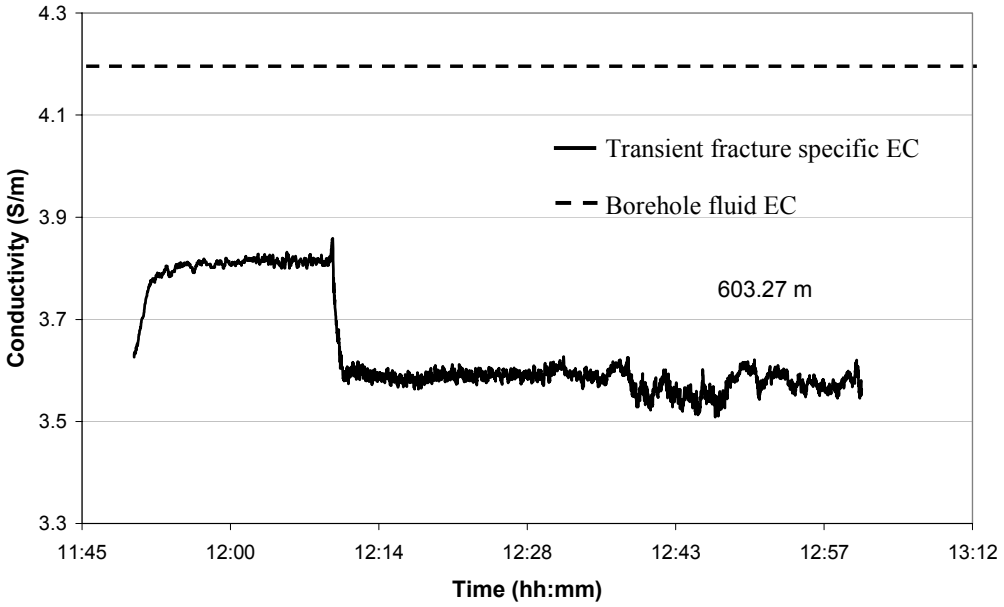

Borehole length: 603.27 m, fracture specific EC: 3.6 S/m
Comment: The obtained conductivity clearly deviates from that of the borehole fluid. There seems to be a leakage in the first 20 minutes of the measurement. Thereafter there are no sign of a major leakage. The curve fluctuates and this may indicate formation of gas or a minor leakage. However the fluctuations are small enough to obtain a reasonable stable conductivity.

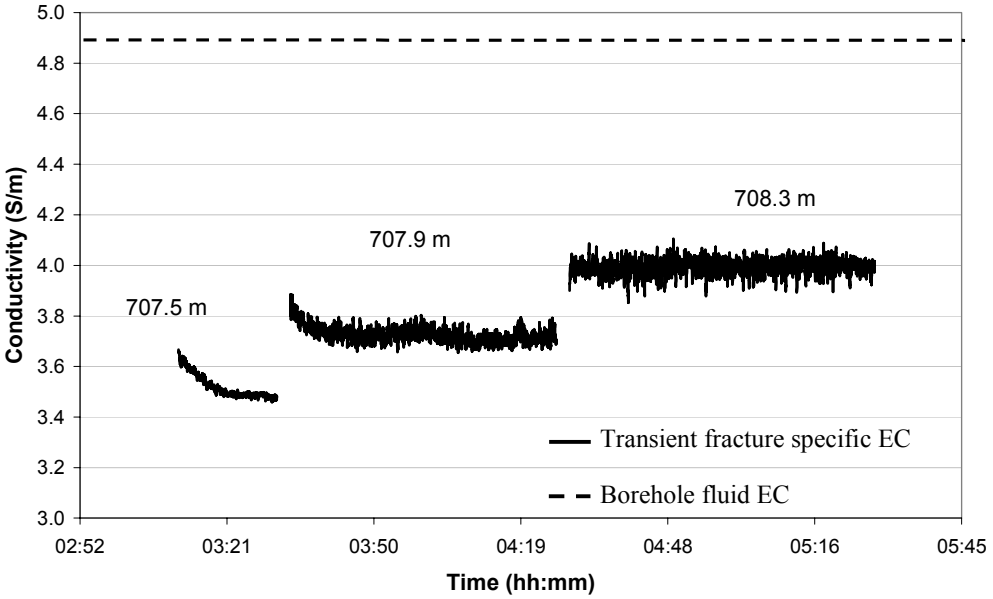

Borehole length: 707.7 m (707.5 and 707.9 m), fracture specific EC: 3.6 S/m
Comment: Three curves were obtained from three nearby fractures. The curve taken at 708.3 did not display the characteristic shape of going from an initial value and stabilize at an end value and was therefore dismissed. The conductivity taken at 707.5 clearly deviates from that of the borehole fluid and there is no sign of leakage. The curve is non-fluctuating and there is no sign of gas formation or of other problems. The conductivity taken at 707.9 clearly deviates from that of the borehole fluid and there is no sign of major leakage. The curve fluctuates and this may indicate formation of gas or a minor leakage. However the fluctuations are small enough to obtain a reasonable stable conductivity. As it is likely that the fractures are interconnected a single value was chosen at the borehole length 707.7 m.

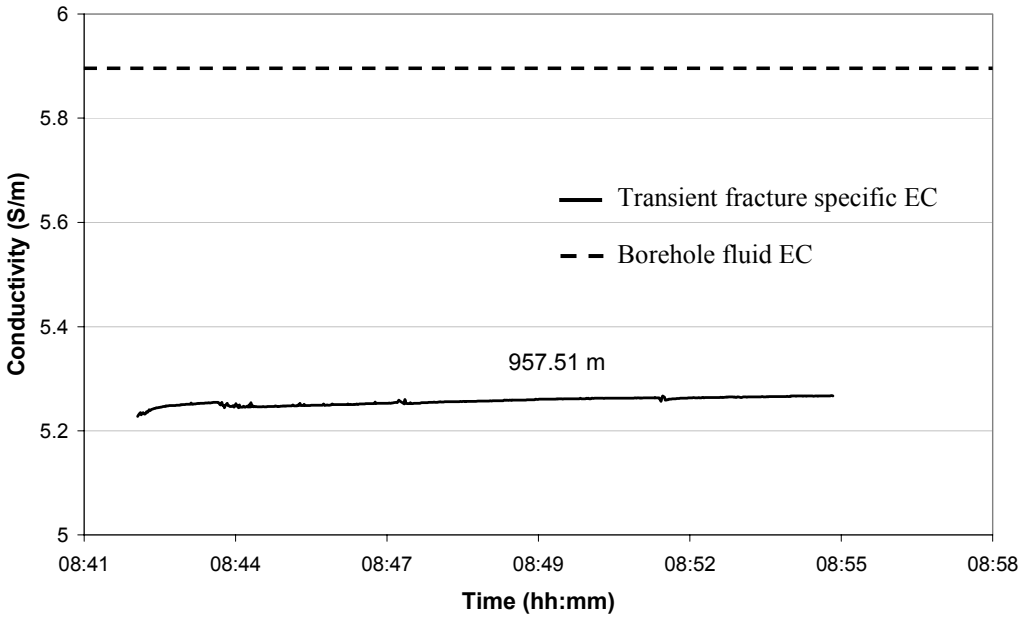

Borehole length: 957.51 m, fracture specific EC: 5.3 S/m
Comment: The curve did not display the characteristic shape of going from an initial value and stabilize at an end value and therefore one could suspect some leakage. However, as this is in the lower end of the borehole the fracture specific EC should be close to that of the borehole fluid, as the borehole fluid is pumped upwards. Therefore the resistivity obtained did not seem unreasonable and was kept. The curve is non-fluctuating and there is no sign of gas formation.

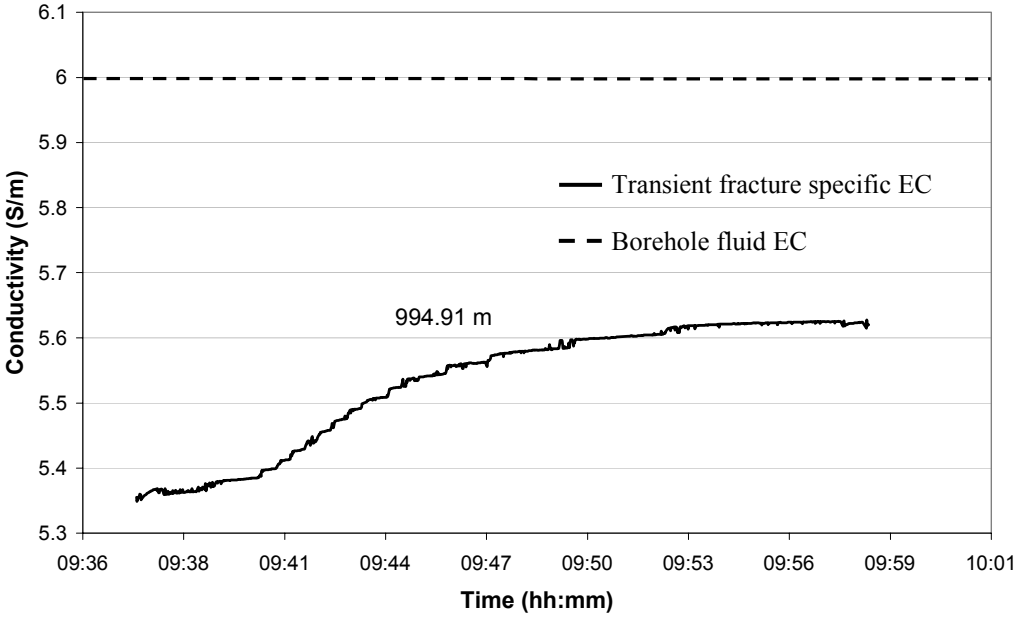

Borehole length: 994.91 m, fracture specific EC: 5.6 S/m
Comment: The obtained conductivity clearly deviates from that of the borehole fluid and there is no sign of leakage. Initially the sealed off borehole section is likely to contain groundwater from the fracture at 957.51 m. The curve is non-fluctuating and there is no sign of gas formation or of other problems.

Appendix B4: In-situ borehole fluid EC in KSH02

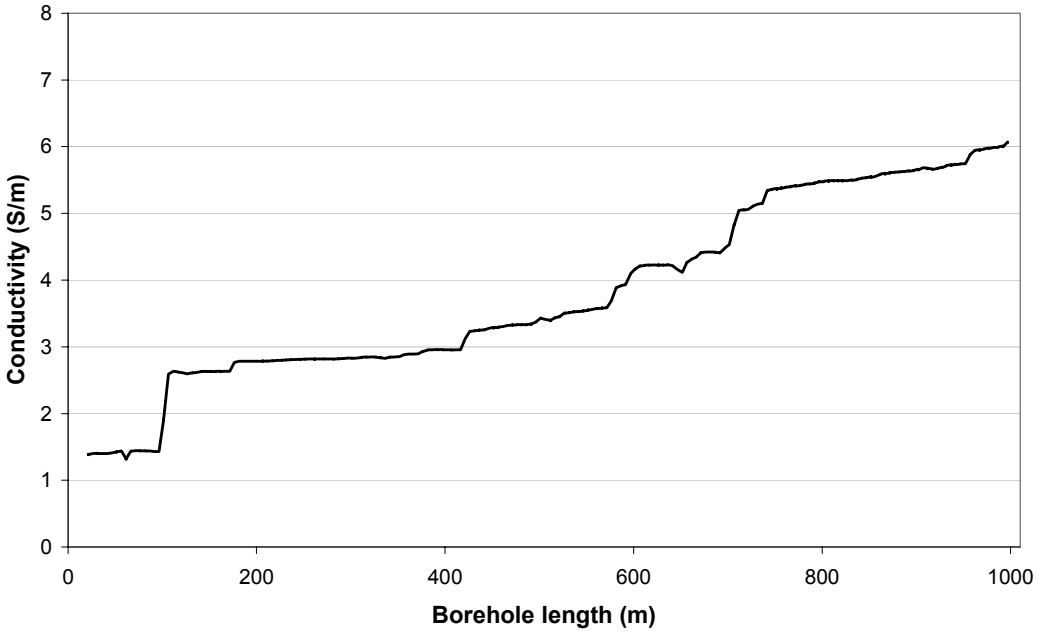

Borehole length: 1,000 m, fracture specific EC: 6.0 S/m
Comment: Above the borehole fluid EC log taken after extensive pumping by the difference flow measurements is shown. It is notable that the conductivity of the borehole fluid at the end of the borehole is around 6 S/m. This could indicate a hydraulically conductive fracture below 997 m, where the difference flow log was not used. It is assumed that the groundwater EC at a borehole length of 1,000 m is 6.0 S/m.

Appendix C

Appendix C1: In-situ and laboratory formation factors KSH01A

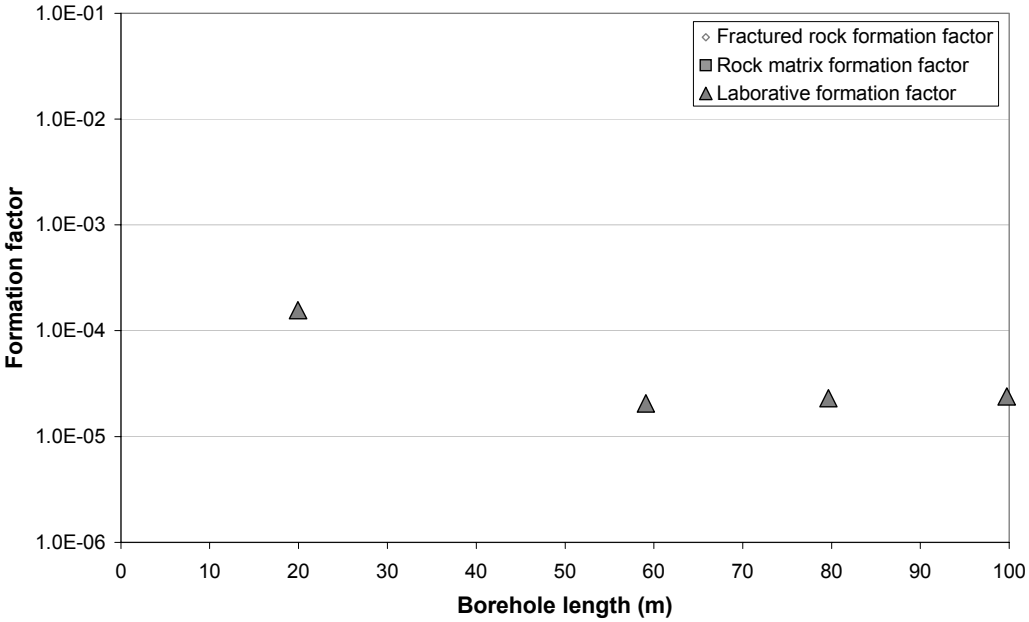

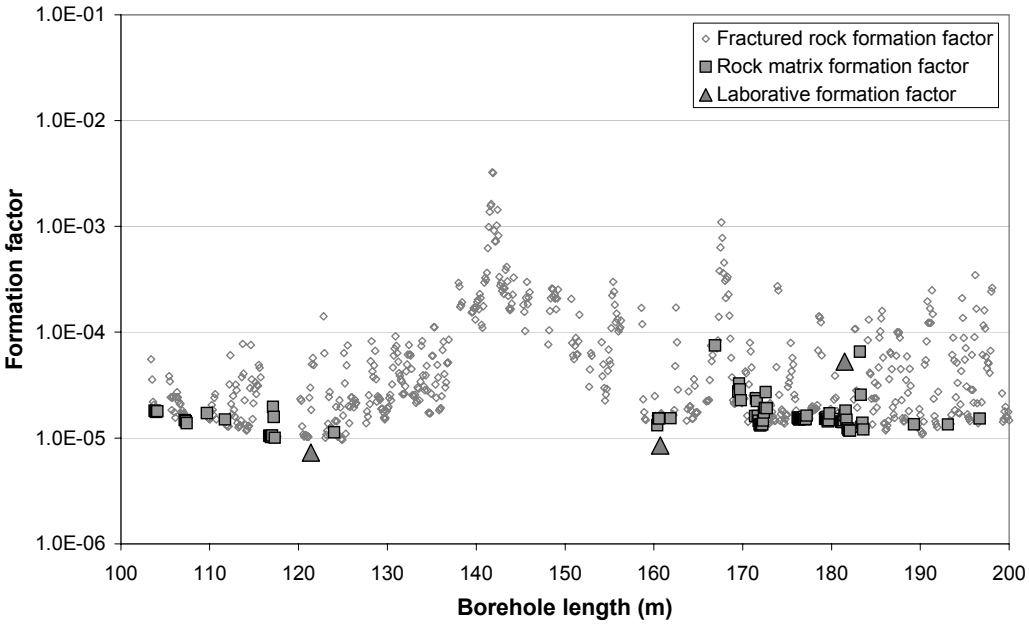

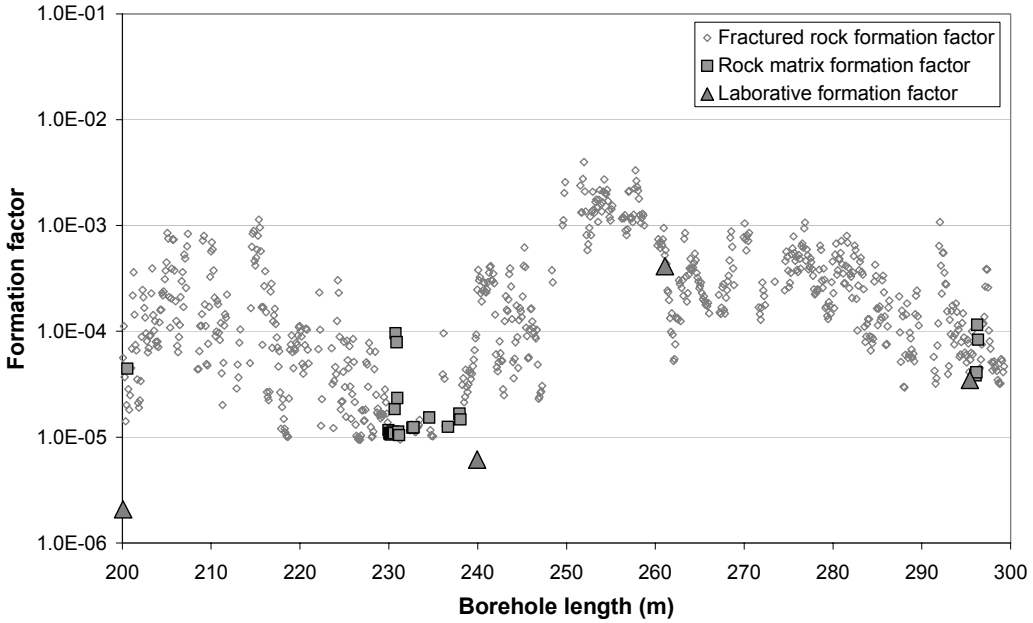
Fractured rock formation factor
Rock matrix formation factor
Laborative formation factor
Formation factor
1.0E-01
1.0E-02
1.0E-03
1.0E-04
1.0E-05
1.0E-06
200
210
220
230
240
250
260
270
280
290
300
Borehole length (m)

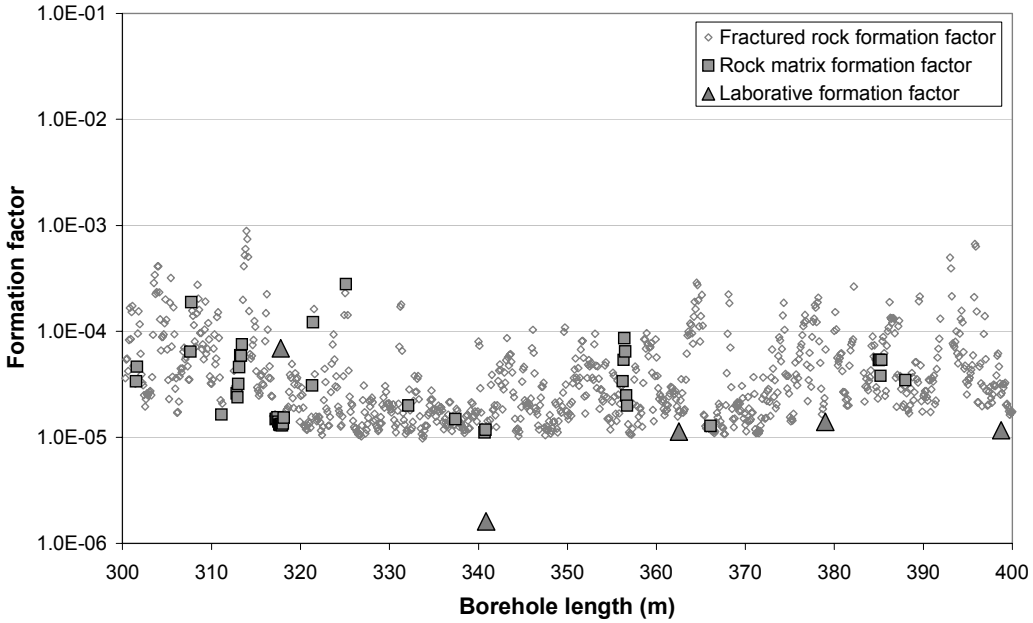
Fractured rock formation factor
Rock matrix formation factor
Laborative formation factor
Formation factor
1.0E-01
1.0E-02
1.0E-03
1.0E-04
1.0E-05
1.0E-06
300
310
320
330
340
350
360
370
380
390
400
Borehole length (m)

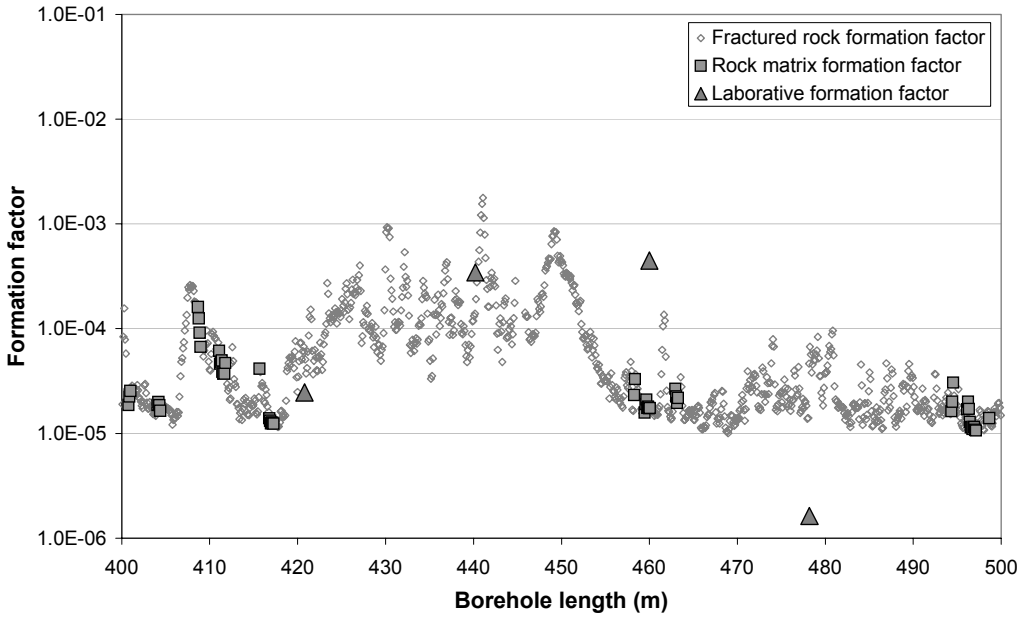
Fractured rock formation factor
Rock matrix formation factor
Laborative formation factor
Formation factor
1.0E-01
1.0E-02
1.0E-03
1.0E-04
1.0E-05
1.0E-06
400
410
420
430
440
450
460
470
480
490
500
Borehole length (m)

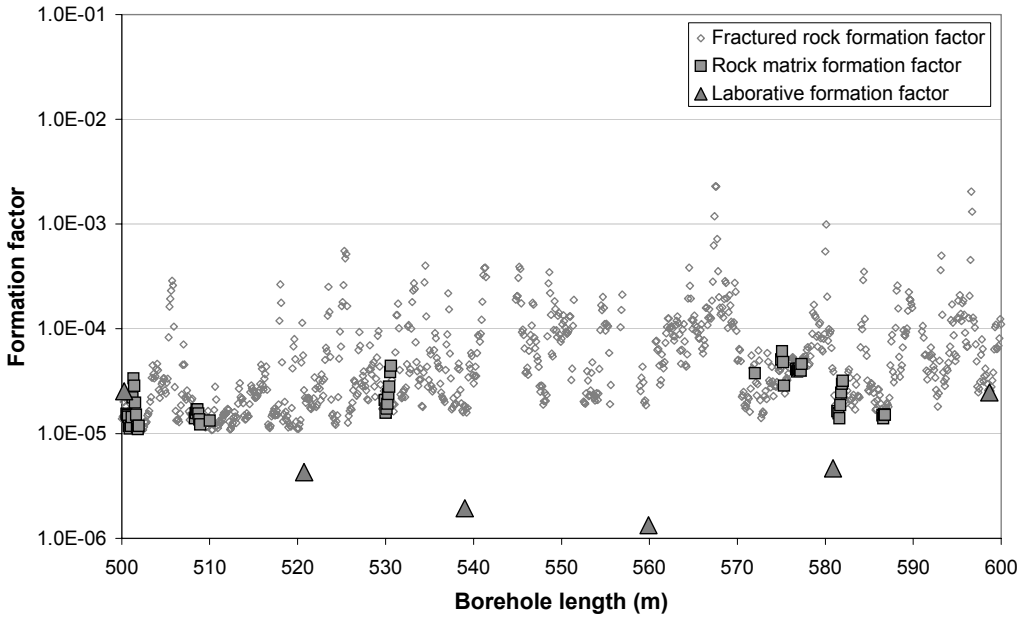
Fractured rock formation factor
Rock matrix formation factor
Laborative formation factor
Formation factor
1.0E-01
1.0E-02
1.0E-03
1.0E-04
1.0E-05
1.0E-06
500
510
520
530
540
550
560
570
580
590
600
Borehole length (m)

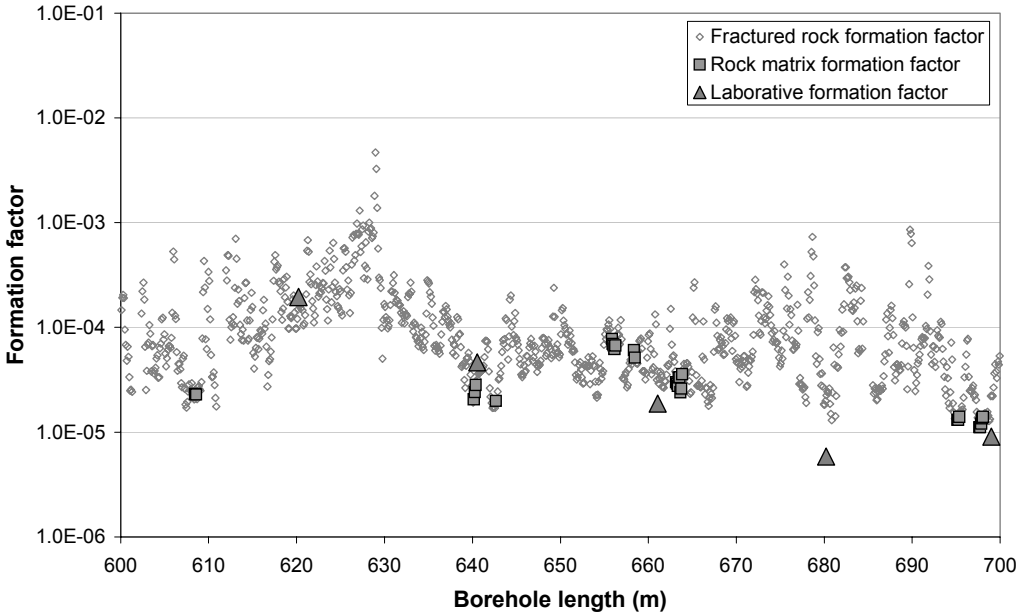
Fractured rock formation factor
Rock matrix formation factor
Laborative formation factor
Formation factor
1.0E-01
1.0E-02
1.0E-03
1.0E-04
1.0E-05
1.0E-06
600
610
620
630
640
650
660
670
680
690
700
Borehole length (m)

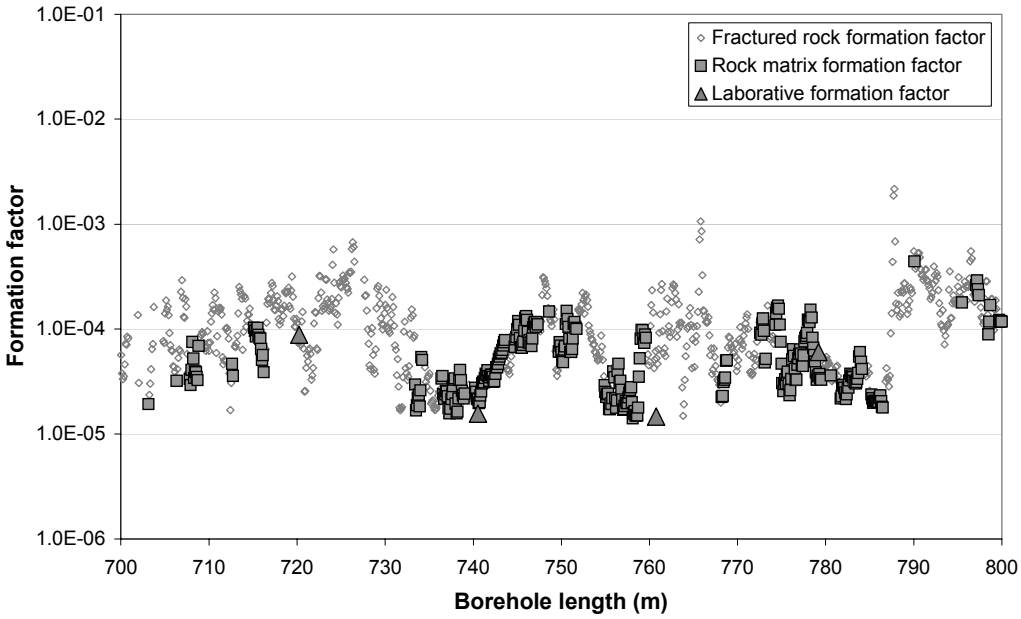
Fractured rock formation factor
Rock matrix formation factor
Laborative formation factor
Formation factor
1.0E-01
1.0E-02
1.0E-03
1.0E-04
1.0E-05
1.0E-06
700
710
720
730
740
750
760
770
780
790
800
Borehole length (m)

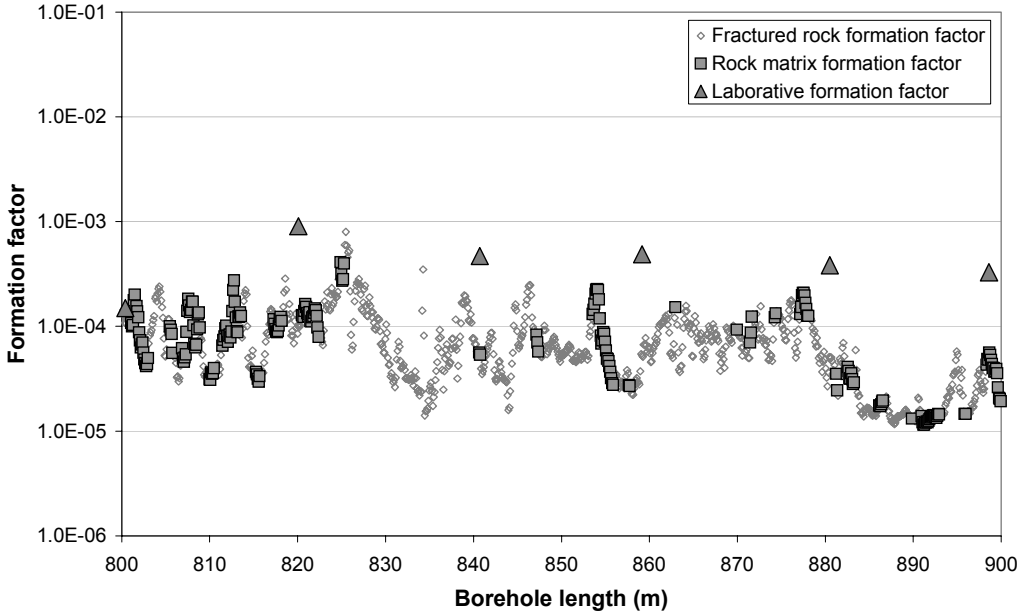
Fractured rock formation factor
Rock matrix formation factor
Laborative formation factor
Formation factor
1.0E-01
1.0E-02
1.0E-03
1.0E-04
1.0E-05
1.0E-06
800
810
820
830
840
850
860
870
880
890
900
Borehole length (m)

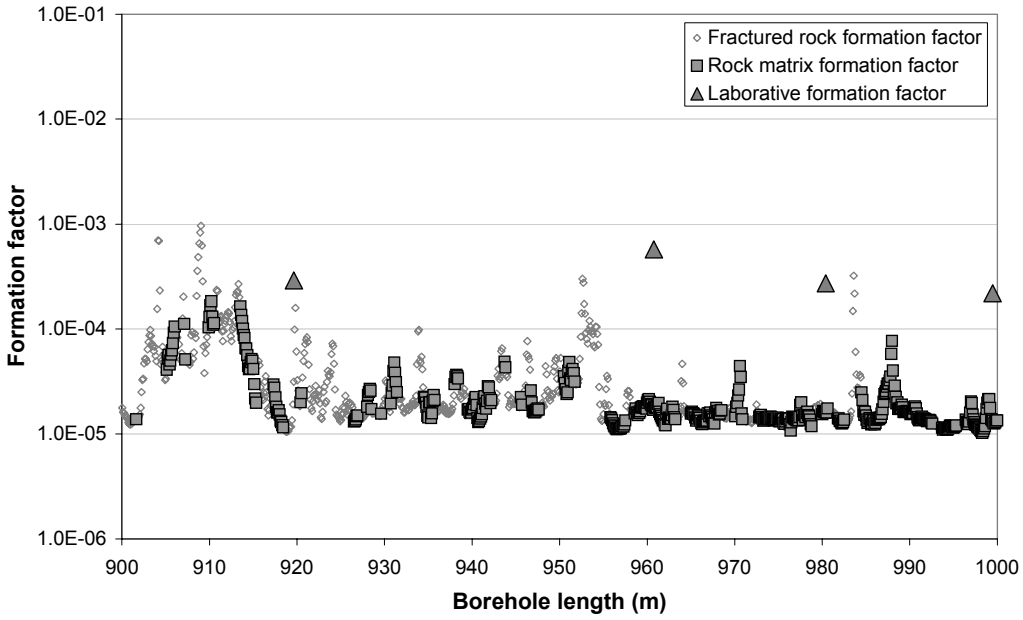
Fractured rock formation factor
Rock matrix formation factor
Laborative formation factor
Formation factor
1.0E-01
1.0E-02
1.0E-03
1.0E-04
1.0E-05
1.0E-06
900
910
920
930
940
950
960
970
980
990
1000
Borehole length (m)

Appendix C2: In-situ and laboratory formation factors KSH02

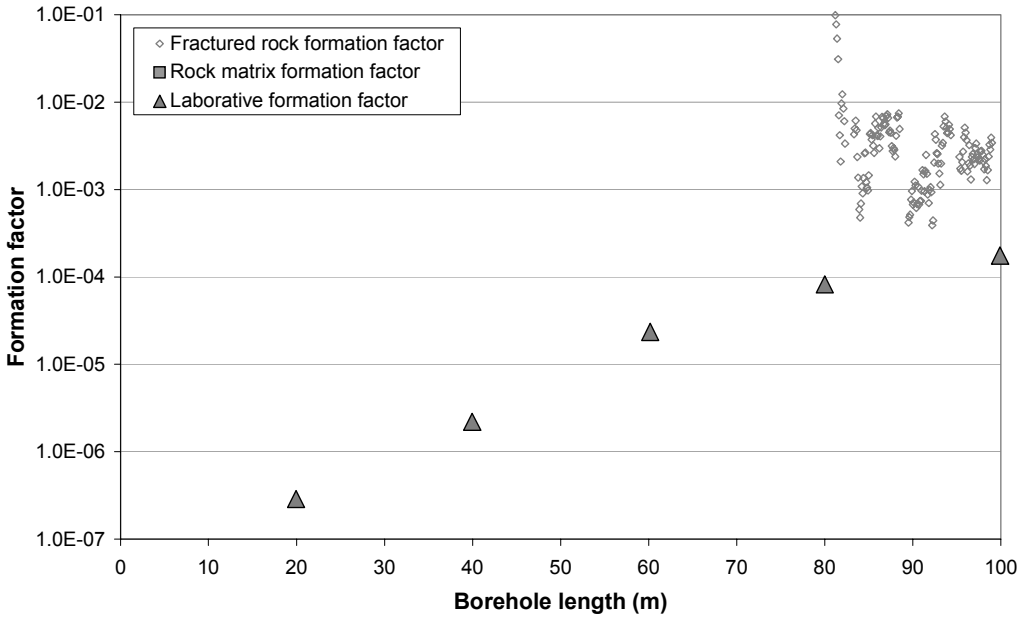

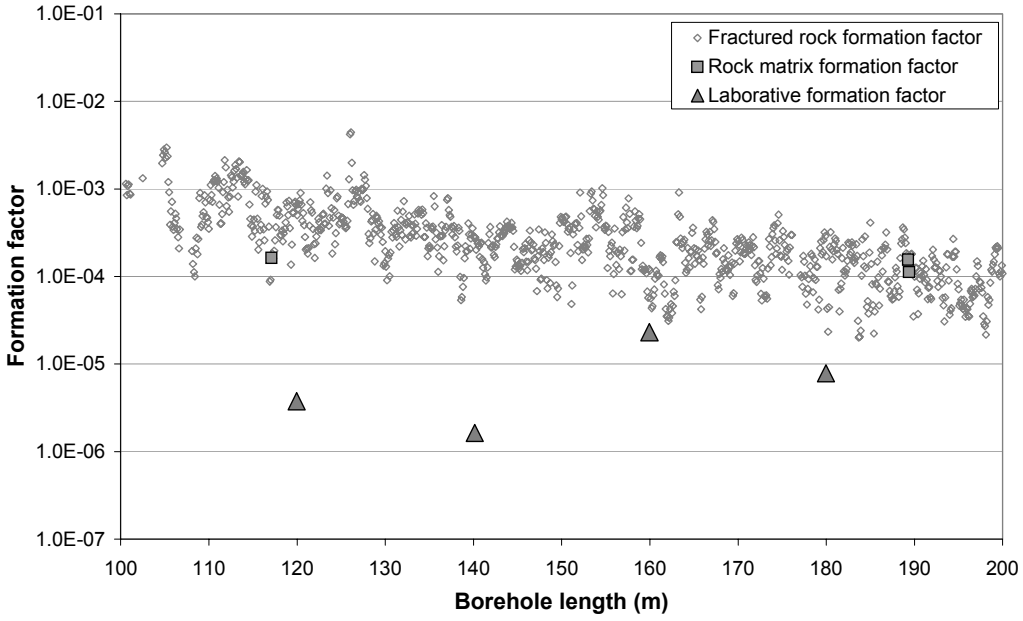

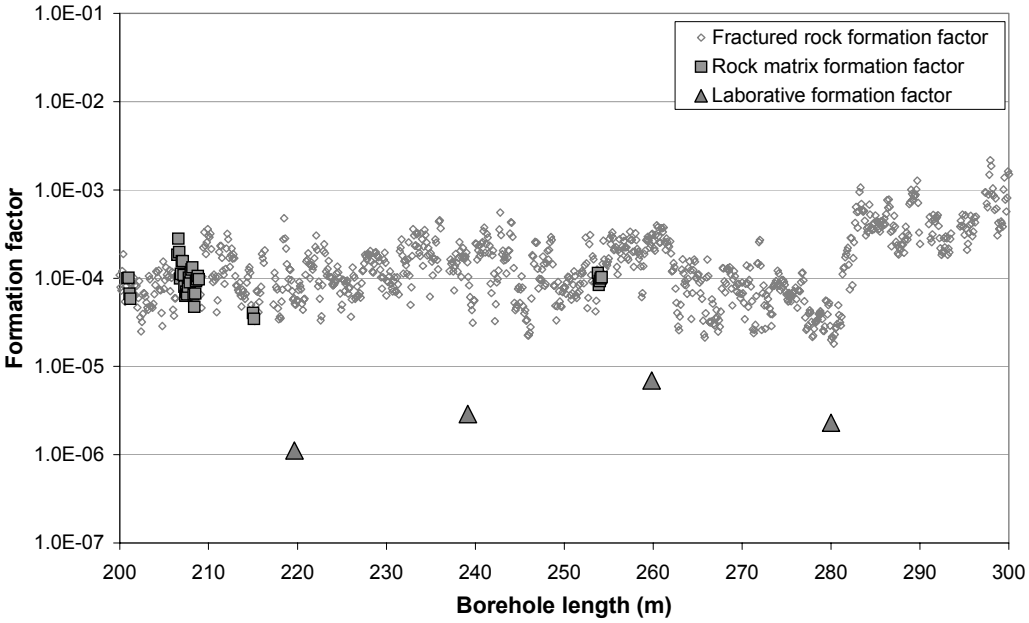
Fractured rock formation factor
Rock matrix formation factor
Laborative formation factor
Formation factor
1.0E-01
1.0E-02
1.0E-03
1.0E-04
1.0E-05
1.0E-06
1.0E-07
200
210
220
230
240
250
260
270
280
290
300
Borehole length (m)

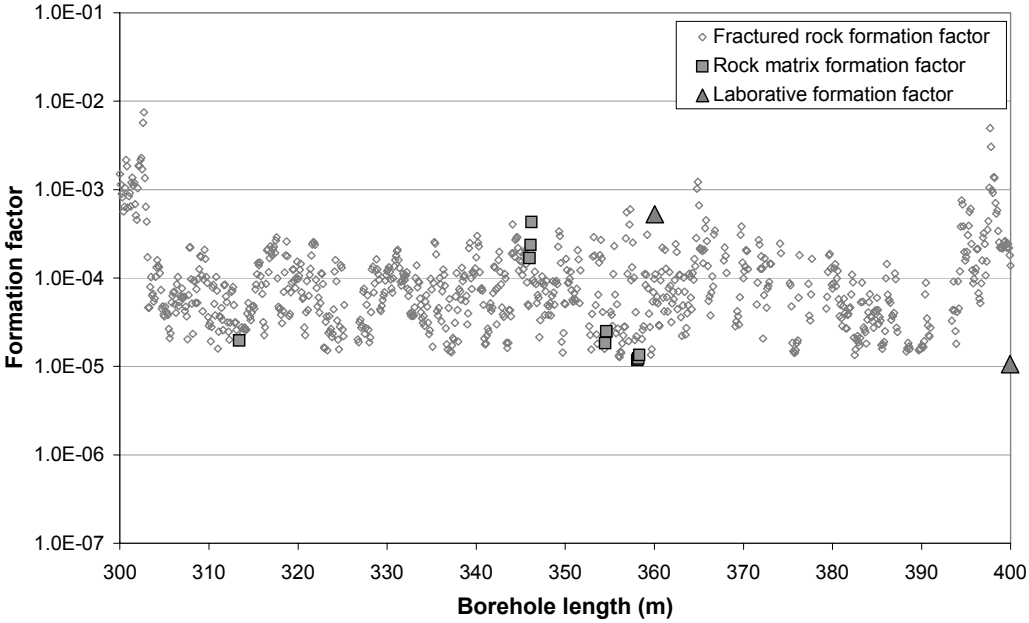
Fractured rock formation factor
Rock matrix formation factor
Laborative formation factor
Formation factor
1.0E-01
1.0E-02
1.0E-03
1.0E-04
1.0E-05
1.0E-06
1.0E-07
300
310
320
330
340
350
360
370
380
390
400
Borehole length (m)

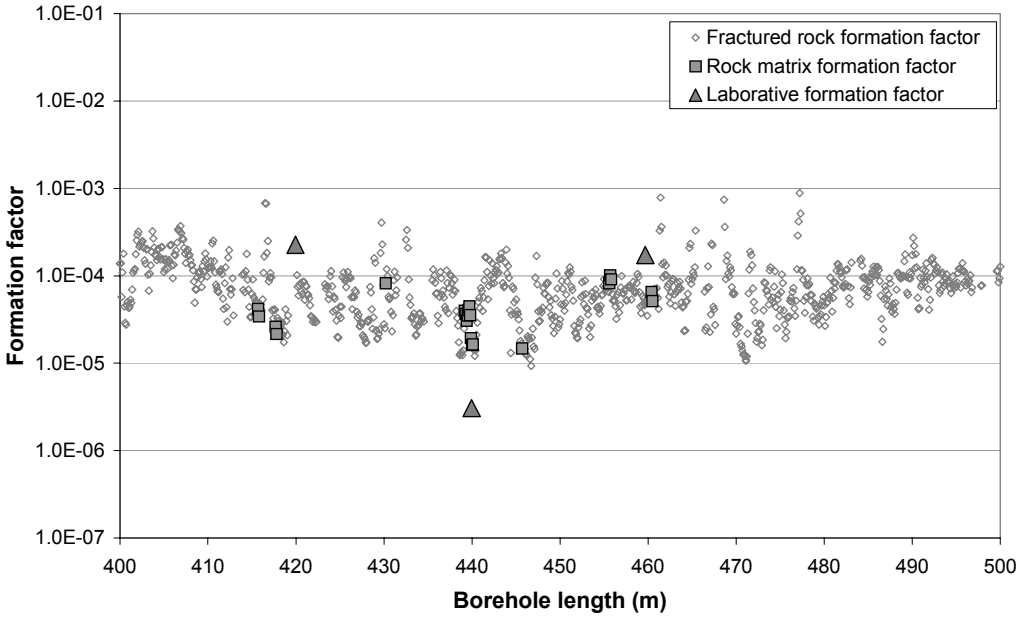
Fractured rock formation factor
Rock matrix formation factor
Laborative formation factor
Formation factor
1.0E-01
1.0E-02
1.0E-03
1.0E-04
1.0E-05
1.0E-06
1.0E-07
400
410
420
430
440
450
460
470
480
490
500
Borehole length (m)

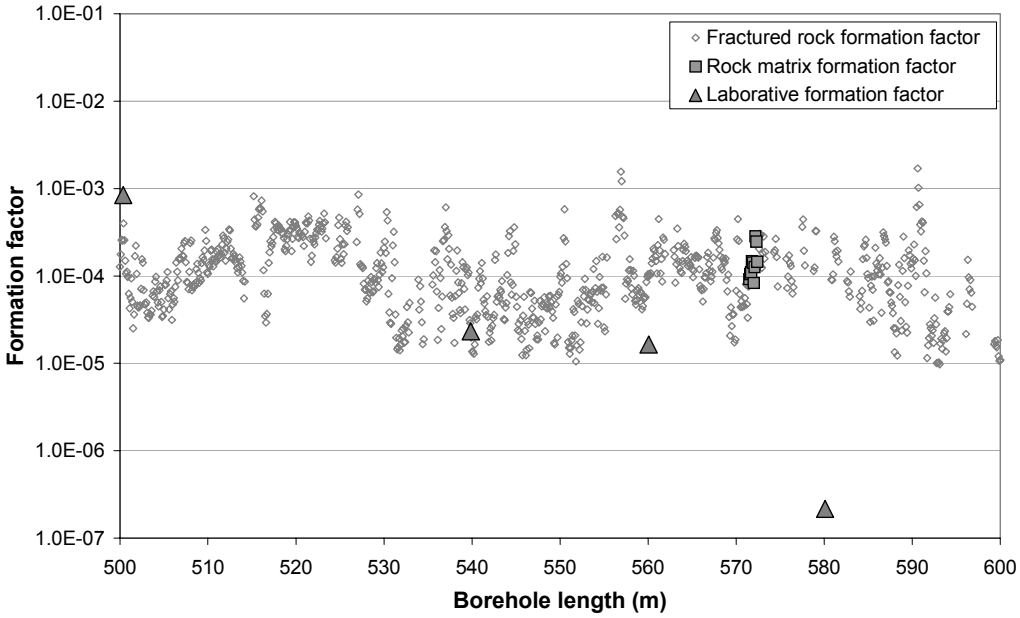
Fractured rock formation factor
Rock matrix formation factor
Laborative formation factor
Formation factor
1.0E-01
1.0E-02
1.0E-03
1.0E-04
1.0E-05
1.0E-06
1.0E-07
500
510
520
530
540
550
560
570
580
590
600
Borehole length (m)

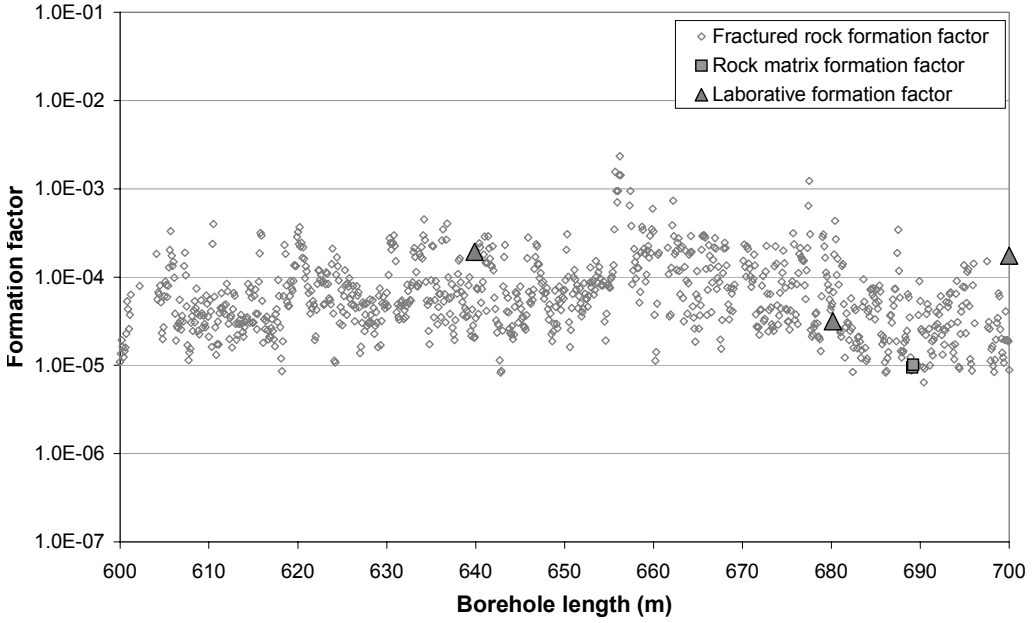
Fractured rock formation factor
Rock matrix formation factor
Laborative formation factor
Formation factor
1.0E-01
1.0E-02
1.0E-03
1.0E-04
1.0E-05
1.0E-06
1.0E-07
600
610
620
630
640
650
660
670
680
690
700
Borehole length (m)

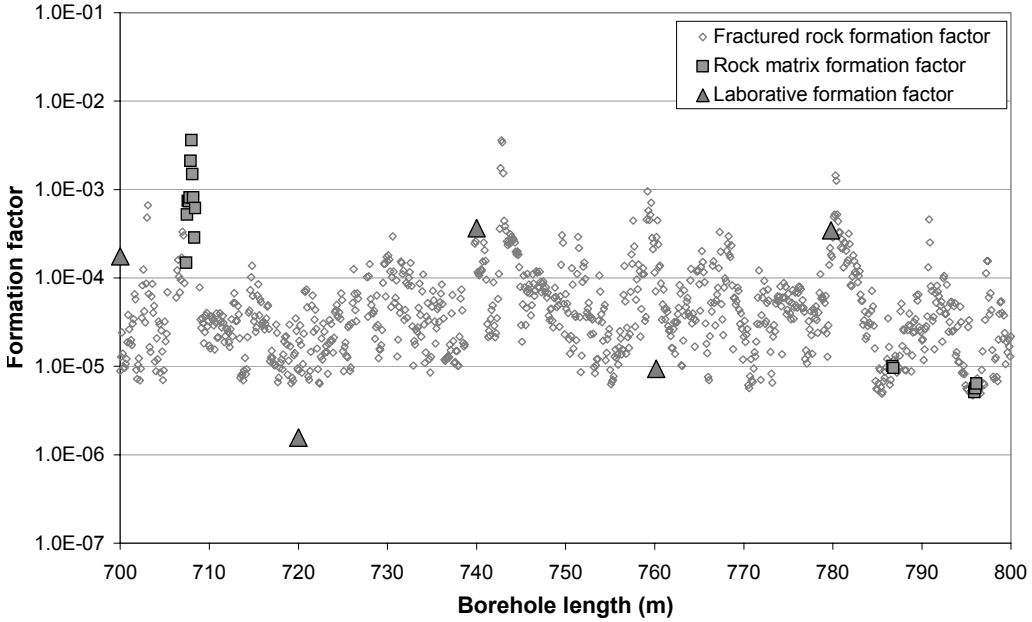
Fractured rock formation factor
Rock matrix formation factor
Laborative formation factor
Formation factor
1.0E-01
1.0E-02
1.0E-03
1.0E-04
1.0E-05
1.0E-06
1.0E-07
700
710
720
730
740
750
760
770
780
790
800
Borehole length (m)

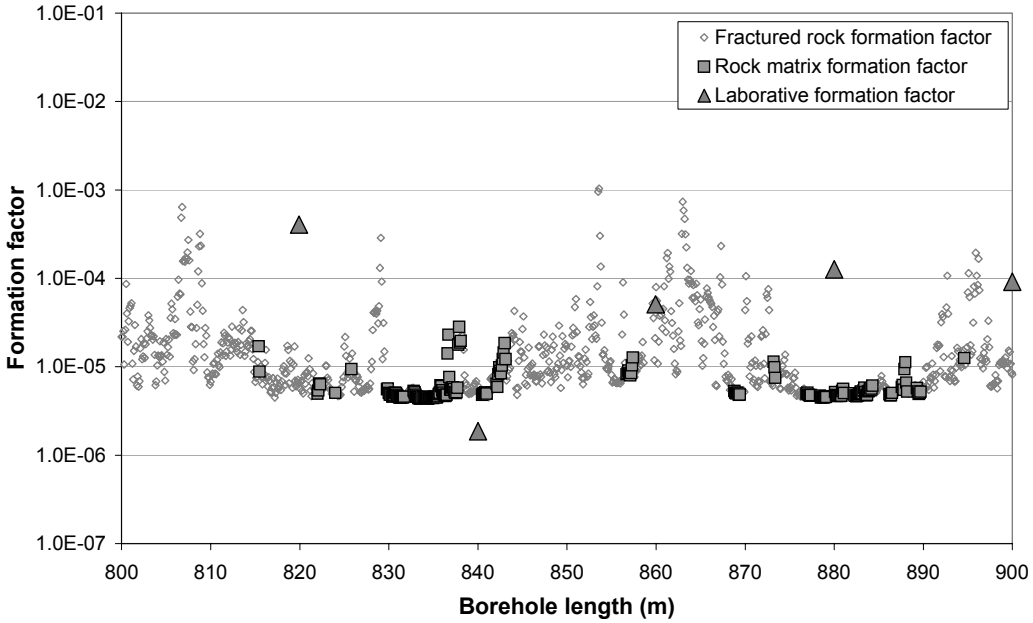
Fractured rock formation factor
Rock matrix formation factor
Laborative formation factor
Formation factor
1.0E-01
1.0E-02
1.0E-03
1.0E-04
1.0E-05
1.0E-06
1.0E-07
800
810
820
830
840
850
860
870
880
890
900
Borehole length (m)

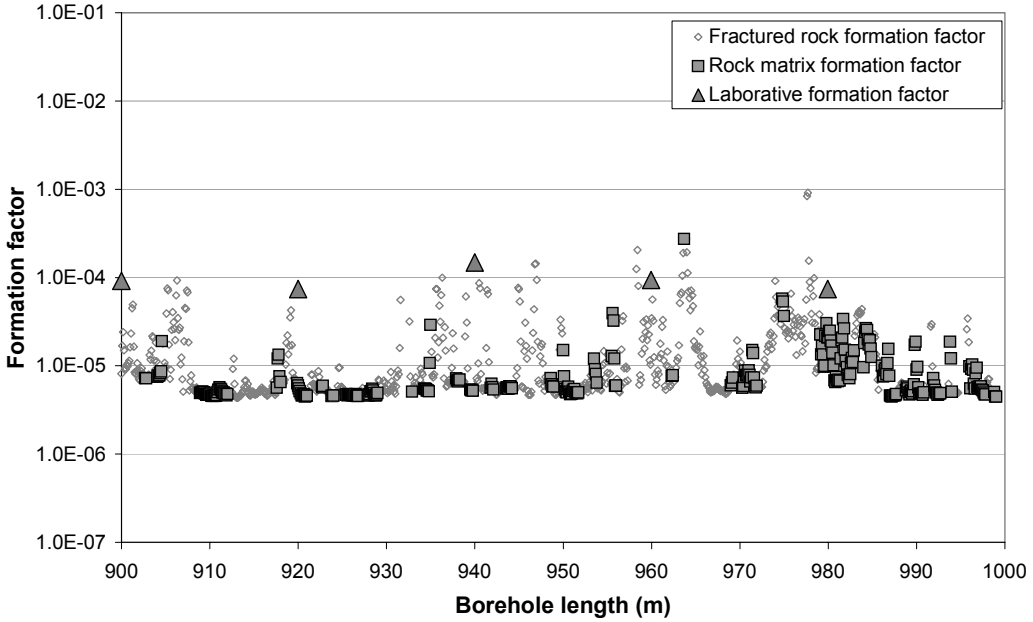
Fractured rock formation factor
Rock matrix formation factor
Laborative formation factor
Formation factor
1.0E-01
1.0E-02
1.0E-03
1.0E-04
1.0E-05
1.0E-06
1.0E-07
900
910
920
930
940
950
960
970
980
990
1000
Borehole length (m)

Appendix C3: Comparison of laboratory and in-situ formation factors KSH01A

BH Length (m)	FF Laboratory	FF In-situ	BH Length (m)	FF Laboratory	FF in-situ
19.95	1.56×10^{-4}		559.90	1.34×10^{-6}	
59.11	2.06×10^{-5}		580.87	4.66×10^{-6}	
79.64	2.31×10^{-5}		598.65	2.48×10^{-5}	
99.70	2.40×10^{-5}		620.22	1.95×10^{-4}	
121.40	7.28×10^{-6}		640.55	4.64×10^{-5}	2.43×10^{-5}
160.71	8.49×10^{-6}	1.46×10^{-5}	661.06	1.87×10^{-5}	
181.46	5.28×10^{-5}	1.46×10^{-5}	680.20	5.87×10^{-6}	
200.10	2.08×10^{-6}	4.43×10^{-5}	699.00	9.06×10^{-6}	
239.95	6.15×10^{-6}		720.24	8.82×10^{-5}	
261.07	4.12×10^{-4}		740.53	1.56×10^{-5}	2.38×10^{-5}
295.40	3.47×10^{-5}		760.75	1.46×10^{-5}	
317.77	6.92×10^{-5}	1.40×10^{-5}	779.19	6.03×10^{-5}	3.91×10^{-5}
340.87	1.61×10^{-6}	1.14×10^{-5}	800.40	1.49×10^{-4}	1.18×10^{-4}
362.54	1.14×10^{-5}		820.08	9.04×10^{-4}	1.27×10^{-4}
378.97	1.40×10^{-5}		840.70	4.70×10^{-4}	5.50×10^{-5}
398.74	1.17×10^{-5}		859.15	4.88×10^{-4}	
420.77	2.47×10^{-5}		880.50	3.84×10^{-4}	
440.22	3.46×10^{-4}		898.60	3.29×10^{-4}	4.77×10^{-5}
460.00	4.48×10^{-4}	1.84×10^{-5}	919.65	2.91×10^{-4}	
478.20	1.63×10^{-6}		960.77	5.72×10^{-4}	1.84×10^{-5}
500.30	2.53×10^{-5}	1.49×10^{-5}	980.40	2.73×10^{-4}	1.62×10^{-5}
520.75	4.29×10^{-6}		999.45	2.19×10^{-4}	1.53×10^{-5}
539.00	1.95×10^{-6}				

BH Length = Borehole length.
FF Laboratory = Formation factor obtained in the laboratory
FF In-situ = Mean value of in-situ rock matrix formation factors from within 0.5 m of BH Length.

Appendix C4: Comparison of laboratory and in-situ formation factors KSH02

BH Length (m)	FF Laboratory	FF In-situ	BH Length (m)	FF Laboratory	FF In-situ
19.95	2.88×10^{-7}		539.85	2.33×10^{-5}	
39.95	2.20×10^{-6}		560.05	1.64×10^{-5}	
60.17	2.36×10^{-5}		580.10	2.17×10^{-7}	
80.00	8.22×10^{-5}		639.88	1.93×10^{-4}	
99.90	1.76×10^{-4}		680.15	3.16×10^{-5}	
119.95	3.76×10^{-6}		700.00	1.75×10^{-4}	
140.15	1.63×10^{-6}		720.00	1.56×10^{-6}	
159.95	2.31×10^{-5}		740.00	3.66×10^{-4}	
179.95	7.85×10^{-6}		760.16	9.39×10^{-6}	
219.65	1.12×10^{-6}		779.81	3.46×10^{-4}	
239.15	2.89×10^{-6}		819.90	4.06×10^{-4}	
259.82	6.93×10^{-6}		840.00	1.87×10^{-6}	4.81×10^{-6}
280.00	2.31×10^{-6}		859.95	5.09×10^{-5}	
360.05	5.26×10^{-4}		880.00	1.27×10^{-4}	4.82×10^{-6}
399.95	1.06×10^{-5}		900.00	9.17×10^{-5}	7.47×10^{-6}
419.95	2.26×10^{-4}		920.00	7.40×10^{-5}	5.31×10^{-6}
439.95	3.06×10^{-6}	2.96×10^{-5}	940.00	1.48×10^{-4}	5.29×10^{-6}
459.68	1.72×10^{-4}		959.95	9.35×10^{-5}	
500.37	8.40×10^{-4}		979.95	7.41×10^{-5}	2.00×10^{-5}

BH Length = Borehole length.
FF Laboratory = Formation factor obtained in the laboratory
FF In-situ = Mean value of in-situ rock matrix formation factors from within 0.5 m of BH Length.

Appendix D

Appendix D1: Histograms of rock matrix formation factor KSH01A

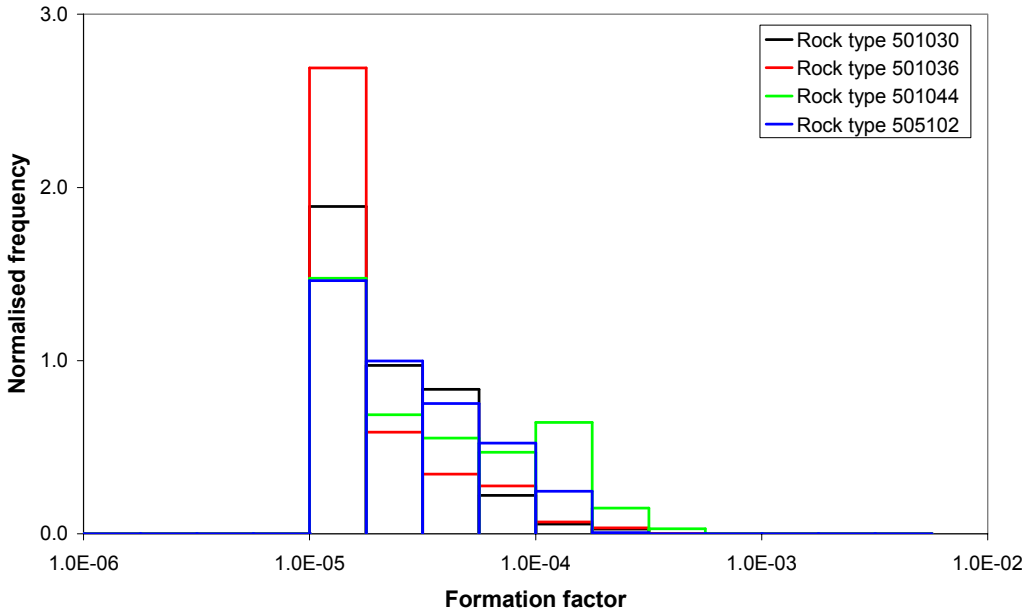

Number of data points: 501030: 144 501036: 116 501044: 535 505102: 473

Rock types:
501030 = Dioritoide
501036 = Quartz monzonite to monzodiorite, equigranular to weakly porphyritic
501044 = Granite to quartz monzodiorite, generally porphyritic
505102 = Mafic rock, fine-grainedAppendix D1: Distribution of rock matrix formation factor KSH01A

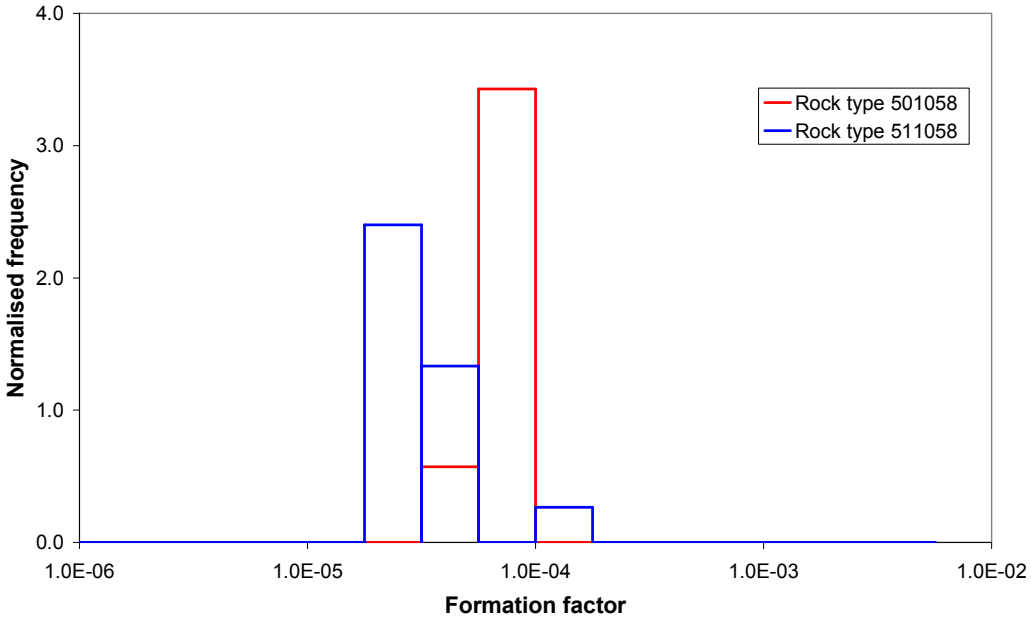

Number of data points: 501058: 7 511058: 15

Rock types:
501058 = Granite, medium- to coarse-grained
511058 = Granite, fine- to medium-grained

Appendix D2: Histograms of fractured rock formation factor KSH01A

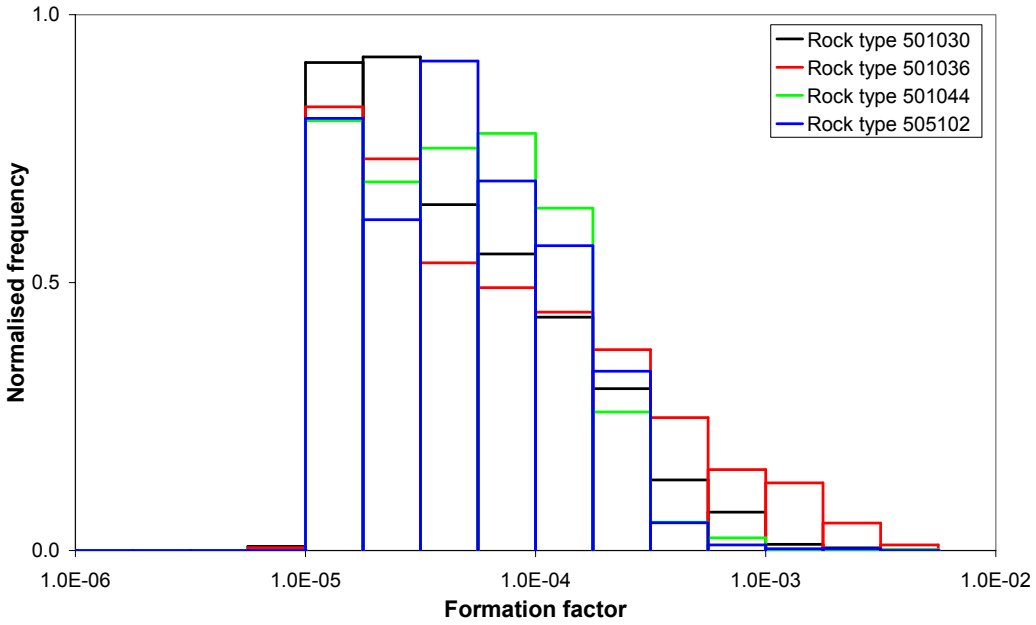

Number of data points: 501030: 3056 501036: 1483 501044: 2179 505102: 1160

Rock types:
501030 = Dioritoide
501036 = Quartz monzonite to monzodiorite, equigranular to weakly porphyritic
501044 = Granite to quartz monzodiorite, generally porphyritic
505102 = Mafic rock, fine-grained.

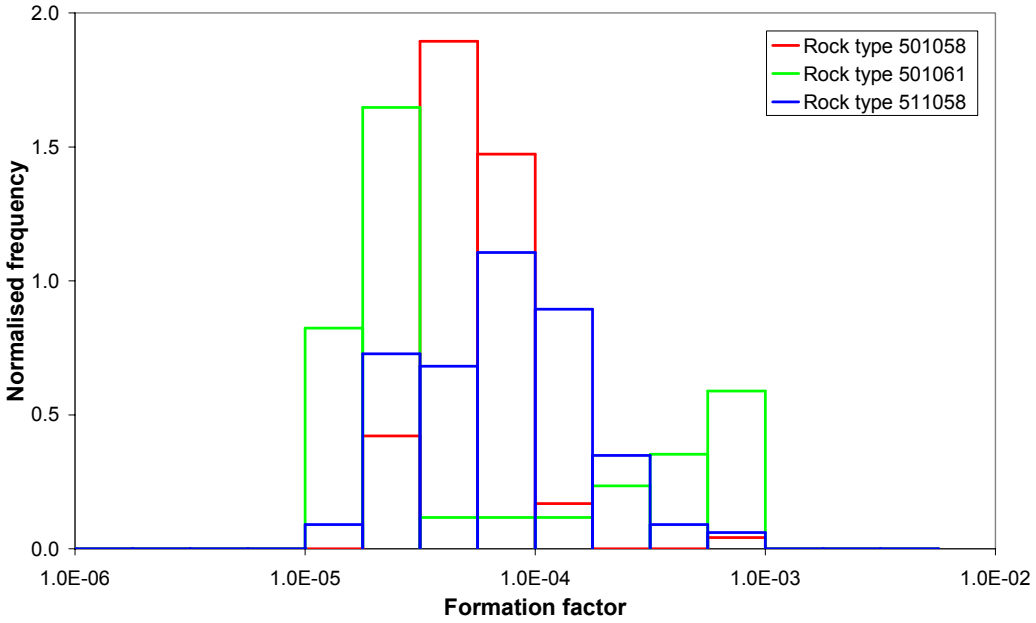

Number of data points: 501058: 95 501061: 34 511058: 264

Rock types:
501058 = Granite, medium- to coarse-grained
501061 = Pegmatite
511058 = Granite, fine- to medium-grained

Appendix D3: Histograms of rock matrix formation factor KSH02

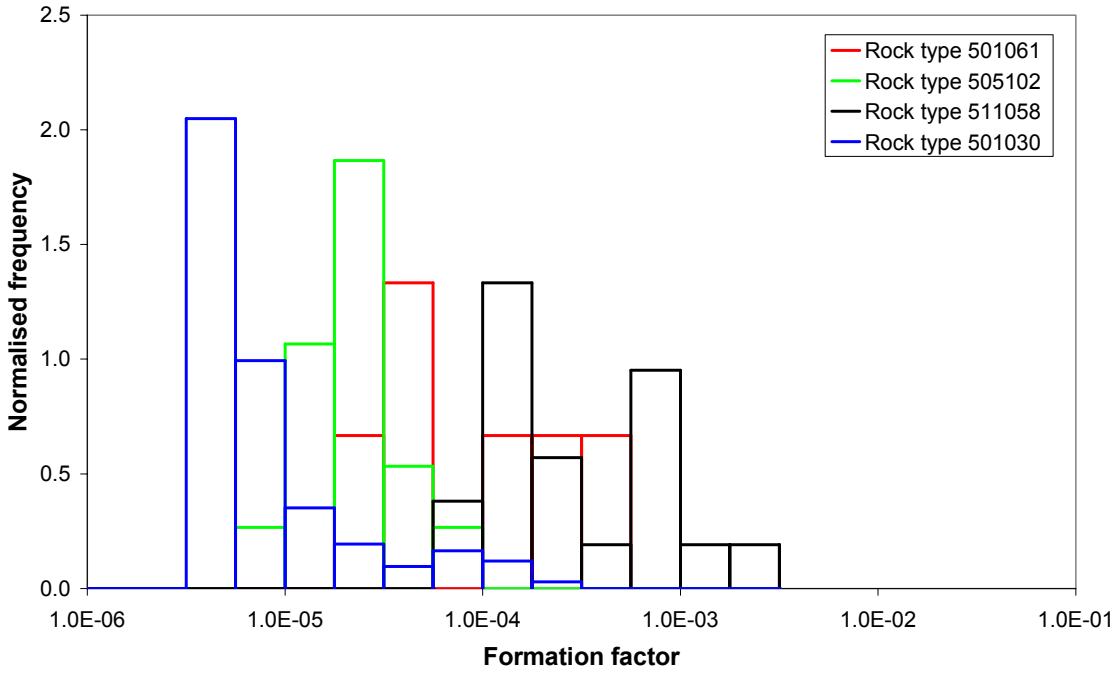

Number of data points: 501030: 3535 511058: 21 501061: 6 505102: 15

Rock types:
501030 = Dioritoide
511058 = Granite, fine- to medium-grained
501061 = Pegmatite
505102 = Mafic rock, fine-grained

Appendix D4: Histograms of fractured rock formation factor KSH02

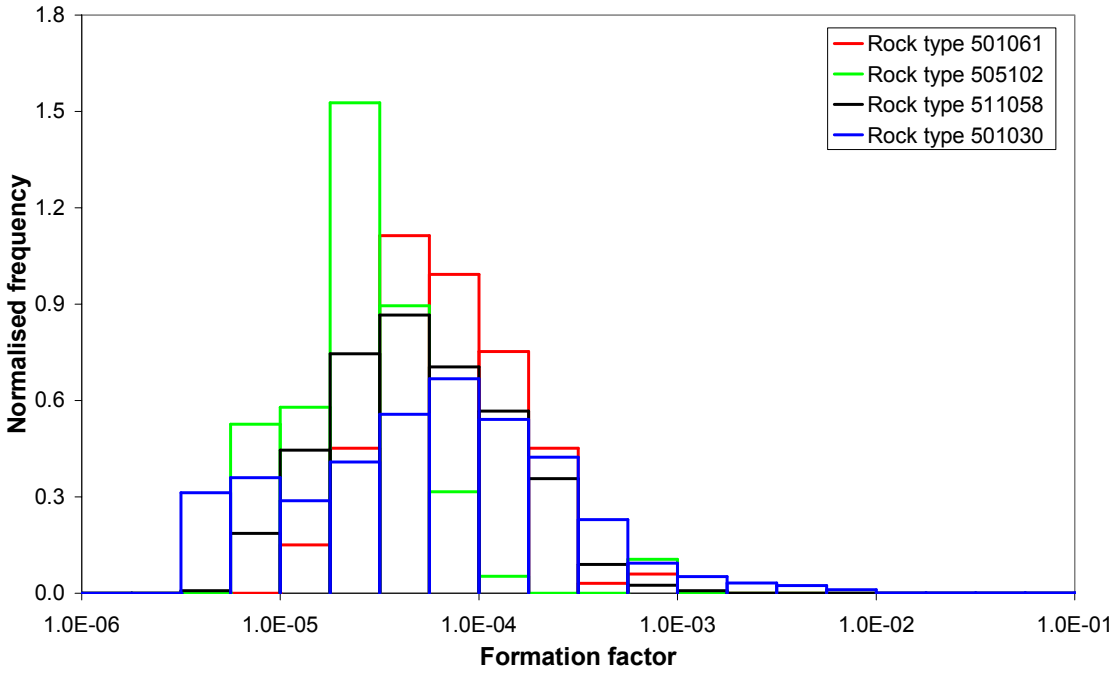

Number of data points: 501030: 7789 511058: 494 501061: 133 505102: 76

Rock types:
501030 = Dioritoide
511058 = Granite, fine- to medium-grained
501061 = Pegmatite
505102 = Mafic rock, fine-grained